

Quantum Chemical Studies of Macropolyhedral Boranes and Related Clusters

INAUGURAL – DISSERTATION

zur
Erlangung der Doktorwürde
der
Naturwissenschaftlich-Mathematischen
Gesamtfakultät
der
Ruprecht-Karls-Universität
Heidelberg

Vorgelegt von
M.Phil. Farooq Ahmad Kiani
aus: Chakwal
2006

Short Summary in English

Density functional studies were carried out on the boron hydride clusters in order to explore the rules governing their structures and relative stabilities. Structural increments assigned to the disfavoring structural features in the 11-vertex *nido*- and the 12-vertex *closo*-carboranes, heteroboranes, heterocarbaboranes and the 12-vertex *closo*-cyclopentadienyl metallaheterocarbaboranes are used to accurately reproduce the relative stabilities as computed by density functional theory methods. Relative energies of a large number of isomeric structures can be determined by a small number of highly additive structural increments through a simple summation procedure. The structural increments obtained as the energy difference of two isomers differing with respect to one disfavoring structural feature or by a statistical fitting based on a large number of structures exhibit periodic trends, i.e., increase along the period and decrease down the group. They depend primarily on the number of skeletal electrons localized by a given heteroatom and secondly on its electronegativity. Structural increments can be transformed into connection increments to give the relative stabilities of 11-vertex *nido*- and 12-vertex *closo*-clusters with a unique set of increments. Usually more electronegative (smaller) heteroatoms tend to occupy non-adjacent, whereas less electronegative (larger) heteroatoms tend to occupy adjacent vertices in the thermodynamically most stable *closo*-diheterododecaborane isomers. Cyclopentadienyl transition metal fragments have specific ortho, meta and para directing effects to a carbon atom in the thermodynamically most stable isomers of 12-vertex *closo*-cyclopentadienyl metallaheteroboranes.

Furthermore, density functional theory studies were carried out on macropolyhedra in which two cluster fragments have one edge in common, i.e. share two vertices. The turning point from single cluster borane to macropolyhedral borane preference was determined: All *nido*-single cluster boranes are thermodynamically more stable than corresponding macropolyhedral boranes for less than twelve vertexes. Macropolyhedral boranes enjoy thermodynamic stability only for clusters with larger cluster size ($n \geq 12$). For anionic species, a clear cut turning point for macropolyhedral preference is shifted to not less than seventeen vertexes. Extra hydrogen atoms at the open face have a significant influence on the relative stabilities of the single cluster boranes vs. macropolyhedral boranes. The *arachno*-9-vertex and *nido*-10-vertex cluster fragments are the preferred building blocks and are usually present in the thermodynamically most stable macropolyhedral borane isomers. The structural relationships between various macropolyhedral borane classes were clarified: Thermodynamically most stable isomers of two-vertex sharing macropolyhedral boranes are related to each other by the removal of one open face vertex. Cluster increments were devised for various two-vertex sharing macropolyhedral boranes with different cluster sizes. The relative stabilities for the macropolyhedral boranes can be easily estimated by using increments specific to each cluster fragment.

Kurzfassung auf Deutsch

An Borhydrid-Clustern wurden Dichtefunktional-Rechnungen durchgeführt um Regeln zu finden, die ihren Strukturen und relativen Stabilitäten zugrunde liegen. Dazu wurden Strukturinkremente für unvorteilhafte Strukturmerkmale ermittelt, und zwar in 11-Vertex *nido*- und 12-Vertex *closo*-Carboranen, -Heteroboranen und -Carbaheteroboranen sowie 12-Vertex *closo*-Cyclopentadienylmetallacarboranen. Sie reproduzieren die relativen Stabilitäten wie sie aus Dichtefunktional-Rechnungen resultieren sehr genau. Bemerkenswerterweise können die relativen Energien einer sehr großen Anzahl von isomeren Strukturen durch eine recht kleine Anzahl von Strukturinkremente mittels einfacher Summation ermittelt werden, da sich letztere höchst additiv verhalten. Strukturinkremente können als Energiedifferenz zweier Isomere erhalten werden, wenn diese sich in nur in dem einen relevanten Strukturmerkmal unterscheiden, oder durch eine statistische Fittprozedur basierend auf einer größeren Anzahl von verschiedenartigen Strukturen. Sie zeigen periodische Trends, wie zum Beispiel dass sie entlang einer Periode zunehmen und innerhalb einer Gruppe mit steigender Ordnungszahl abnehmen. Sie hängen in erster Linie von der Zahl der Gerüstelektronen ab, die eine bestimmte Heterogruppe zur Clusterbindung beiträgt, und in zweiter Linie von der Elektronegativität des Heteroatoms. Strukturinkremente können auch als Konnektivitätsinkremente ausgedrückt werden. Diese besitzen den Vorzug als einheitlicher Satz von Inkrementen gleichermaßen zur Bestimmung der relativen Stabilitäten von 11-Vertex *nido*- wie auch 12-Vertex *closo*-Clustern herangezogen werden zu können. Üblicherweise neigen elektronegativer (kleinere) Heteroatome dazu, in den thermodynamisch stabilsten *closo*-Diheterododecaboranisomeren nicht-benachbarte Clusterplätze einzunehmen, wohingegen weniger elektronegative (größere) Heteroatome benachbarte Vertices besetzen. Cyclopentadienyl-Übergangsmetallfragmente besitzen in Bezug auf die thermodynamisch stabilsten 12-Vertex *closo*-Cyclopentadienylmetallaheteroboran-Isomere einen spezifischen ortho-, meta- und para-dirigierenden Effekt auf ein Kohlenstoffatom.

Des Weiteren wurden Dichtefunktional-Rechnungen an Makropolyedern durchgeführt, und zwar an Strukturen in denen zwei reguläre Clusterfragmente an einer gemeinsamen Kante verschmolzen sind, sich also zwei Vertices teilen. Es wurde der Wendepunkt ermittelt, an dem die Präferenz bei den Boranen von Einfachcluster- zu Makropolyeder-Strukturen wechselt: Alle *nido*-Cluster sind thermodynamisch stabiler als entsprechende makropolyedrische Borane, solange die Zahl der Vertices kleiner als zwölf ist. Makropolyedrischen Boranen kommt erst bei größeren Molekülen ($n \geq 12$) eine größere thermodynamische Stabilität zu. Bei den Anionen findet man eine deutliche Bevorzugung der Makropolyeder allerdings erst ab 17 Vertices. Die zusätzlichen Wasserstoffatome auf der offenen Fläche der Borane haben einen entscheidenden Einfluss auf die relativen Stabilitäten von Einfach- gegenüber makropolyedrischen Clustern. Die *arachno*-9-Vertex und *nido*-10-Vertex Clusterfragmente sind bevorzugte Bausteine für Makropolyeder und sind meist in den thermodynamisch stabilsten makropolyedrischen Boranisomeren vertreten. Außerdem wurden die strukturellen Beziehungen zwischen den verschiedenen Klassen von Makropolyedern geklärt: Die thermodynamisch stabilsten Isomere von Makropolyedern leiten sich voneinander durch die Entfernung eines Vertices von der offenen Fläche eines Clusterbausteins ab. Clusterinkremente wurden für verschieden große makropolyedrische Borane mit zwei gemeinsamen Vertices ermittelt. Sie erlauben es, die relativen Stabilitäten von Makropolyedern leicht abzuschätzen.

Quantum Chemical Studies of Macropolyhedral Boranes and Related Clusters

INAUGURAL – DISSERTATION

zur
Erlangung der Doktorwürde
der
Naturwissenschaftlich-Mathematischen
Gesamtfakultät
der
Ruprecht-Karls-Universität
Heidelberg

Vorgelegt von
M.Phil. Farooq Ahmad Kiani
aus: Chakwal
2006

Thema

Quantum Chemical Studies
of Macropolyhedral Boranes
and Related Clusters

Gutachter: Prof. Dr. Roland Krämer
Prof. Dr. Peter Comba

Tag der mündlichen Prüfung: 20.10.2006

The research work was carried out from October 2003 until August 2006 in the Inorganic Chemistry Institute of the University of Heidelberg, Germany.

DR. MATTHIAS HOFMANN, I am grateful to you for accepting me as a PhD student, sharing your vast knowledge of chemistry and providing excellent training of handling and presenting scientific projects. I am also thankful to you for providing financial support and very nice company over the years.

Dedicated to

The *Silent Moments*

That lead to

Divine Truths

Contents

1. Introduction	1
1.1. Structural Patterns Between <i>closo</i> -, <i>nido</i> - and <i>arachno</i> -Clusters.	4
1.2. Polyhedral Skeletal Electron pair Theory (PSEPT).	4
1.3. Heteroatom Placement in <i>closo</i> -Clusters.	6
1.3.1. Williams Qualitative Heteroatom Placement Rule.	6
1.3.2. Ott-Gimarc's Charge Preference.	7
1.3.3. Ring-Cap Principle.	8
1.3.4. Tight Bond with Adjacent Matrix (TBAM) approach.	8
1.4. Heteroatom Placement in <i>nido</i> -Clusters.	9
1.5. Macropolyhedral Boranes, Jemmis' <i>mno</i> Rule and its Limitations.	11
1.6. Focus of Current Research Work.	12
1.6.1. A Simple Approach to Derive Structural Increments for <i>nido</i> - and <i>closo</i> - Heteroboranes.	12
1.6.2. Quantum Chemical Studies of Macropolyhedral Boranes.	13
2. Computational Details	15
2.1. 11-Vertex <i>nido</i> -p-block-Heteroboranes (Chapter 3).	15
2.2. The Relative Stabilities of 11-Vertex <i>nido</i> - and 12-Vertex <i>closo</i> -Heteroboranes and -borates: Facile Estimation by Structural or Connection Increments (Chapter 4).	16
2.3. Ortho-, Meta- and Para-Directing Influence of Transition Metal Fragments in 12- vertex <i>closo</i> -Cyclopentadienyl Metallaheteroboranes: Additive Nature of Structural Increments (Chapter 5).	16
2.4. Which <i>nido:nido</i> -Macropolyhedral Boranes are Most Stable (Chapter 6)?	17
2.4.1. Construction of <i>nido</i> -single clusters.	17
2.4.2. Construction of <i>nido:nido</i> -Macropolyhedral Borane Clusters.	17
2.5. Structural Relationships among Two Vertex Sharing Macropolyhedral Boranes (Chapter 7).	18
2.6. Cluster Increment System for Macropolyhedral Boranes (Chapter 8).	19

3. Periodic Trends and Easy Estimation of Relative Stabilities in 11-Vertex <i>nido</i>-p-block-Heteroboranes and –borates -----	21
3.1. Introduction -----	21
3.2. Results and Discussion -----	24
3.2.1. Structural Features for Hetero(carba)boranes and -borates. -----	24
3.2.2. Energy Penalties as Periodic Properties of Heteroatoms in 11-Vertex <i>nido</i> -Cluster. -----	26
3.2.3. Comparisons of the Estimated Relative Stabilities (E_{inc}^{rel}) Derived from Estimated Energy Penalties (E_{inc}) with DFT computed Values (E_{calc}) for the 11-vertex <i>nido</i> -Hetero(carba)boranes and -borates. -----	30
3.2.3.1. Thia(carba)boranes and –borates. -----	30
3.2.3.2. Phosphathiaboranes and -borates. -----	33
3.2.3.3. Seleno(carba)boranes and –borates. -----	34
3.2.3.4. Selenathiaboranes. -----	36
3.2.3.5. Estimated Energy Penalties (E_{inc}) and Corresponding Estimated Relative Stabilities (E_{inc}^{rel}) for Other 11-vertex <i>nido</i> -Hetero(carba)boranes and -borates. ----	36
3.2.4. Prediction of Thermodynamically Most Stable Mixed Heteroboranes and -borates with Three Open Face Heteroatoms.-----	36
3.3. Conclusion -----	39
4. The Relative Stabilities of 11-Vertex <i>nido</i>- and 12-vertex <i>closo</i>-Heteroboranes and –borates: Facile Estimation by Structural or Connection Increments.-----	41
4.1. Introduction. -----	41
4.2. Results and Discussion -----	42
4.2.1. Periodic Trends of Heteroatom Energy Penalties for the 12-Vertex <i>closo</i> -Cluster. -----	42
4.2.2. Redefining $Het_{5k}(2)$ and $HetHet$ in Terms of Connection Increments. -----	46
4.2.3. Heavy Heteroatoms at Adjacent Positions in the Thermodynamically Most Stable 12-Vertex <i>closo</i> -Isomer; a Phenomenon Supported by Experimental Results. --	51
4.3. Conclusion -----	52

5. Ortho-, Meta- and Para-Directing Influence of Transition Metal Fragments in 12-vertex <i>closo</i>-Cyclopentadienyl Metallaheteroboranes: Additive Nature of Structural Increments. -----	55
5.1. Introduction -----	55
5.2. Results and Discussion -----	57
5.2.1. Structural Features in Metallaheteroboranes. -----	58
5.2.2. Ortho-, Meta- and Para-Directing Influence of Metal Atoms to a Carbon Atom in Metallocarboranes. -----	59
5.2.3. Periodic Trends in MC_o and MC_m Energy Penalties and Their Dependence on the Extent of Electrons Localized by a CpM Fragment. -----	61
5.2.4. Additive Nature of Structural Increments in Cyclopentadienyl Iron Containing 12-Vertex <i>closo</i> -Metallaheteroboranes. -----	61
5.2.4.1. $[CpFeC_xB_{11-x}H_{11}]^{(3-x)-}$ ($x = 1,2,3$) isomers. -----	63
5.2.4.2. $[CpFeP_xB_{11-x}H_{11-x}]^{(3-x)-}$ ($x = 1, 2, 3$) isomers. -----	64
5.2.4.3. $[CpFePCB_9H_{10}]^-$, $CpFePC_2B_8H_{10}$ and $CpFeP_2CB_8H_{10}$ isomers. -----	64
5.2.5. Thermodynamically Most Stable $[CpMC_yB_{11-y}H_{11}]^{z-}$ ($y = 0,1,2,3$, $M = Ru, Os, Co, Rh, Ir$) Isomers. -----	65
5.2.6. Relative Stabilities of $(CO)_3CoCB_{10}H_{11}$ Isomers. -----	66
5.3. Conclusion -----	67
6. Which <i>nido:nido</i>-Macropolyhedral Boranes are Most Stable? -----	69
6.1. Introduction -----	69
6.2. Result and Discussion -----	71
6.2.1. Fusion Mode of <i>nido:nido</i> -Macropolyhedral Boranes. -----	71
6.2.2. Turning Point from <i>nido</i> - B_nH_{n+4} Single Cluster to <i>nido:nido</i> - B_nH_{n+4} Macropolyhedral Preference. -----	72
6.2.3. The Effect of Open Face Hydrogen Atoms on the Relative Stabilities of <i>nido</i> Single Cluster Boranes vs. <i>nido:nido</i> Macropolyhedral Boranes. -----	74
6.2.4. Preferred Units for <i>nido:nido</i> -Macropolyhedral Boranes and Borates from 12-19 Vertices. -----	76

6.2.5. Relative Energies ($E_{x,y}$) of Macropolyhedral Boranes in Comparison to the Relative Energies (E_{x+y}) from Summation of Individual Clusters Making the Macropolyhedra. -----	78
6.3. Conclusion -----	80
7. Cluster Increments for Macropolyhedral Boranes -----	81
7.1. Introduction -----	81
7.2. Result and Discussion -----	82
7.2.1. Relative stabilities of various types of macropolyhedral boranes. -----	82
7.2.2. Even <i>nido</i> -clusters are more favorable than odd <i>nido</i> -clusters in macropolyhedra. -----	86
7.2.3. Smaller <i>arachno</i> -clusters are more favorable than larger <i>arachno</i> -clusters. -----	87
7.2.4. Cluster increments reproduce the DFT computed relative stabilities of macropolyhedral boranes with good accuracy. -----	88
7.3. Conclusion -----	90
8. Structural Relationships among Two Vertex Sharing Macropolyhedral Boranes -----	91
8.1. Introduction -----	91
8.2. Results and Discussion -----	93
8.2.1. Thermodynamic Stabilities of Neutral Macropolyhedral Boranes Relative to Corresponding Simple Polyhedral Boranes. -----	93
8.2.2. Importance of Open Face Hydrogen Atoms on the Stabilities of Macropolyhedral vs. Monopolyhedral Boranes. -----	95
8.2.3. The Number of Skeletal Electron Pairs and the Stabilities of Macropolyhedral Boranes Relative to Isomeric Simple Polyhedra. -----	97
8.2.4. Preferred Fragments for Two Vertex Sharing <i>arachno:nido</i> - and <i>arachno:arachno</i> -Macropolyhedral Boranes. -----	98
8.2.5. Structural Relationships between Different Macropolyhedral Borane Classes. ----	99
8.2.6. Comparison of $E_{n+1}-E_n$ for Simple Polyhedral and Macropolyhedral Boranes. ----	101
8.3. Conclusion -----	102
9. Summary and Conclusion -----	103

1. Introduction

Boron and carbon are the only two elements in the Periodic Table that can form complex and extensive series of hydrides. There are, however, profound differences between the hydrides of boron and those of carbon. The skeletons of the carbon hydrides and their relatives are typified by chains and rings e.g., propane; C₃H₈, benzene; C₆H₆, and so on. The boron

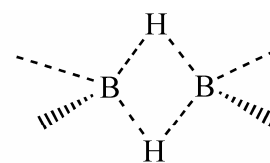


Figure 1.1: B₂H₆ structure

hydrides also called boranes, and their derivatives have quite different structures from those of organic compounds. Instead of rings and chains, they form cages and clusters. This is because the valence shell of boron atom contains only three electrons. One consequence of this is that there are not enough electrons to allow formation of four two-center-two-electron covalent bonds, only three. Hence, a boron compound with only three covalent bonds is electron deficient.¹ The simplest example of this is BH₃ with three filled sp²-orbitals and one empty p-orbital. The empty p-orbital is extremely keen to accept an electron pair from any electron-donating species. In fact, the BH₃ does not exist as a monomer and dimerises to B₂H₆. The molecular structure of B₂H₆ defied contemporary chemical valency concepts in the third and fourth decades of the 20th century and constitutes two boron atoms bridged by two hydrogen atoms and four terminal hydrogens, two on each boron atom (Figure 1.1). Eight of the 12 valence electrons are involved in the four terminal B-H bonds. Only four electrons are left over to bind the bridging hydrogen atoms. The bonds between the two boron atoms which include the “bridging” hydrogen atoms are referred to as a three-center-two-electron (3c-2e) bond. The electronic structure is similar to that of ethylene, the only difference being the two protons embedded into the bridging bonds. The chemical bonding in B₂H₆ is much different from the classical concepts. Three-center, two-electron bonds in boron compounds can also be formed by overlap of three orbitals from three corners of an equilateral triangle of boron atoms.¹ The bonding MO enjoys orbital overlap in the centre of this boron triangle and contains one pair of electrons. This allows for the existence of boron-cage compounds. Three-dimensional structures that consist of BBB triangles and involve resonance between 2c-2e BB bonds and 3c-2e BBB bonds, in addition to terminal B-H bonds on the outside of the structure are called polyhedral boron hydrides. Boron hydride cages and clusters can be quite small, as in the case of diborane; B₂H₆, or tetraborane; B₄H₁₀, but can also get much bigger. [B₁₂H₁₂]²⁻ is one typical example,

¹ Huheey, J. E.; Keither, E. A.; Keither, R. L. *Inorganic Chemistry. Principles of Structure and Reactivity*, 4th ed.; Harper Collins: New York, 1993.

1. INTRODUCTION

with a twelve-boron symmetrical skeleton that takes the form of a regular single icosahedral cluster (Fig. 1.2a).¹ Alternatively, binary boron hydride clusters could be made by joint fusion of two or more single clusters exhibiting varying degrees of intimacy ranging from a single covalent bond linkage to the sharing of an entire deltahedral face or wedge. One such example is B₂₀H₁₆ in which two icosahedral units share a wedge or four vertexes (Figure 1.2b).² Compounds with fused cages have also been termed macropolyhedral boranes.

Single clusters as well as macropolyhedral boranes can get very complicated when heteroatoms, e.g. carbon, sulfur, nitrogen atoms etc. are incorporated into these cages and clusters. The presence of heteroatoms also results in various possible skeletal isomers, e.g., carbon atoms at different positions relative to each other in C₂B₁₀H₁₂,³ produce ortho (1,2-), meta (1,7-), or para (1,12-) isomers (Figure 1.3). Not only carbon, but also most other elements, can substitute a boron

atom or a BH vertex in the clusters. A number of examples for phosphaboranes,⁴ thiaboranes⁵ and azaboranes⁶ are experimentally known. Skeletal isomers are also possible for macropolyhedral boranes when heteroatoms are incorporated. For example, a single vertex sharing metallaborane can have

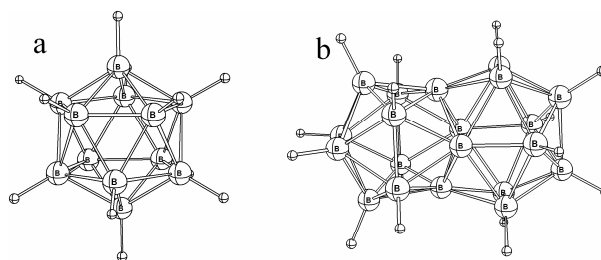


Figure 1.2: a) [B₁₂H₁₂]²⁻ icosahedron b) B₂₀H₁₆ structure with four shared vertexes between two icosahedral [B₁₂H₁₂]²⁻ single clusters

² a) Friedman, L. B.; Dobrott, R. D.; Lipscomb, W. N. *J. Am. Chem. Soc.* **1963**, *85*, 3506. b) Miller, H. C.; Muetterties, E. L. *J. Am. Chem. Soc.* **1963**, *85*, 3506.

³ a) Bobinsky, J. J. *J. Chem. Ed.* **1964**, *41*, 500. b) Heying, T. L.; Ager, J. W.; Clark, S. L.; Mangold, D. J.; Goldstein, H. L.; Hillman, M.; Polak, R. J.; Szymanski, J. W. *Inorg. Chem.* **1963**, *2*, 1089. c) Potenza, J. A.; Lipscomb, W. N. *J. Am. Chem. Soc.* **1964**, *86*, 1874. d) Potenza, J. A.; Lipscomb, W. N. *Inorg. Chem.* **1964**, *3*, 1673. e) Schroeder, H.; Vickers, G. D. *Inorg. Chem.* **1963**, *2*, 1317. f) Grafstein, D.; Dvorak, J. *Inorg. Chem.* **1963**, *2*, 1128. g) Pepetti, S.; Heying, J. L. *J. Am. Chem. Soc.* **1964**, *86*, 2295. h) Fein, M. M.; Bobinsky, J.; Mays, N.; Schwartz, N. N.; Cohen, M. S. *Inorg. Chem.* **1963**, *2*, 1111.

⁴ See for example, a) Little, J. L.; Kester, J. G.; Huffman, J. C.; Todd, L. J. *Inorg. Chem.* **1989**, *28*, 1087-1091. b) Štíbr, B.; Holub, J.; Bakardjiev, M.; Pavlík, I.; Tok, O. L.; Císařová, I.; Wrackmeyer, B.; Herberhild, M. *Chem. Eur. J.* **2003**, *9*, 2239-2244.

⁵ See for example, Pretzer, W. R., Rudolph R. W., *J. Am. Chem. Soc.* **1976**, *98*, 1441-1447 b) Kang, S. O., Carroll, P. J., Sneddon, L. G. *Inorg. Chem.* **1989**, *28*, 961-964 c) Zimmerman, G. J., Sneddon, L. G., *J. Am. Chem. Soc.* **1981**, *103*, 1102-1111. d) Thompson, D. A., Rudolph, R. W. *J. Chem. Soc. Chem. Commun.* **1976**, *19*, 770-771

⁶ See for example, a) Bicerano, J.; Lipscomb, W. N. *Inorg. Chem.* **1980**, *19*, 1825-1827.

different heteroatom positions (Figure 1.4). Such sandwiched metallaheteroboranes have been considered as precursors for molecular rotors and locks.⁷

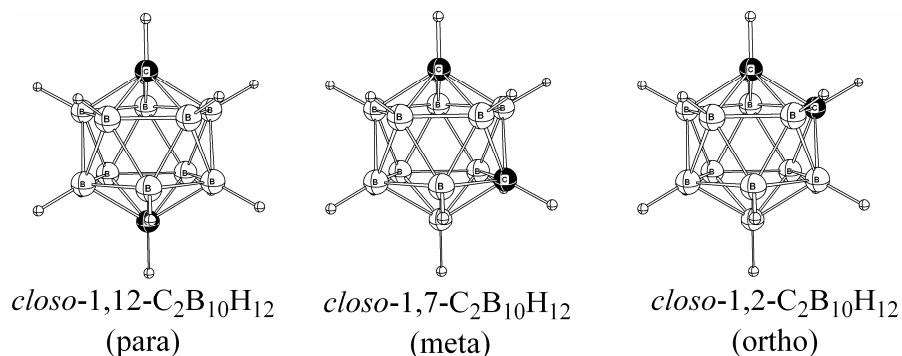


Figure 1.3: Three isomers of *closo*- $C_2B_{10}H_{12}$

The chemistry of boron hydrides exhibits many unique features, demonstrating exceptional ability in molecular, ionic, and solid state environments to form very stable compounds exhibiting structures based on icosahedral and other deltahedral units. In addition, boron forms a variety of very stable cage anions including some of the most weakly coordinating anions,⁸ and strongest Bronsted acids,⁹ currently known. The use of polyhedral boron hydride clusters in synthesis of new materials,⁷ and in boron neutron capture therapy¹⁰ is well documented. The hydride chemistry of boron is unusually rich providing diverse examples of multicenter bonding, which have stimulated numerous theoretical and computational studies. The next sections include numerous theoretical advancements which played a key role in understanding the chemistry of deltahedral boron hydrides.

⁷ Hawthorne, M. F.; Skelton, J. M.; Zink, J. I.; Bayer, M. J.; Liu, C.; Livshits, E.; Baer, R.; Neuhauser, D.; *Science*, **2004**, *303*, 1849-1851.

⁸ King, R. B.; Editor. In *Boron Chemistry at the Millennium*. In: *J. Organomet. Chem.*, **1999**, *581*, 1999, 210 pp.

⁹ See for example, a) Reed, C. A.; Kim, K.-C.; Bolskar, R. D.; Mueller, M. J. *Science*, **2000**, *289*, 101. b) Stoyanov, E. S.; Hoffmann, S. P.; Juhasz, M. Reed, C. A. *J. Am. Chem. Soc.* **2006**, DOI: 10.1021/ja058581l, published online. c) Juhasz, M.; Hoffmann, S.; Stoyanov, E.; Kim, K.-C.; Reed, C. A. *Angew. Chem., Intl. Ed.* **2004**, *43*, 5352-5355.

¹⁰ a) Hawthorne, M. F.; Maderia, A. *Chem. Rev.*, **1999**, *99*, 3421. b) Nakanishi, A.; Guan, L.; Kane, R. R.; Kasamatsu, H.; Hawthorne, M. F. *Proc. Natl. Acad. Sci. USA*, **1999**, *96*, 238.

1.1. Structural Patterns Between *closo*-, *nido*- and *arachno*-Clusters

In 1971, Williams pointed out that the known series of deltahedral fragments, characteristic of *nido*-polyboranes, *nido*-carboranes, and the *nido*-carbocation, $C_5H_5^+$, could almost always be derived from the unique series of most spherical *closo*-deltahedra (with 6-12 vertexes) by the removal of one high- coordinated vertex from each deltahedron and that the *arachno*-deltahedral fragments could

subsequently be derived (from the *nido*-fragments) by the removal of one additional high-coordinated vertex neighbouring the open faces (see Figure. 1.5).¹¹ The most spherical deltahedra are always those with the most uniformly or most homogeneously connected vertexes. Various *closo*-clusters with five to twelve vertexes are shown in Figure 1.5. All *nido*-deltahedral fragments obtained from these most spherical deltahedra by the removal of one most highly coordinated vertex are also shown. Removal of another most highly coordinated vertex generally gives rise to *arachno*-deltahedra.

1.2. Polyhedral Skeletal Electron pair Theory (PSEPT).

Wade was the first to associate cluster shapes with the specific skeletal electron count.¹² The electrons provided by the cluster atoms for cluster bonding are called skeletal electrons. Since each boron atom has one out of three electrons tied up in a terminal B-H bond, it can donate two electrons to the cluster. Thus, n number of boron atoms in a cluster can donate 2n skeletal electrons. According to this rule, all *closo*-clusters require one electron pair in addition to the skeletal electron pairs provided by n BH vertexes. Thus, all *closo*-clusters require n+1 skeletal electron pairs. If there are extra frame work electrons in one of these polyhedral hydrides, the structures will change to accommodate the extra framework electrons.

Wade's rules designate these distorted structures *nido* for n+2 skeletal electron pairs, and *arachno* for n+3 skeletal electron pairs. The remaining cluster fragment remains the same, when a BH vertex is removed from a *closo*-cluster, but its two skeletal electrons remain with the cluster. Additional H^+ to accommodate for the additional negative charge are located at the open face. Thus total requirement of number of skeletal electrons of a given *closo*-cluster, and the derived *nido*- and *arachno*-cluster

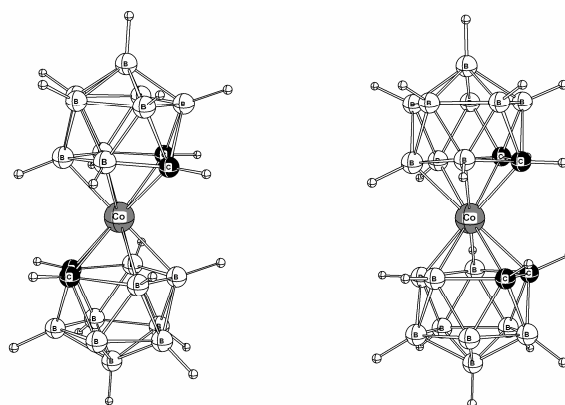


Figure 1.4: Cobalt sandwich isomers of 11-vertex dicarbaboranes

¹¹ Williams, R. E. *Inorg. Chem.* **1971**, *10*, 210-214.

¹² a) Wade, K. *Adv. Inorg. Chem. Radiochem.* **1976**, *18*, 1-66. b) Wade, K. In *Metal Interactions with Boron Clusters*; Grimes, R. N., Ed.; Plenum Press: New York, 1982; Chapter 1, pp 1– 41.

1. INTRODUCTION

fragments is same. That is the total electronic requirement of $n+1$ skeletal electron pairs for a 12-vertex *closo*-cluster, $n+2$ skeletal electron pairs for an 11-vertex *nido*-cluster and $n+3$ skeletal electron pairs for a 10-vertex *arachno*-cluster result in 13 skeletal electron pairs.

Shore¹³ first prepared and structurally characterized $B_5H_9(PMe_3)_2$, $[B_5H_{12}]^-$, and $B_6H_{10}(PMe_3)_2$, three molecules which contain $n+4$ skeletal electron pairs and these structures represent the first well-established members of the *hypho*¹⁴ class of boranes. The *hypho* structures are even more open than the *arachno* and *nido* counterparts, as expected. Table 1.1 lists the experimentally known homonuclear *closo*, *nido*, *arachno* and *hypho*-structures.

In the case of metallaboranes and metallaheteroboranes, the d-electrons

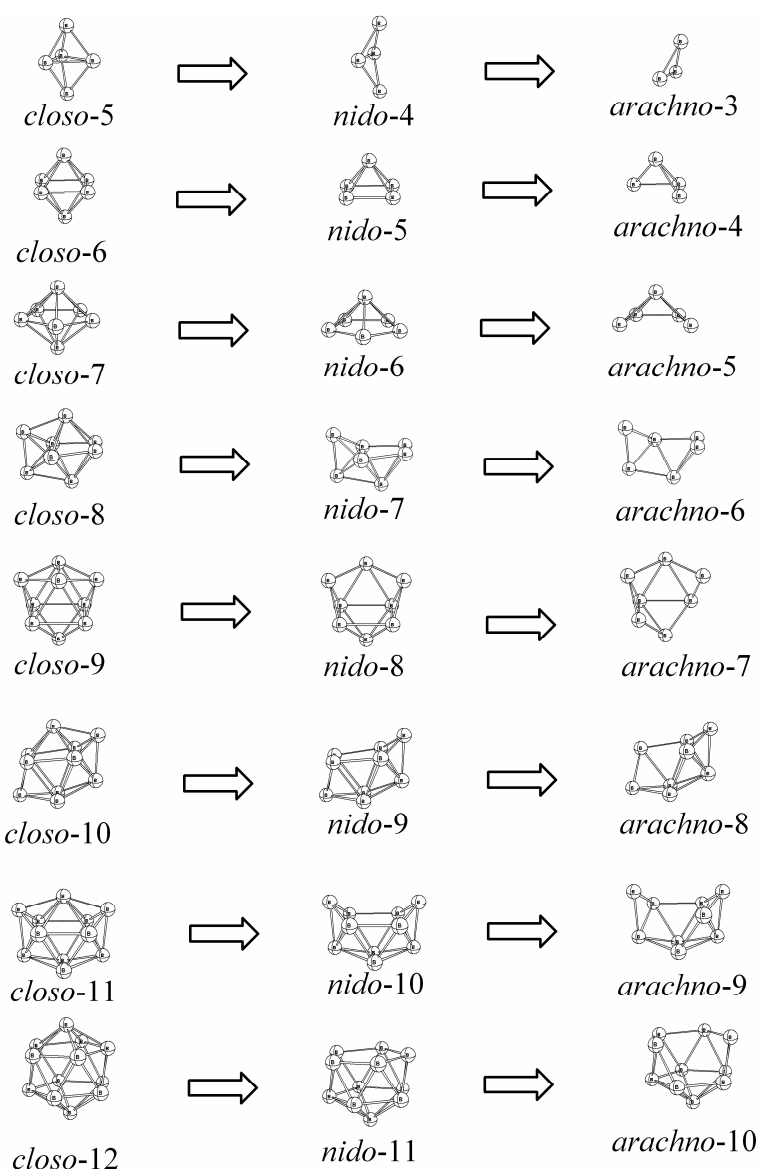


Figure 1.5: Geometrical Systematics in boron hydride clusters

in effect are not included as framework electrons. Mingos¹⁵ has generalized such premises to give the number of skeletal electrons per metal vertex as $u + x - 12$ where u is the number of valence electrons on the metal and x is the number of electrons donated by exocluster ligands and substituents. In this formalism moieties such as $Fe(CO)_3$ and $Co(\pi-C_5H_5)$ are analogous to a BH vertex while $Ni(\pi-C_5H_5)$

¹³ Mangion, M.; Hertz, R. K.; Denniston, M. L.; Long, J. R.; Claytm W. R.; Shore, S. G. *J. Am. Chem. Soc.*, **1976**, *98*, 449-453.

¹⁴ Rudolph, R. W.; Thompson, D. A. *Inorg. Chem.*, **1974**, *13*, 2779-2782.

¹⁵ Mingos, D. M. P. *Nature, Phys. Sci.*, **1972**, *236*, 99-102.

1. INTRODUCTION

behaves like a CH vertex. There are numerous examples consistent with the latter analogies, e.g., *closo*-(C₆H₅)₂C₂Fe₃(CO)₉¹⁶ is analogous to *closo*-C₂B₃H₅. Similar analogies exist for various other metallaheteroboranes.

Table 1.1. Some experimentally known *closo*, *nido* and *arachno* polyhedral borane structures.

Name	Series	Examples	Note
<i>closo</i> ("cage")	B _n H _n ²⁻	n = 6-12	<i>closo</i> polyhedral cage
	B _n H _{n+4}	B ₂ H ₆ , B ₅ H ₉ , B ₆ H ₁₀ , B ₉ H ₁₃ , B ₁₀ H ₁₄	removal of 1 vertex from <i>closo</i>
<i>nido</i> ("nest")	[B _n H _{n+3}] ⁻	[B ₄ H ₇] ⁻ , [B ₅ H ₈] ⁻ , [B ₆ H ₉] ⁻ , [B ₉ H ₁₂] ⁻ , [B ₁₀ H ₁₃] ⁻	removal of 1 H _b from B _n H _{n+4}
	B _n H _{n+2} ²⁻	[B ₁₀ H ₁₂] ²⁻ , [B ₁₁ H ₁₃] ²⁻	removal of 2 H _b from B _n H _{n+4}
<i>arachno</i> ("spider web")	B _n H _{n+6}	B ₄ H ₁₀ , B ₅ H ₁₁ , B ₆ H ₁₂ , B ₈ H ₁₄	removal of one vertex from <i>nido</i>
	[B _n H _{n+5}] ⁻	[B ₂ H ₇] ⁻ , [B ₃ H ₈] ⁻ , [B ₅ H ₁₀] ⁻ , [B ₉ H ₁₄] ⁻	
	[B _n H _{n+4}] ²⁻	[B ₁₀ H ₁₄] ²⁻	
<i>hypho</i> ("net")	B _n H _{n+8}	Only known as adducts: B ₅ H ₉ ·2L	removal of 1 vertex from <i>arachno</i>
	[B _n H _{n+7}] ⁻		
	[B _n H _{n+6}] ²⁻	[B ₅ H ₁₁] ²⁻	

1.3. Heteroatom Placement in *closo*-Clusters

1.3.1. Williams Qualitative Heteroatom Placement Rule.

There are two qualitative rules that explain the replacement of a heteroatom in the polyhedral borane clusters:

- a) Thermodynamically most stable isomers have heteroatoms at positions of lowest connectivity.
- b) The heteroatoms occupy nonadjacent vertexes, if equivalently connected sites are available.

In most of the known examples of heteroboranes with one or more heteroatoms, e.g., *closo*-[CB₁₁H₁₂]⁻¹⁷ and *nido*-SB₁₀H₁₂^{18,19} the heteroatoms contribute more skeletal electrons, as compared to boron atoms. Moreover, they inductively attract the skeletal electrons away from the boron atoms thus

¹⁶ Blount, J. F.; Dahl, L. F.; Hoogzand, C.; Huebel, W. *J. Am. Chem. Soc.* **1966**, *88*, 292-301.

¹⁷ Knoth, W. H.; Little, J. L.; Lawrence, J. R.; Scholer, F. R.; Todd, L. J. *Inorg. Syn.* **1968**, *11*, 33-41.

¹⁸ Kang, S. O.; Sneddon, L. G. *Inorg. Chem.* **1988**, *27*, 3298-3300.

¹⁹ Pretzer, W. R.; Rudolph, R. W. *J. Am. Chem. Soc.* **1976**, *98*, 1441-1447.

producing more electron deficient environment for BH vertexes. A more electron deficient center tends to have higher connectivity.²⁰

Hence the boron atoms tend to occupy the positions of higher connectivity. As a result the heteroatoms are located at the positions of lowest connectivity as is the case in all *closo* heteroborane clusters. E.g., In the case of *closo*-[CB₉H₁₀]⁻ (Figure 1.6), there are two different types of cage vertexes present. Two cage vertexes have a total connectivity of four (4k

vertexes) while the remaining eight vertexes have a cage atom connectivity of five (5k vertexes). A carbon atom tends to occupy the least coordinated position in the thermodynamically most stable isomer as exemplified in Figure 1.6b. Rearrangement of 2-[CB₉H₁₀]⁻ to 1-[CB₉H₁₀]⁻, is associated with the release of energy.

In the case of *closo*-C₂B₁₀H₁₂ (Figure 1.3), all the vertexes are equivalently connected (i.e. 5k), and the carbon atoms tend to be apart from each other in the thermodynamically most stable isomer, i.e. *para*-C₂B₁₀H₁₂. The *ortho*- and *meta*- isomers of C₂B₁₀H₁₂ are far less stable as compared to the *para*-isomer due to the positions of carbon atoms.

1.3.2. Ott-Gimarc's Charge Preference

Ott and Gimarc have used topological charge stabilization considerations to predict the qualitative ordering of stabilities of positional isomers among the various classes of *closo*-carboranes, C₂B_{n-2}H_n, 5 ≤ n ≤ 12.²¹ The rule of topological charge stabilization states that the positions of heteroatoms in a structure are related to the distribution of atomic charges that are determined by connectivity or topology for an isoelectronic, isostructural, homoatomic reference system. They used Mulliken net atomic populations calculated from extended Hückel wave functions. The predicted order of stabilities agrees perfectly with what can be deduced from experiments. For example, the uniform reference frame for the trigonal-bipyramidal [B₅H₅]²⁻ structure (Figure 1.7) shows the normalized charges to be negative at the apical positions and positive at the equatorial sites. Topological charge stabilization says that electronegative heteroatoms, like the carbon atoms in C₂B₃H₅, prefer to be at sites where electron density is already greatest in the uniform reference frame. Therefore, the three possible isomeric carboranes should follow the decreasing order of stability: 1,5-C₂B₃H₅ > 1,2-C₂B₃H₅ > 2,3-C₂B₃H₅. The

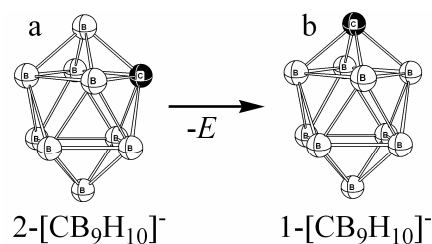


Figure 1.6: Two isomers of *closo*-[CB₁₀H₁₀]⁻. *closo*-2-[CB₁₀H₁₀]⁻ is thermodynamically less stable than the *closo*-1-[CB₁₀H₁₀]⁻ isomer.

²⁰ Williams, R. E. *Chem. Rev.* **1992**, 92, 177-207; references therein.

²¹ Ott, J. J.; Gimarc, B. M. *J. Am. Chem. Soc.* **1986**, 108, 4303-4308.

1,5-isomer shows a perfect match between the negative charges in the reference frame and the location of the more electronegative heteroatoms. Hence, 1,5- $C_2B_3H_5$ is the most stable isomer. The 1,2-isomer complies in only one of the two positions, while in the 2,3-isomer neither carbon atom occupies a site of greater electron density and hence the structure is the least stable isomer.

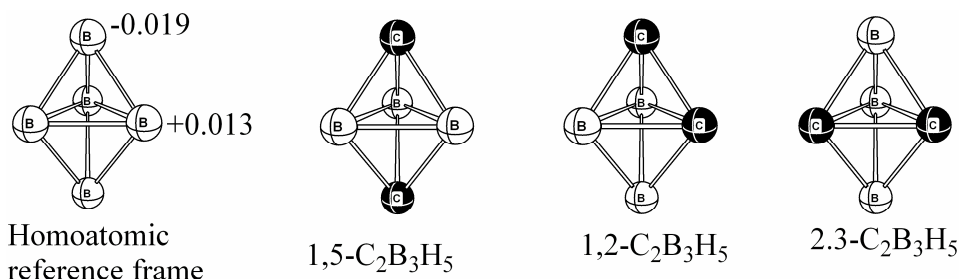


Figure 1.7: The relative stabilities of 1,5-, 1,2- and 2,3- $C_2B_3H_5$ isomers can be predicted with the help of Mulliken Charges of the Homoatomic reference frame.

1.3.3. Ring-Cap Principle

Jemmis and Schleyer²² extended the planar $(4n + 2)$ Hückel rule to the aromaticity of three-dimensional delocalized systems using the “six interstitial electron” concept. They pointed to the need of orbital overlap compatibility. The radial extension of the π -orbitals of the capping atom should optimally match the ring size. *closo*-Carboranes that can be formally divided into rings and caps follow a six-electron rule. The relative stabilities of various isomers for a given carborane depend on the size of the ring on which the polyhedral structure is based. With three- and four-membered rings the CH group fits in as the best cap; the overlap of the orbitals of CH with the orbitals of three- and four-membered borocycles is favorable. The BH group with more diffuse orbitals overlaps better with the orbitals of a five-membered ring. Thus, *closo*-1- $[CB_6H_7]^-$ is less stable than *closo*-2- $[CB_6H_7]^-$ because in the former, the H-C cap combines with a five-membered ring, while in the latter, the H-C cap is attached to a four-membered ring. More diffuse orbitals such as those of BeH, Li, and transition-metal fragments should stabilize polyhedra based on six-membered rings.

1.3.4. Tight Bond with Adjacent Matrix (TBAM) approach

The tight bond with adjacent matrix (TBAM) approach²³ is based on bond energies and electronegativities of adjacent atoms and can be used to predict the relative stabilities of various positional isomers in a given heteronuclear *closo*-icosahedral borane clusters. Given the knowledge of

²² a) Jemmis, E. D. *J. Am. Chem. Soc.* **1982**, *104*, 7017-7020. b) Jemmis, E. D.; Schleyer, P. v. R. *J. Am. Chem. Soc.* **1982**, *104*, 4781-4788.

²³ Teo, B. K.; Strizhev, A. *Inorg. Chem.* **2002**, *41*, 6332-6342.

the number of bonds of each kind and the assumption that only the nearest neighbor interactions (i.e., the bonds) contribute to the cluster's total energy, the "total bond energy" of a cluster can be calculated by summing up the contributions from each type of bond in the cluster which in turn can be obtained by multiplying the numbers of bonds (N_{AA} , N_{BB} , and N_{AB} for a binary system) of each type (AA, BB, and AB, respectively) by the corresponding bond energies (E_{AA} , E_{BB} , and E_{AB} , respectively) within the cluster core, as follows:

$$E_{\text{total}} = N_{AA}E_{AA} + N_{BB}E_{BB} + N_{AB}E_{AB}$$

The bond energies of homonuclear bonds involving main-group elements can be found in the literature.¹ The energy of a heteronuclear bond of type AB can be estimated by the following empirical equation.²³

$$E_{AB} = 1/2(E_{AA} + E_{BB}) + 96.23(\chi_A - \chi_B)^2$$

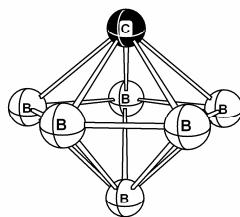
Here, E_{AA} and E_{BB} are the covalent bond energies, and χ_A and χ_B are Pauling's electronegativities²⁴ for the corresponding elements. The second term in the above equation is due to the ionic character of the covalent bond caused by the disparity of the electronegativities of the constituents.

Knowing the energies of homonuclear (AA and BB) and heteronuclear (AB) bonds, the energies of clusters can be calculated. One limitation of this approach is that it cannot differentiate between 1,7- and 1,12-isomers of A_2B_{10} clusters. Moreover, relative stabilities can be evaluated only for octahedral or icosahedral structures, as they have all equivalently connected vertexes.

1.4. Heteroatom Placement in *nido*-Clusters.

Williams' qualitative rules are sufficient for the heteroatom placement in *closo*-carboranes. However, less symmetric *nido*-clusters afford large number of possible isomers mainly due to open face hydrogen atom positions and a possible incorporation of up to four carbon atoms. In order to correctly predict the relative stabilities of various isomeric *nido*-heteroboranes, some more rules are needed. Such quantitative rules (structural increments or energy penalties) governing heteroatom and hydrogen atom

closo-1-[CB₆H₇]⁻



closo-2-[CB₆H₇]⁻

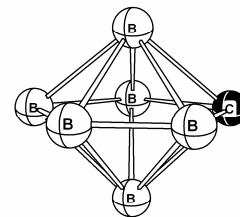


Figure 1.8: Ring-cap Principle: The H-C cap fits best with the four membered ring as in *closo*-2-[CB₆H₇]⁻ which is thermodynamically most stable than the *closo*-1-[CB₆H₇]⁻, in which H-C cap overlaps a five membered ring.

²⁴ Pauling, L. *The Nature of the Chemical Bond*, 3rd ed.; Cornell University Press: Ithaca, NY, 1960.

1. INTRODUCTION

placement permit the prediction of correct relative stability orders of various 6-,²⁵ 10-²⁶ and 11-vertex *nido*-boron hydride, carborane and heteroborane structures.²⁷ Specific architectural features, recognized to be unfavorable, are assigned "energy penalty" values that allow the projection of comprehensive thermodynamic stability values via a simple additivity procedure. These values match the *ab initio*²⁵ or density functional theory^{26,27} results with surprising precision. Some structural features and their corresponding energy penalties for 11-vertex *nido*-carboranes are shown in Figure 1.9. By summing up the energy penalties for each structural feature in a given isomer, the relative stabilities of all possible *nido*-hetero(car)borane isomers for a given formula can be accurately determined.²⁵⁻²⁷

Using this structural increment approach, the relative stabilities of various *nido*-carboranes and hetero(car)boranes can be easily determined. DFT computed relative stabilities of 202 carbon, nitrogen and phosphorus containing 11-vertex *nido*-heteroboranes were quite accurately reproduced using this structural increment approach (Figure 1.10).^{26,27}

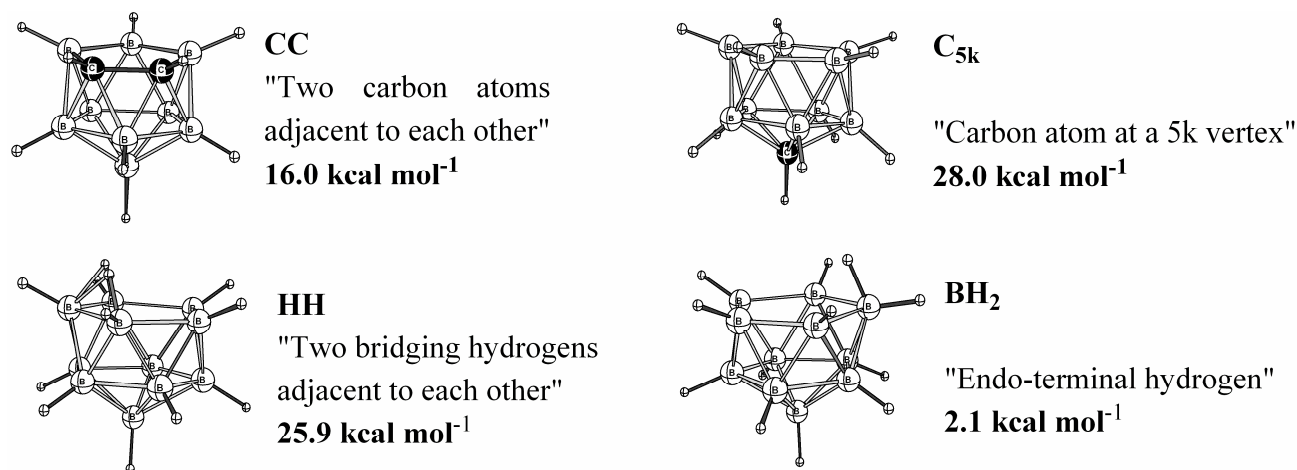


Figure 1.9: Important structural features and corresponding energy penalties (structural increments) for the 11-vertex *nido*-carboranes family.

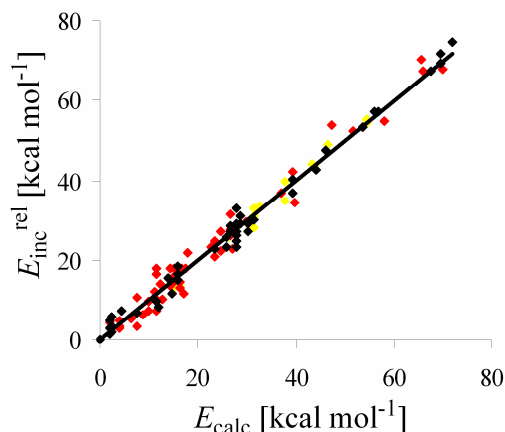
The study of structural increments for 11-vertex *nido*-carboranes resulted in solving a number of conflicts, e.g., the presence of carbon atoms at the position of higher connectivity in experimentally known structures. Structural increments are capable to predict when and how the effect of hydrogen atom placement should dominate that of carbon atom placement. This study also identified

²⁵ Hofmann, M.; Fox, M. A.; Greatrex, R.; Schleyer, P. v. R.; Williams, R. E. *Inorg. Chem.* **2001**, *40*, 1790-1801.

²⁶ Kiani, F. A.; Hofmann, M. *Eur. J. Inorg. Chem.* **2005**, *12*, 2545-2553.

²⁷ a) Kiani, F. A.; Hofmann, M. *Inorg. Chem.* **2004**, *43*, 8561-8571. b) Kiani, F. A.; Hofmann, M. *Inorg. Chem.* **2005**, *44*, 3746-3754.

experimentally unknown *nido*-hetero(car)boranes that are thermodynamically more stable than known positional isomers.²⁵⁻²⁷



Heteroboranes	N _{isomer}	ΔE_{\max}	RMS
Carba-	61	5.6	2.42
Phospha-	95	6.6	2.75
Aza-	46	4.7	2.39
Total	202		

Figure 1.10: Structural increments ($E_{\text{inc}}^{\text{rel}}$) correctly reproduce the DFT computed relative stabilities for 202 11-vertex *nido*-heteroboranes.

1.5. Macropolyhedral Boranes, Jemmis' *mno* Rule and its Limitations.

A large number of homonuclear as well as heteronuclear boranes with more than one cluster unit is experimentally known. They exhibit different architectural patterns, i.e., those with cluster units joined by a two center-two electron,²⁸ or by a three center-two electron bond,²⁹ as well as those in

Electron count by *mno* rule
 $m = 2$
 $n = 18$
 $p = 2$
 Sum = 22 electron pairs

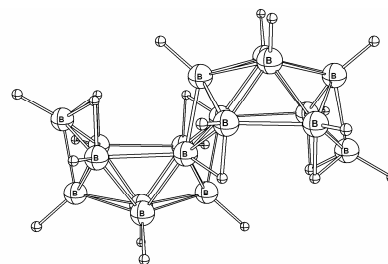


Figure 1.11: Application of the *mno* rule to $B_{18}H_{22}$ macropolyhedral borane structure

which cluster units share one vertex, e.g., $B_{14}H_{22}$,³⁰ two vertexes, e.g., $B_{18}H_{22}$,³¹ three vertexes, e.g., $B_{20}H_{18}L_2$ compounds,³² or even four vertexes, e.g., $B_{20}H_{16}$.² Nevertheless, these so-called

²⁸ See for example, a) Srinivas, G. N.; Hamilton, T. P.; Jemmis, E. D.; McKee, M. L.; Lammertsma, K. *J. Am. Chem. Soc.* **2000**, *122*, 1725-1728. b) Hawthorne, M. F.; Pilling, R. L.; Stokely, P. F.; Garrett, P. M. *J. Am. Chem. Soc.* **1963**, *85*, 3704-3705. c) Hawthorne, M. F.; Pilling, R. L.; Stokely, P. F. *J. Am. Chem. Soc.* **1965**, *87*, 1893-1899. d) Watson-Clark, R. A.; Knobler, C. B.; Hawthorne, M. F. *Inorg. Chem.* **1996**, *35*, 2963-2966.

²⁹ See for example, Hawthorne, M. F.; Pilling, R. L. *J. Am. Chem. Soc.* **1966**, *88*, 3873-3874.

³⁰ Rathke, J.; Schaeffer, R. *Inorg. Chem.* **1974**, *13*, 3008-3011.

³¹ Simpson, P. G.; Lipscomb, W. N. *J. Chem. Phys.* **1963**, *39*, 26-34.

macropolyhedral boranes still remain a large area to be explored³³ both theoretically as well as experimentally. Except for Jemmis' *mno* rule³⁴ that gives the skeletal electron requirement for macropolyhedral boranes, no considerable theoretical work has ever been done in the field. According to the *mno* rule, $m + n + o + p$ number of electron pairs are necessary for a macropolyhedral system to be stable. Here, m is the number of polyhedra, n is the number of vertexes, o is the number of single-vertex-sharing condensations and p is the number of missing vertexes. For *nido* and *arachno* arrangements, one and two additional pairs of electrons are required. Wade's $n + 1$ rule is a special case of the *mno* rule, where $m = 1$ and $o = 0$. B₂₀H₁₆ (Figure 1.2b), for example has $m = 2$ and $n = 20$, leading to 22 electron pairs. Application of the *mno* rule to B₁₈H₂₂ (Figure 1.11)³⁵ results in a total of 22 skeletal electron pairs as $m = 2$, $n = 18$ and $p = 2$. The generality of the *mno* rule was demonstrated by applying it to a variety of known macropolyhedral boranes and heteroboranes.³⁴

However, unlike Wade's skeletal electron count principle for single clusters, which associates the number of skeletal electrons with definite cluster shapes, the *mno* rule does not specify architectures or cluster shapes based on the given number of skeletal electrons. As a result it is impossible to decide which structure out of a large number of possibilities is the preferred target for synthesis or is the thermodynamically most stable one.

1.6. Focus of Current Research Work

1.6.1. A Simple Approach to Derive Structural Increments for *nido*- and *closo*-Heteroboranes

Structural increment studies for various *nido*-heteroboranes obtained so far are highly accurate but need the computations of a large number of isomers. In this thesis, a simple approach is applied in which the structural increment for a given disfavoring structural feature is obtained by computing two isomers differing only with respect to one particular structural feature. The simplified approach successfully

³² See for example, a) Enemark, J. H.; Friedman, L. B.; Lipscomb, W. N. *Inorg. Chem.* **1966**, *5*, 2165-2173. b) Cheek, Y. M.; Greenwood, N. N.; Kennedy, J. D.; McDonald, W. S. *J. Chem. Soc., Chem. Commun.* **1982**, *1*, 80-81.

³³ a) Kennedy, J. D. In *Advances in Boron Chemistry*; Siebert, W., Ed.; Royal Society of Chemistry: Cambridge, U.K., 1997; p 451. b) Grimes, R. N. In *Metal Interactions with Boron Clusters*; Plenum Press: New York, 1982. c) McGrath, T. D.; Jelinek, T.; Stibr, B.; Thornton-Pett, M.; Kennedy, J. D. *J. Chem. Soc., Dalton Trans.* **1997**, *15*, 2543-2545.

³⁴ a) Jemmis, E. D.; Balakrishnarajan, M. M.; Pancharatna, P. D.; *J. Am. Chem. Soc.* **2001**, *123*, 4313-4323. b) Jemmis, E. D.; Balakrishnarajan, M. M.; Pancharatna, P. D. *Chem. Rev.* **2002**, *102*, 93-144.

³⁵ Two isomers C₂ and C_i symmetry and two-vertex sharing pattern, each with two 10-vertex *nido*-cluster fragments are experimentally known. See a) Pitochelli, A. R.; Hawthorne, M. F. *J. Am. Chem. Soc.* **1962**, *84*, 3218. b) Simpson, P. G.; Lipscomb, W. N. *J. Chem. Phys.* **1963**, *39*, 26-34. c) Simpson, P. G.; Lipscomb, W. N. *Proc. Natl. Acad. Sci. U.S.A.* **1962**, *48*, 1490-1491.

applies to various 11-vertex *nido*-heteroboranes to predict their relative stabilities (Chapter 3) and can be extended to the 12-vertex *closo*-cluster to reproduce the relative stabilities of various 11-vertex *nido*- and 12-vertex *closo*-clusters with a single set of increments. The thermodynamically most stable 12-vertex *closo* $\text{Het}_2\text{B}_{10}\text{H}_{10}$ isomers (where Het = heteroatom) with two small, more electronegative heteroatoms have heteroatoms at para positions (Williams rule), while those with large less electronegative heteroatoms occupy ortho positions (Chapter 4). Various CpM groups (Cp = cyclopentadienyl, M = a group-8, -9 or -10 metal) in the 12-vertex *closo*-cyclopentadienyl metallaheteroboranes have specific ortho, meta and para directing effects to other cluster heteroatoms (Chapter 5).

1.6.2. Quantum Chemical Studies of Macropolyhedral Boranes

Computational studies were carried out to determine the turning point from smaller *nido*-single cluster boranes to isomeric *nido:nido*-macropolyhedral boranes in terms of thermodynamic stability. The studied *nido:nido*-macropolyhedral boranes include a large number of two vertex sharing macropolyhedral boranes.^{34b,35} Structures of two vertex sharing macropolyhedral boranes can be classified according to the cluster shape of fused clusters: i.e. *nido:nido*-, *arachno:nido*- and *arachno:arachno*- macropolyhedral boranes (Chapter 6). A cluster increment system was proposed for various macropolyhedral boranes with two units of different cluster sizes fused through two vertexes. The relative stabilities for the macropolyhedral boranes can be easily estimated by using an increments specific for each cluster fragment (Chapter 7). For a given number of vertexes (n), the thermodynamically most stable *nido:nido*- B_nH_{n+4} macropolyhedral borane isomer is structurally related to the thermodynamically most stable *arachno:nido*- $\text{B}_{n-1}\text{H}_{n+5}$ and *arachno:arachno*- $\text{B}_{n-2}\text{H}_{n+6}$ isomers through successive removal of one open face vertex (Chapter 8).

2. Computational Details

All the geometry optimizations, single point energies and frequency calculations were carried out using the Gaussian 98 and 03 programs.¹ Basis sets and/or additional diffuse or polarization functions where used are indicated below, separately for each chapter.

2.1. 11-Vertex *nido*-p-block-Heteroboranes (Chapter 3).

For all hetero(carba)boranes and -borates except stanna, stiba and tellura(carba)boranes and -borates, geometries were consecutively optimized at RB3LYP/3-21G and RB3LYP/6-31G(d). All presented structures are local minima at RB3LYP/6-31G(d). Single point energies were computed at RB3LYP/6-311+G(d,p). Zero point vibrational energies from RB3LYP/6-31G(d) frequency calculations were included to derive the relative energies for all the isomers.

For stanna, stiba and telluraboranes, geometries were optimized at the RB3LYP/LANL2DZ level with additional d-polarization functions² for Sn, Sb, Te, B and C atoms ($\zeta = 0.183, 0.211, 0.237, 0.388,$

¹ a) Frisch, M. J.; Trucks, G. W.; Schlegel, H. B.; Scuseria, G. E.; Robb, M. A.; Cheeseman, J. R.; Zakrzewski, V. G.; Montgomery, J. A., Jr.; Stratmann, R. E.; Burant, J. C.; Dapprich, S.; Millam, J. M.; Daniels, A. D.; Kudin, K. N.; Strain, M. C.; Farkas, O.; Tomasi, J.; Barone, V.; Cossi, M.; Cammi, R.; Mennucci, B.; Pomelli, C.; Adamo, C.; Clifford, S.; Ochterski, J.; Petersson, G. A.; Ayala, P. Y.; Cui, Q.; Morokuma, K.; Malick, D. K.; Rabuck, A. D.; Raghavachari, K.; Foresman, J. B.; Cioslowski, J.; Ortiz, J. V.; Stefanov, B. B.; Liu, G.; Liashenko, A.; Piskorz, P.; Komaromi, I.; Gomperts, R.; Martin, R. L.; Fox, D. J.; Keith, T.; Al-Laham, M. A.; Peng, C. Y.; Nanayakkara, A.; Gonzalez, C.; Challacombe, M.; Gill, P. M. W.; Johnson, B. G.; Chen, W.; Wong, M. W.; Andres, J. L.; Head-Gordon, M.; Replogle, E. S.; Pople, J. A. *Gaussian 98*, revision A.6; Gaussian, Inc.: Pittsburgh, PA, 1998. b) Frisch, M. J.; Trucks, G. W.; Schlegel, H. B.; Scuseria, G. E.; Robb, M. A.; Cheeseman, J. R.; Montgomery, Jr., J. A.; Vreven, T.; Kudin, K. N.; Burant, J. C.; Millam, J. M.; Iyengar, S. S.; Tomasi, J.; Barone, V.; Mennucci, B.; Cossi, M.; Scalmani, G.; Rega, N.; Petersson, G. A.; Nakatsuji, H.; Hada, M.; Ehara, M.; Toyota, K.; Fukuda, R.; Hasegawa, J.; Ishida, M.; Nakajima, T.; Honda, Y.; Kitao, O.; Nakai, H.; Klene, M.; Li, X.; Knox, J. E.; Hratchian, H. P.; Cross, J. B.; Bakken, V.; Adamo, C.; Jaramillo, J.; Gomperts, R.; Stratmann, R. E.; Yazyev, O.; Austin, A. J.; Cammi, R.; Pomelli, C.; Ochterski, J. W.; Ayala, P. Y.; Morokuma, K.; Voth, G. A.; Salvador, P.; Dannenberg, J. J.; Zakrzewski, V. G.; Dapprich, S.; Daniels, A. D.; Strain, M. C.; Farkas, O.; Malick, D. K.; Rabuck, A. D.; Raghavachari, K.; Foresman, J. B.; Ortiz, J. V.; Cui, Q.; Baboul, A. G.; Clifford, S.; Cioslowski, J.; Stefanov, B. B.; Liu, G.; Liashenko, A.; Piskorz, P.; Komaromi, I.; Martin, R. L.; Fox, D. J.; Keith, T.; Al-Laham, M. A.; Peng, C. Y.; Nanayakkara, A.; Challacombe, M.; Gill, P. M. W.; Johnson, B.; Chen, W.; Wong, M. W.; Gonzalez, C.; and Pople, J. A.; *Gaussian 03*, Revision B.03, Gaussian, Inc., Pittsburg, PA 2003.

² Huzinaga, S.; Andzelm, J.; Gaussian basis sets for molecular calculations. Elsevier, Amsterdam, 1984, pp 23-25

0.600, respectively). Single point energies were determined at B3LYP/SDD together with p-polarization function for H ($\zeta = 1.000$) and d-polarization function for Sn, Sb, Te, B and C² along with an sp set of diffuse functions for Sn, Sb, Te ($\zeta = 0.0231, 0.0259, 0.0306$, respectively)³ as well as for B and C ($\zeta = 0.0315$ and 0.0438 , respectively).⁴

2.2. The Relative Stabilities of 11-Vertex *nido*- and 12-Vertex *closo*-Heteroboranes and –borates: Facile Estimation by Structural or Connection Increments (Chapter 4).

All structures were optimized at the RB3LYP/LANL2DZ level of density functional theory with d-type polarization functions² for B ($\zeta = 0.388$), Al ($\zeta = 0.198$), Ga ($\zeta = 0.207$), In ($\zeta = 0.160$), Tl ($\zeta = 0.146$), C ($\zeta = 0.600$), Si ($\zeta = 0.262$), Ge ($\zeta = 0.207$), Sn ($\zeta = 0.183$), Pb ($\zeta = 0.164$), N ($\zeta = 0.864$), P ($\zeta = 0.340$), As ($\zeta = 0.293$), Sb ($\zeta = 0.211$) and Bi ($\zeta = 0.185$) followed by frequency calculations and zero point energy calculations at the same level. Single point energies of the optimized geometries were computed at the RB3LYP/SDD level with additional d-type polarization functions,² p-type polarization function for hydrogen atoms ($\zeta = 1.000$) and an sp set of diffuse functions for B, C, and N ($\zeta = 0.0315, 0.0438$ and 0.0639 , respectively),⁴ for Al, Si and P ($0.0318, 0.0331$ and 0.0348 , respectively)⁵ and for Ga, Ge, As, In, Sn, Sb, Tl, Pb and Bi ($0.0205, 0.0222, 0.0287, 0.0223, 0.0231, 0.0259, 0.0170, 0.0171$ and 0.0215 , respectively).³ The relative energies reported for isomeric structures correspond to the RB3LYP/SDD//RB3LYP/LANL2DZ+ZPE level.

2.3. Ortho-, Meta- and Para-Directing Influence of Transition Metal Fragments in 12-vertex *closo*-Cyclopentadienyl Metallaheteroboranes: Additive Nature of Structural Increments (Chapter 5).

Geometry optimizations, frequency calculations and zero point energy computations of various [CpMP_xC_yB_{11-(x+y)}H_{11-x}]^{z-} metallaboranes (where M = Fe, Co, Ni) were performed at the RB3LYP/6-31G(d) level, followed by single point energy calculations at the RB3LYP/6-311+G(d,p) level. For M = Ru, Os, Rh, Ir, Pd and Pt, the structures were optimized at the RB3LYP/LANL2DZ level using d-polarization functions for B, C and P ($\xi = 0.388, 0.600, 0.340$, respectively)² with frequency and zero point energy calculations at the same level. Single point energies were determined at RB3LYP/SDD with additional p-type polarization functions for Ru, Os, Rh, Ir, Pd, Pt and H ($\xi = 0.081, 0.077, 0.086, 0.081, 0.091, 0.086$ and 1.000)² and d-polarization functions for B, C and P.²

³ These values were optimized for the atomic ground state anion, using ROHF with a flexible ECP basis set, by Ted Packwood at NDSU. Diffuse functions for these and other heteroatoms may be found at the website: <http://phoenix.liu.edu/~nmatsuna/gamess/refs/basis.refs.html>

⁴ Clark, T.; Chandrasekhar, J; Spitznagel, G. W.; Schleyer, P. v. R.; *J. Comput. Chem.* **1983**, *4*, 294-301

⁵ Spitznagel, G. W. Diplomarbeit, Erlangen, **1982**.

2.4. Which *nido:nido*-Macropolyhedral Boranes are Most Stable (Chapter 6)?

2.4.1. Construction of *nido*-single clusters

Basic skeletons for single *nido*-polyhedral borane clusters with the number of vertexes, $n = 4-19$ were obtained by removing one highest coordinate vertex⁶ from *closo*-deltahedra with five to 20 vertexes. The structures for five to 12 vertex *closo*-clusters are most spherical deltahedra and are well known from experiments.⁷ For 13-17 vertexes, the optimized *closo*-geometries reported by Schleyer, Najafian and Mebel were used.⁸ Metal free thirteen⁹ and fourteen¹⁰ vertex *closo*-carboranes have been recently synthesized. The *closo*-structures with 14 and 15 vertexes correspond to deltahedra proposed by Frank and Kasper.¹¹ For 16-vertexes, the *closo*-polyhedron with two squares proposed in ref. 8 which is thermodynamically more stable than that proposed by Frank and Kasper¹¹ or by Brown and Lipscomb¹² was used. For 18 through 20 vertexes, various *closo*-clusters were computed and the *nido*-structures were obtained by removal of the highest coordinate vertex from the most stable *closo*-deltahedra. The skeleton of a 19-vertex *nido*-deltahedron was obtained by optimizing a D_{6d} symmetric *closo*-[B₂₀H₂₀]²⁻ structure as proposed by Brown and Lipscomb.¹² Addition of four hydrogen atoms to edges of the open face of these basic skeletons resulted in numerous *nido*-B_nH_{n+4} isomers. The energy of each most stable *nido*-B_nH_{n+4} ($n = 4-19$) structure was compared with the most stable isomeric *nido:nido*-macropolyhedral borane.

2.4.2. Construction of *nido:nido*-Macropolyhedral Borane Clusters.

Different *nido* single cluster boranes were used as building blocks for two vertex sharing *nido:nido*-macropolyhedral boranes. Formally, two vertex sharing *nido:nido*-macropolyhedra result from the

⁶ A *nido*-B₁₂H₁₆ starting *nido*-geometry derived from a 13-vertex *closo* cluster by the removal of a 5-coordinate rather than 6-coordinate vertex was also optimized but converged to a macropolyhedron. However, a similar starting geometry for [B₁₂H₁₅]⁻ persisted.

⁷ a) Muetterties, E. L.; Boron Hydride Chemistry, Academic Press, New York, N. Y. 1975, pp12-16. b) Wade, K. Chem. Br., **1975**, *11*, 177-183. c) Wade, K. *Adv. Inorg. Chem. Radiochem.* **1976**, *18*, 1-66. d) Lipscomb, W. N. Boron Hydrides, Benjamin, W. A., New York, N. Y., 1963. pp 13-15 and 19-24.

⁸ Schleyer, P. v. R.; Najafian, K.; Mebel, A. M. *Inorg. Chem.* **1998**, *37*, 6765-6772.

⁹ a) Burke, A.; Ellis, D.; Giles, B. T.; Hodson, B. E.; Macgregor, S. A.; Rosair, G. M.; Welch, A. J. *Angew. Chem. Intl. Ed.* **2003**, *42*, 225-228. b) Grimes; R. N.; *Angew. Chem.* **2003**, *115*, 1232; *Angew. Chem. Intl. Ed.* **2003**, *42*, 1198-1200.

¹⁰ Deng, L.; Chan, H. S.; Xie, Z. *Angew. Chem., Int. Ed.* **2005**, *44*, 2128-2131.

¹¹ Frank, F. C.; Kasper, J. S. *Acta Crystallogr.* **1958**, *11*, 184-190.

¹² Brown, L. D.; Lipscomb, W. N. *Inorg. Chem.* **1977**, *16*, 2989-2996.

2. COMPUTATIONAL DETAIL

condensation reaction of two *nido*-boranes releasing B_2H_6 . Hence, the number of vertexes of a given macropolyhedron is always two less than the sum of number of vertexes of the two *nido*-clusters that build it up. Sharing of two vertexes between any two *nido* single clusters (**3** – **12**) results in a number of possible *nido:nido*-macropolyhedral combinations for each B_nH_{n+4} formula. For example, for *nido:nido*- $B_{14}H_{18}$, the following combinations are possible; *nido*(8):*nido*(8)-, *nido*(7):*nido*(9)-, *nido*(6):*nido*(10)-, *nido*(5):*nido*(11)-, *nido*(4):*nido*(12)- $B_{14}H_{18}$. For any of these options, there are more than one choice of connecting sites and different bridging hydrogen positions on the open face. Hence a large number of structural isomers is possible.

Starting *nido*-geometries derived from *closo* clusters were initially optimized with density functional theory methods at the RB3LYP/3-21G level. Further geometry optimization as well as frequency calculations for the most stable RB3LYP/3-21G optimized *nido*-geometries as well as isomeric *nido:nido*-macropolyhedral starting geometries were performed at RB3LYP/6-31G(d) with symmetry restrictions, where applicable. Only a few macropolyhedral *nido:nido*-structures belong to symmetry point groups higher than C_1 . Finally, single point energies were computed at RB3LYP/6-311+G(d,p). All the structures presented in this paper are local minima at RB3LYP/6-31G(d). Relative energies reported for all the B_nH_{n+4} and $[B_nH_{n+3}]^-$ isomers considered for $n = 4-19$, correspond to the RB3LYP/6-311+G(d,p)//RB3LYP/6-31G(d)+ZPE level of theory.

2.5. Cluster Increment System for Macropolyhedral Boranes (Chapter 7)

The macropolyhedral borane clusters were constructed by sharing two vertexes between the individual cluster fragments. Two individual cluster fragments, due to different possible connecting sites or due to different bridging open face hydrogen positions, may give rise to more than one possible isomer. Resulting geometries were optimized initially at the RB3LYP/3-21G level within symmetry restrictions, where applicable. Further geometry optimization and frequency determinations were performed at the RB3LYP/6-31G(d) level. Single point energies were determined at RB3LYP/6-311+G(d,p) level. The relative energies reported here are the RB3LYP/6-311+G(d,p)//RB3LYP/6-31G(d)+ZPE energies, where ZPE denotes zero point energy corrections.

The most stable isomers, which in each case, were used to derive cluster increments. All cluster fragments were initially given arbitrary increments with respect to a zero increment for one cluster of their own kind. The increments were assigned to *nido*-clusters with respect to zero increment for 10-vertex *nido*-cluster and to *arachno*-clusters with respect to zero increment for 5-vertex *arachno*-fragment. A statistical fitting procedure resulted in more accurate cluster increments which reproduce the DFT computed relative stabilities of various macropolyhedral boranes within 6 kcal mol⁻¹ limit.

2.6. Structural Relationships among Two Vertex Sharing Macropolyhedral Boranes (Chapter 8).

Different starting geometries for each particular mono- or macropolyhedral borane were first optimized at RB3LYP/3-21G using the Gaussian 03 program.^{1b} The most stable clusters were subjected to RB3LYP/6-31G* geometry optimization. Geometries for most macropolyhedral boranes belong to the C_1 symmetry point group. However, a few geometries were optimized with symmetry restrictions. Frequency calculations at the RB3LYP/6-31G* level proved the stationary points to be local minima on the respective potential energy surfaces. Single point energies were computed at RB3LYP/6-311+G**. The final relative energies were corrected for zero point vibrational energies computed at the RB3LYP/6-31G*.

The geometries of various *arachno*- B_nH_{n+6} ($n = 4-18$) were obtained by the removal of one most highly coordinated vertex from the respective parent *nido*-clusters ($n = 5-19$, Chapter 6). Placement of six open face endo-hydrogen atoms resulted in numerous isomers. Similarly, initial *hypho*- B_nH_{n+8} ($n = 4-17$) geometries were obtained by the removal of another most highly coordinated vertex from *arachno*-clusters followed by open face hydrogen atom placement.

Two vertex sharing macropolyhedral boranes are formally obtained by the fusion of two polyhedral clusters releasing a B_2H_6 unit. Therefore, macropolyhedral boranes have two vertexes less than the sum of the number of vertexes of individual clusters. Different open face edges may contribute the shared vertexes connecting the two individual units, resulting in numerous skeletal isomers. The different distribution patterns of open face bridged (or endo-terminal) hydrogen atoms produces even larger number of isomers. In most *arachno:nido*-macropolyhedral boranes, the more open *arachno*-part contains five open face hydrogen atoms in addition to three open face hydrogen atoms on the *nido*-part. However, in some cases, one hydrogen atom of the *arachno*-part is attached as an exo-substituent to one boron atom of the shared B_2 unit. One or two hydrogen atoms in the *arachno:arachno*-macropolyhedral boranes may also be exo-substituted to one or two boron atoms of the shared B_2 unit.

3. Periodic Trends and Easy Estimation of Relative Stabilities in 11-Vertex *nido*-p-block-Heteroboranes and -borates

3.1. Introduction

The 11-vertex *nido*-cluster represents the most diverse family of heteroboranes and -borates. Many reactions are known,¹ to incorporate a hetero fragment into a smaller *nido*- or *arachno*- cluster leading to 11-vertex *nido*-heteroboranes. Removal of one vertex from a 12-vertex *closo*-heteroborane cluster also leads to 11-vertex *nido*-heteroboranes and -borates.^{1a,2} Experimentally known 11-vertex *nido*-heteroborane and -borate clusters include group 14 heteroatoms, i.e., carbon,³ silicon,⁴ germanium⁵ and tin^{3b-c,6} group-15 heteroatoms, i.e., nitrogen, phosphorus,^{1a-b} arsenic^{2b,7} and antimony,⁸ group 16

¹ For example see a) Štibr, B. *Collect. Czech. Chem. Commun.*, **2002**, *67*, 843-868; references therein. b) Haubold, W. ; Keller, W. ; Sawitzki, G.; *Angew. Chem., Int. Ed. Engl.* **1988**, *27*, 925. c) Shedlow, A. M.; Sneddon, L. G. *Inorg. Chem.* **1998**, *37*, 5269-5277.

² For example see a) Todd, L. J.; Little, J. L.; Silverstein, H. T. *Inorg. Chem.* **1969**, *8*, 1698-1703. b) Little, J. L.; Whitesell, M. A.; Chapman, R. W.; Kester, J. G.; Huffman, J. C.; Todd, L. J. *Inorg. Chem.* **1993**, *32*, 3369-3372.

³ For example see a) Williams, R. E. *Chem. Rev.* **1992**, *92*, 177-207; references therein. b) Fox, M. A.; Goeta, A. E.; Hughes A. K.; Johnson, A. L. *J. Chem. Soc. Dalton Trans.* **2002**, *9*, 2009-2019. c) Fox, M. A.; Greatrex, R.; Nikrahi, A.; Brain, P. T.; Picton, M. J.; Rankin, D. W. H.; Robertson, H. E.; Bühl, M.; Li, L.; Beaudet, R. A. *Inorg. Chem.* **1998**, *37*, 2166-2176. d) Dirk, W.; Paetzold, P.; Radacki, K. Z. *Anorg. Allg. Chem.* **2001**, *627*, 2615-2618.

⁴ a) Dopke, J. A.; Bridges, A. N.; Schmidt, M. R., Gaines, D. F. *Inorg. Chem.*, **1996**, *35*, 7186-7187. b) Wesemann, L.; Englert, U.; Seyferth, D. *Angew. Chem.*, **1995**, *107*, 2345-2436; *Angew. Chem., Int. Ed. Engl.*, **1995**, *34*, 2236-2238. c) Dopke, J. A.; Powel, D. R.; Hayashi, R. K., Gaines, D. F. *Inorg. Chem.*, **1998**, *37*, 4160-4161.

⁵ a) Wesemann, L.; Trinkaus, M.; Ruck, M. *Angew. Chem., Int. Ed.* **1999**, *38*, 2375-2377. b) Wesemann, L.; Ramjoie, Y.; Trinkaus, M.; Spaniol, T. P. *Eur. J. Inorg. Chem.* **1998**, *9*, 1263-1268. c) Wesemann, L.; Ramjoie, Y.; Trinkaus, M.; Ganter, B. *Inorg. Chem.* **1997**, *36*, 5192-5197. d) Loffredo, R. E.; Norman, A. D. *J. Am. Chem. Soc.* **1971**, *93*, 5587-5588.

⁶ a) Greenwood, N. N.; Youll, B. *J. Chem. Soc., Dalton Trans.* **1975**, *2*, 158-162. b) Dupont, T. J.; Loffredo, R. E.; Haltiwanger, R. C.; Turner, C. A.; Norman, A. D. *Inorg. Chem.* **1978**, *17*, 2062-2067. c) Loffredo, R. E.; Dupont, T. J.; Haltiwanger, R. C.; Norman, A. D. *J. Chem. Soc., Chem. Commun.*

3. 11-VERTEX NIDO HETEROBORANES

heteroatoms, i.e., sulfur,⁹ selenium¹⁰ and tellurium.^{10a-c,11} Williams' qualitative rules predict isomers with low coordinate heteroatoms and separated heteroatoms to be preferred.^{3a,12} While these rules

1977, 4, 121-122. d) Loffredo, R. E.; Drullinger, L. F.; Slater, J. A.; Turner, C. A.; Norman, A. D. *Inorg. Chem.* **1976**, 15, 478-480.

⁷ a) Todd, L. J.; Burke, A. R.; Garber, A. R.; Silverstein, H. T.; Storhoff, B. N. *Inorg. Chem.*, **1970**, 9, 2175-2179. b) Bould, J.; Kennedy, J. D.; Ferguson, G.; Tony D. F.; O'Riordan, G. M.; Spalding, T. R. *Dalton Trans.* **2003**, 23, 4557-4564. c) O'Connell, D.; Patterson, J. C.; Spalding, T. R.; Ferguson, G.; Gallagher, J. F.; Li, Y.; Kennedy, J. D.; Macias, R.; Thornton-Pett, M.; Holub, J. *J. Chem. Soc., Dalton Trans.* **1996**, 15, 3323-3333. d) Fontaine, X. L. R.; Kennedy, J. D.; McGrath, M.; Spalding, T. R. *Magn. Reson. Chem.* **1991**, 29, 711-720. e) Wright, W. F.; Garber, A. R.; Todd, L. J. *J. Magn. Reson.* **1978**, 30, 595-602. f) Little, J. L.; Pao, S. S. *Inorg. Chem.* **1978**, 17, 584-587. g) Little, J. L.; Pao, S. S.; Sugathan, K. K. *Inorg. Chem.* **1974**, 13, 1752-1756. h) Hanusa, T. P.; Roig de Parisi, N.; Kester, J. G.; Arafat, A.; Todd, L. J. *Inorg. Chem.* **1987**, 26, 4100-4102. i) Little, J. L. *Inorg. Chem.* **1979**, 18, 1598-1600. j) Yamamoto, T.; Todd, L. J. *J. Organomet. Chem.* **1974**, 67, 75-80. k) Colquhoun, H. M.; Greenhough, T. J.; Wallbridge, M. G. H. *J. Chem. Research*, **1979**, 7, 248.

⁸ Valnot, J. Y. *Synthesis* **1978**, 8, 590-592.

⁹ Pretzer, W. R.; Rudolph, R. W. *J. Am. Chem. Soc.* **1976**, 98, 1441-1447.

¹⁰ a) Ferguson, G.; Gallagher, J. F.; McGrath, M.; Sheehan, J. P.; Spalding, T. R.; Kennedy, J. D. *J. Chem. Soc., Dalton Trans.* **1993**, 1, 27-34. b) Ferguson, G.; Parvez, M.; MacCurtain, J. A.; Dhubhghaill, O. N.; Spalding, T. R.; Reed, D. *J. Chem. Soc., Dalton Trans.* **1987**, 4, 699-704. c) Little, J. L.; Friesen, G. D.; Todd, L. J. *Inorg. Chem.* **1977**, 16, 869-872. d) Faridooon; Dhubhghaill, O. N.; Spalding, T. R.; Ferguson, G.; Kaitner, B.; Fontaine, X. L. R.; Kennedy, J. D. *J. Chem. Soc., Dalton Trans.* **1989**, 9, 1657-1668. e) Ferguson, G.; Hampden-Smith, M. J.; Dhubhghaill, O. Ni; Spalding, T. R. *Polyhedron* **1988**, 7, 187-193. f) Barriola, A. M.; Hanusa, T. P.; Todd, L. J. *Inorg. Chem.* **1980**, 19, 2801-2802. g) Reed, D.; Ferguson, G.; Ruhl, B. L.; Dhubhghaill, O. N.; Spalding, T. R. *Polyhedron*, **1988**, 7, 17-23.

¹¹ a) Faridooon; S., Trevor R.; Ferguson, G.; Kennedy, J. D.; Fontaine, X. L. R. *J. Chem. Soc., Chem. Commun.* **1989**, 14, 906-908. b) Faridooon, O.; Dhubhghaill, O. Ni; Spalding, T. R.; Ferguson, G.; Kaitner, B.; Fontaine, X. L. R.; Kennedy, J. D. *J. Chem. Soc., Dalton Trans.* **1988**, 11, 2739-2745. c) Thornton-Pett, M.; Kennedy, J. D.; Spalding, F.; Spalding, T. R. *Act. Cryst.* **1995**, C51, 840-843. d) Ferguson, G.; O'Connell, D.; Spalding, T. R. *Act. Cryst.* **1994**, C50, 1432-1434. e) Ferguson, G.; Gallagher, J. F.; Sheehan, J. P.; Spalding, T. R.; Kennedy, J. D.; Macias, R. *J. Chem. Soc., Dalton Trans.* **1993**, 20, 3147-3148. f) Sheehan, J. P.; Spalding, T. R.; Ferguson, G.; Gallagher, J. F.; Kaitner, B.; Kennedy, J. D. *J. Chem. Soc., Dalton Trans.* **1993**, 1, 35-42. g) Faridooon; McGrath, M.; Spalding, T. R.; Fontaine, X. L. R.; Kennedy, J. D.; Thornton-Pett, M. *J. Chem. Soc., Dalton Trans.* **1990**, 6, 1819-1829. h) Ferguson, G.; Lough, A. J.; Faridooon; McGrath, M. N.; Spalding, T. R.; Kennedy, J. D.; Fontaine, X. L. R. *J. Chem. Soc., Dalton Trans.* **1990**, 6, 1831-1839. i) Ferguson, G.; Gallagher, J. F.; Sheehan, J. P.; Spalding, T. R. *J. Organomet. Chem.* **1998**, 550, 477-480. j) Ferguson, G.; Kennedy, J. D.; Fontaine, X. L. R.; Faridooon; S., Trevor, R. *J. Chem. Soc., Dalton Trans.* **1989**, 2, 383. k) Mceneaney, P. A.; Spalding, T. R.; Ferguson, G. *J. Chem. Soc., Dalton Trans.* **1997**, 2, 145-147. l) Ferguson, G.; Kennedy, J. D.; Fontaine, X. L. R.; Faridooon; S., Trevor R. *J. Chem. Soc., Dalton Trans.* **1988**, 10, 2555-2564.

suffice to select the most stable *closo*-heteroboranes, the presence of additional endo-hydrogen atoms, the large number of isomers and possibly irresolvable conflicts ask for more sophisticated rules to predict the most favorable isomer in the case of *nido*-clusters.

A set of quantitative rules was presented which reproduced the stability order of 6-vertex *nido*-carboranes on the basis of 15 structural increments.¹³ Disfavoring structural features, e.g. neighboring carbon atoms, were identified and so called energy penalties were derived by a statistical fitting procedure. Applying these energy penalties additively, the stability order of isomeric 6-vertex *nido*-(carba)boranes and -borates can easily be derived by a paper and pencil approach. With only nine such fitted quantitative rules, the relative stability order of numerous 11-vertex *nido*-(carba)boranes and -borates¹⁴ was successfully reproduced. The approach was applied to the 10-vertex *nido*-(carba)boranes and -borates,¹⁵ and to the 11-vertex *nido*-mixed hetero(carba)boranes and -borates¹⁶ with H-C, P, H-P, N and H-N heteroatoms. This work¹³⁻¹⁶ quantified Williams' rules^{3a,12} by corresponding energy penalties for each heteroatom and introduced some more rules due to open face hydrogen characteristics of the *nido*-cluster. These quantitative rules allow not only to predict the thermodynamically most stable isomer but to easily estimate a stability order of various isomers.¹⁴⁻¹⁵ Furthermore, these energy penalties successfully elaborate which two heteroatoms are more favorable choices for adjacent positions in the thermodynamically most stable mixed *nido*-heteroboranes. For example, quantitative rules indicate 7,8,10- rather than 7,8,9-, 7,9,10-, and 7,9,8- positions for the heteroatoms in *nido*-P₂CB₈H₉⁻ to be thermodynamically most stable.¹⁶

Previously, energy penalties (E_{inc}) were determined by statistical fitting to a large number of structures.¹³⁻¹⁶ The procedure gives accurate values but requires extensive computations. Estimated energy penalties, (E_{inc}^{\wedge}), which are the energy difference of two suitable reference structures differing with respect to one structural feature only, are usually very close to the energy penalties arising from

¹² a) Williams, R. E. *Inorg. Chem.* **1965**, *87*, 3513-3515. b) Williams, R. E. *In Progress in Boron Chemistry* Brotherton, R. J., Steinberg, H., Eds.; Pergamon Press: England, 1970; Vol. 2, Chapter 2, p 57.

¹³ Hofmann, M.; Fox, M. A.; Greatrex, R.; Schleyer, P. v. R.; Williams, R. E. *Inorg. Chem.* **2001**, *40*, 1790-1801.

¹⁴ Kiani, F. A.; Hofmann, M. *Inorg. Chem.*, **2004**, *43*, 8561-8571.

¹⁵ Kiani, F. A.; Hofmann, M. *Eur. J. Inorg. Chem.* **2005**, *12*, 2545-2553.

¹⁶ Kiani, F. A.; Hofmann, M. *Inorg. Chem.* **2005**, *44*, 3746-3754.

statistical fitting to a large number of isomers.¹⁶ This is to be expected when structural features behave additively. For instance, the estimated energy penalty for adjacent carbon atoms, i.e., the energy difference of 7,8-C₂B₉H₁₁²⁻ and 7,9-C₂B₉H₁₁²⁻ is 16.3 kcal mol⁻¹, very close to the statistically fitted value (16.0 kcal mol⁻¹) derived from 20 carboranes.^{14,16} Here, the relative stability order ($E_{\text{inc}}^{\text{rel}}$) is presented for 11-vertex *nido*-sila, germana, stanna, arsa, stiba, thia, selena and tellura(carba)boranes and -borates, phosphathiaboranes and -borates and selenathiaboranes produced by E_{inc} which are more approximate but easier to determine and are accurate enough for the interpretation of general trends.

The numbering scheme for the 11-vertex *nido*-cluster is shown in Figure 3.1. The apical position is numbered as 1. The vertices next to the apex (middle belt) are given numbers 2-6, while the vertices of the open face are numbered from 7 to 11 where 7 is connected to 2 and 3. There are six cage vertices with connections to five other cluster atoms, $k_c = 5$ and five peripheral vertices with $k_p = 4$, where, c and p denote cage and peripheral vertices, respectively. In the literature, different numbering patterns have been used for mixed heteroboranes.

3.2. Results and Discussion

3.2.1. Structural Features for Hetero(carba)boranes and -borates.

Different structural features for hetero(carba)boranes and -borates are shown in Figure 3.2 and their energy penalties are listed in Chart 3.1. Energy penalties for carbon in Chart 3.1 are statistically fitted values taken from ref. 14. For all other heteroatoms, the energy penalties are estimated as the energy difference of two structures which differ with respect to one structural feature only.

Het_{5k}(1) and Het_{5k}(2) A heteroatom at a 5k position (1-6) rather than a 4k position (7-11) is indicated by the structural feature Het_{5k}.¹⁶ The apical position (number 1) differs from positions 2-6: the former has only 5k neighbors, the later has two 4k and three 5k neighbors. Hence, higher energy penalties are observed for position 1, i.e., Het_{5k}(1), as compared to positions 2 through 6, i.e., Het_{5k}(2).¹⁶ Estimated Het_{5k}(1) energy penalties for a given heteroatom were obtained by comparing the 7- and 1-isomers of HetB₁₀H₁₀⁽⁶⁻ⁿ⁾⁻ and that of Het_{5k}(2) by comparing 7- and 2- isomers of HetB₁₀H₁₀⁽⁶⁻ⁿ⁾⁻ (Figure 3.2a), where Het = H-C, H-Si, N, H-N, P or H-P etc. and n = number of electrons donated by a given hetero group.

$E_{\text{inc}}^{\text{Het}_{5k}(1)}$ and $E_{\text{inc}}^{\text{Het}_{5k}(2)}$ for different heteroatoms are listed in Chart 3.1. For the carbon atom at a 5k position in heterocarbaboranes, the statistically fitted energy penalty of 28.0 kcal mol⁻¹ obtained

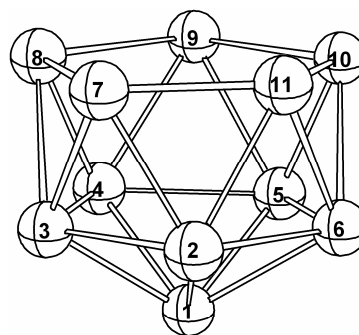


Figure 3.1: Numbering scheme for the 11-vertex *nido*-cluster.

3. 11-VERTEX *NIDO* HETEROBORANES

originally from 11-vertex *nido*-carboranes will be used.¹⁴

HetHet' Heteroatom apart isomers are generally more favorable than heteroatom adjacent isomers in heteroboranes and -borates.^{3a,12,14-16} The structural feature HetHet' gives the amount of destabilization caused by two adjacent heteroatoms. For example 7,8-C₂B₈H₁₀²⁻ with two adjacent carbon atoms (CC) is 16.3 kcal mol⁻¹ less stable than carbon apart 7,9-isomer.^{14,16}

The structural feature HetHet' gives the amount of destabilization caused by two adjacent heteroatoms. For example 7,8-C₂B₈H₁₀²⁻ with two adjacent carbon atoms (CC) is 16.3 kcal mol⁻¹ less stable than carbon apart 7,9-isomer.^{14,16} The estimated energy penalties for HetHet' were obtained by comparing the 7,8- and 7,9-isomers of HetHet' B₉H₉^(8-n-n') (Figure 3.2b), where Het or Het' may be equal or different heteroatoms and n and n' are the number of electrons donated by Het and

Het'. When Het and Het' are three electron donating heteroatoms ($\sum n = 6$), the structures to be compared are dianions, but they are neutral and monoanionic for two four electron donating heteroatoms ($n+n' = 8$) and one three and one four electron donating heteroatom ($n+n' = 7$), respectively. HetHet' energy penalties for two adjacent carbon atoms, CC,¹⁴ and two adjacent phosphorus atoms, PP,¹⁶ are 16.0 and 10.7 kcal mol⁻¹, respectively. HetHet' energy penalties for Het' = Het and for Het' = C are listed in Chart 3.1. The energy

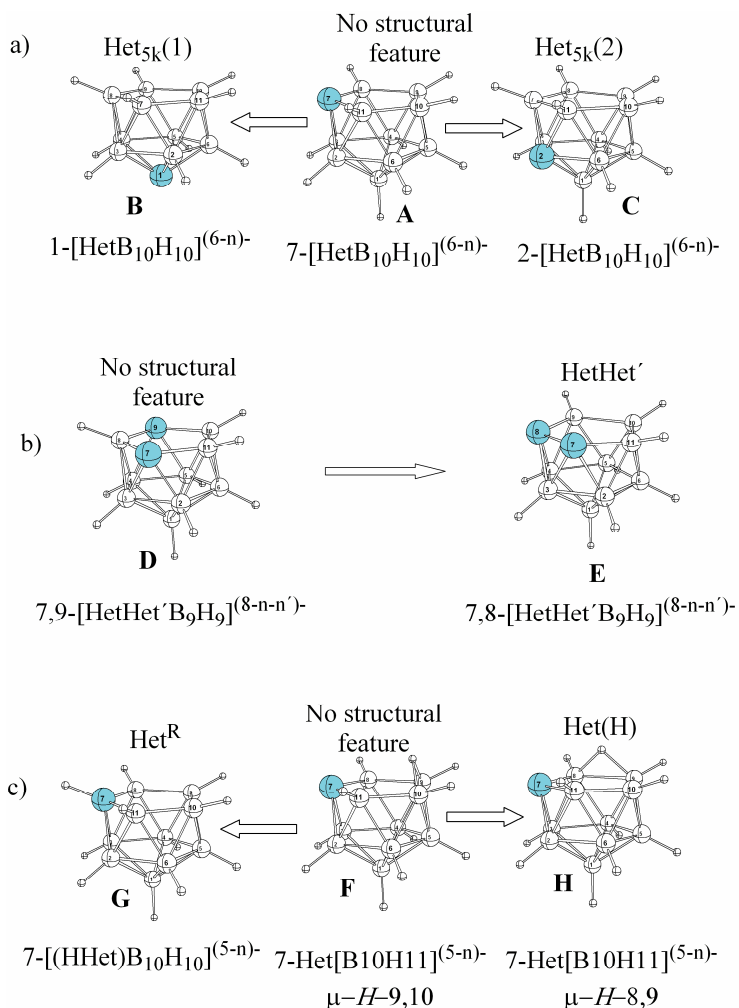


Figure 2: a) A heteroatom (Het) at a 5k apical position (vertex number 1, structure B) or in the middle belt (positions 2 through 6, structure C) rather than at the open face (positions 7 through 11, structure A) represents the structural features Het_{5k}(1) and Het_{5k}(2), respectively. b) Heteroatom adjacent (E) rather than heteroatom apart isomer (D) represent the structural feature HetHet', where Het and Het' may be equal or different heteroatoms. n and n' are the number of electrons donated by heteroatoms Het and Het' c) μ -H-8,9 (hydrogen bridge adjacent to heteroatom, H) rather than μ -H-9,10 (hydrogen bridge far away from heteroatom, F) in *nido*-7-HetB₁₀H₁₁⁽⁵⁻ⁿ⁾⁻, represent the structural feature Het(H). Hydrogen as an exo-substituent (G) rather than bridged between positions 9 and 10 (F) produces the structural feature Het^R.

respectively. HetHet' energy penalties for Het' = Het and for Het' = C are listed in Chart 3.1. The energy

penalties for a heteroatom adjacent to a bare phosphorus atom (HetP) and to an exo-substituted phosphorus atom (HetP^R) are listed in Table 3.1. Very similar energy penalties were derived for CC (i.e., two adjacent carbon atoms) in carboranes (16.0 kcal mol⁻¹),¹⁴ phosphacarbaboranes (18.3 kcal mol⁻¹),¹⁶ exo-substituted azacarbaboranes (15.4 kcal mol⁻¹)¹⁶ and thiocarbaboranes (17.7 kcal mol⁻¹). Hence, an average value of 17.0 kcal mol⁻¹ for $E_{\text{inc}}\text{CC}$ is used in all heterocarbaboranes considered in this work.

Het(H) This structural feature presents the amount of destabilization caused by a heteroatom (Het) adjacent to a hydrogen bridge. Comparing *nido*-7-HetB₁₀H₁₁⁽⁵⁻ⁿ⁾⁻ isomers, (n = number of electrons donated by Het) with μ -H-8,9 and μ -H-9,10 hydrogen positions, directly gives an estimated energy penalty for the structural feature Het(H) (Figure 3.2c). This structural feature has a relatively small destabilizing effect. For example, the energy penalty for C(H) was determined to be 2.2 kcal mol⁻¹ for carboranes.¹⁴ The energy penalties of other heteroatoms adjacent to a hydrogen bridge are listed in Chart 3.1. The largest Het(H) energy penalty (9.4 kcal mol⁻¹) is observed for the four electron donating P^R heterogroup, while tin has the smallest (even negative) energy penalty $E_{\text{inc}}\text{Sn(H)} = -1.7$ kcal mol⁻¹. It is the only negative energy penalty observed for any heteroatom structural features in 11-vertex *nido*-heteroboranes.

Het^R This structural feature allows to compare bare (3-electron donating) and exo-substituted (4-electron donating) group 14 heteroatoms. *nido*-7-HetB₁₀H₁₁²⁻ (μ -H-9,10) and *nido*-7-(HHet)B₁₀H₁₁²⁻ (Figure 3.2c) give a direct estimate of the energy penalty of Het^R for group 15 heteroatoms. Generally, three electron donating nitrogen and phosphorus atoms (N and P) have smaller energy penalties as compared to four electron donating exo-substituted nitrogen and phosphorus (N^R and P^R) atoms.¹⁶ The same is true for bare arsenic (As) and antimony (Sb) atoms in the 11-vertex *nido*-cluster which have generally smaller energy penalties as compared to exo-substituted arsenic (As^R) and antimony (Sb^R) atoms (see Chart 3.1).

3.2.2. Energy Penalties as Periodic Properties of Heteroatoms in 11-Vertex *nido*-Cluster.

In this section, the general trends of HetHet', Het_{5k}(1) and Het_{5k}(2) energy penalties will be discussed.

HetHet and HetC energy penalties decrease along group 14 (C → Sn), 15 (N → Sb) and 16 (S → Te) and increase along the periods (C → N, Si → S, Ge → Se, Sn → Te, see Chart 3.1). The magnitude of energy penalties depends largely upon the extent of electron localization which is determined primarily by the number of electrons donated by a heteroatom and secondarily by the electronegativity of the heteroatom. All the heteroatoms in Chart 3.1 formally donate more than two electrons (two electrons are donated by a BH vertex) to the total of 26 skeletal electrons required in an 11-vertex *nido*-cluster and hence cause stronger electron localization as compared to a BH vertex.

3. 11-VERTEX *NIDO* HETEROBORANES

 Chart 3.1. Relative trends of energy penalties kcal mol⁻¹ for different features in 11-vertex *nido*-hetero(carba)boranes and -borates.

Het ^a		χ^b									
HetHet ^d		r pm ^c		Het _{5k} (1) ^f		Het _{5k} (2) ^g		Het(H) ^h			
HetC ^e											
Group 14			Group 15 (bare)			Group 15(Exo-Substituted)			Group 16		
C	2.55 ⁱ	77	N	3.04	75	N^R	3.04	75	O	3.44 ^j	73
16.0	28.0		40.7	44.3		63.6^k	65.6		---	---	
16.0	28.0		23.4	41.1		36.9	49.9		---	---	
	2.2			0.5			6.7		---	---	
Si	1.90	111	P	2.19	106	P^R	2.19	106	S	2.58	102
8.7	45.0		12.0	31.5		36.9	56.7		45.0^l	52.2	
8.5	33.6		14.7	27.8		20.1	43.1		31.2	43.8	
	4.9			4.3			6.8			6.2	
Ge	2.01	122	As	2.18	119	As^R	2.18	119	Se	2.55	116
4.2	54.2		6.9	32.3		26.8	79.7		35.1	48.2	
7.7	44.2		16.0	28.5		17.3	---		30.3	40.7	
	4.2			3.8			3.4			6.1	
Sn	1.96	141	Sb	2.05	138	Sb^R	2.05	138	Te	2.1	135
3.1	69.7		3.8	31.8		15.8	92.6		29.3	45.0	
2.4	---		15.7	29.0		12.5	26.2		28.6	34.8	
	-1.7			4.5			1.2			6.3	

^a Heteroatom ^b Electronegativity values, see Pauling, L. *The Nature of the Chemical Bond* Cornell University Press: Ithaca, New York, 1960. ^c Covalent radii in pico meter, see Huheey, J. E.; Keiter, E. A.; Keiter R. L. *Inorganic Chemistry: Principles of Structure and Reactivity*, 4th edition, HarperCollins, New York, USA, 1993. ^d The energy penalty for two identical adjacent heteroatoms and ^e the energy penalty for a heteroatom adjacent to a carbon atom in the 11-vertex *nido*-cluster. ^f Het_{5k}(1) is the structural feature for a heteroatom at a 5k apical position (vertex number 1) rather than the ideal 4k open face positions. ^g Het_{5k}(2) is the structural feature for a heteroatom at vertices 2 through 6 rather than at the ideal 4k open face positions. ^h Structural feature Het(H) denotes the amount of destabilization caused by a heteroatom adjacent to a bridged hydrogen atom. ⁱ Statistically fitted values taken from ref. 14. For all other heteroatoms, energy penalties are estimated by comparing two suitable reference structures which differ with respect to one structural feature. ^j Initial starting 11-vertex *nido*-oxaborane geometries did not survive geometry optimizations due to the expected very high energy penalties of the oxygen atom. ^k The N^RN^R energy penalty could not be accurately obtained as the structure rearranged. The rough energy penalty derived by fixing N7-B2 and N8-B2 distances to be 1.775 Å was even higher (76.5 kcal mol⁻¹). ^l The energy penalty for SS (45 kcal mol⁻¹) also needed to be derived by fixing the S(7)-S(8) bond distance to be 2.34 Å.

3. 11-VERTEX *NIDO* HETEROBORANES

Two adjacent heteroatoms result in a larger degree of electron localization on two adjacent vertices and hence a positive HetHet energy penalty. This HetHet energy penalty is more positive for three electron donating group 15 heteroatoms as compared to the three electron donating group 14 heteroatoms. This is due to the larger electronegativity of three electron donating group-15 members. Four electron donating group-15 members have even higher electron localization due to four rather than three electrons localized at one vertex.

Group-16 heteroatoms have even higher energy penalties as compared to group-15 heteroatoms due to larger electronegativity of the group-15 heteroatoms. It is interesting to note that neighboring NH groups have such a large destabilizing effect that the energy penalty could only be estimated by fixing the N(7)-B(2) and N(8)-B2 distances as the cluster shape was destroyed upon free geometry optimization.¹⁶ Considering the general trends, the energy penalties for oxygen should be the largest but none of the five structural features for 11-vertex *nido*-oxaboranes could be determined as none of the oxaborane starting geometries optimized to a *nido*-11-vertex cluster geometry.

Among the heteroatoms in Chart 3.1, oxygen is the only for which no experimentally known 11-vertex *nido*-heteroborane exists. The smallest HetHet energy penalty (3.1 kcal mol⁻¹) is found for tin (on the left bottom of Chart 3.1).

Geometric consequences also seem to be important: Incorporation of one

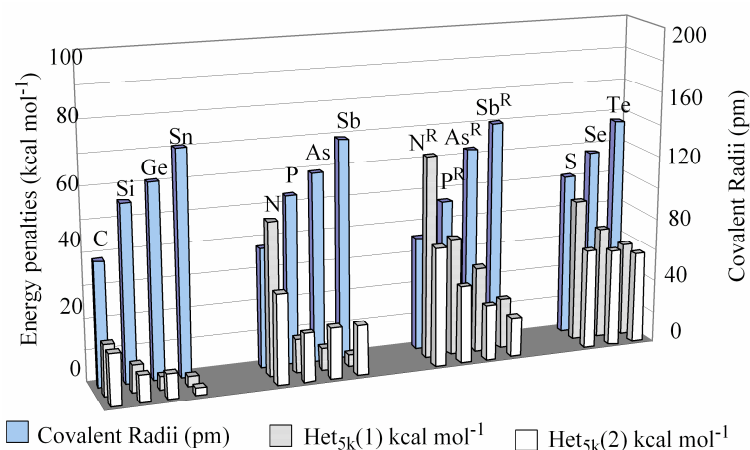


Figure 3.3: Covalent radii, HetHet and HetC energy penalties kcal mol⁻¹ for group 14, group 15 and group 16 heteroatoms. HetHet and HetC energy penalties for heteroatoms increase with decrease in covalent radii.

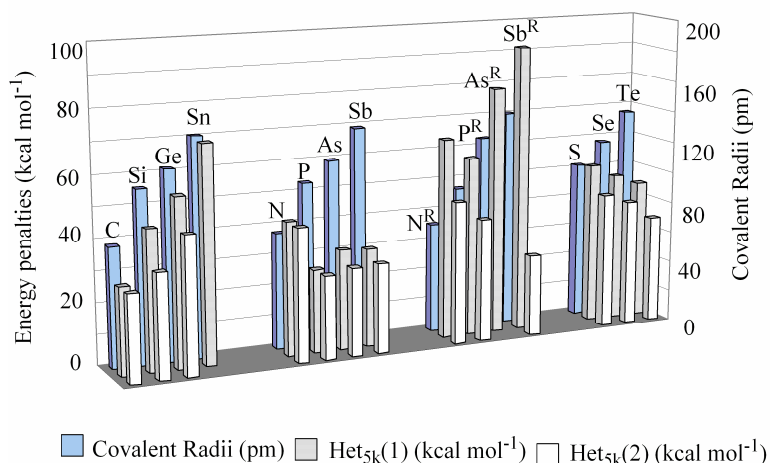


Figure 3.4: Het_{5k}(1) and Het_{5k}(2) energy penalties kcal mol⁻¹ for group 14 heteroatoms decrease with decreasing covalent radii but increase for group 16 heteroatoms. Group 15 heteroatoms have mixed trends.

large heteroatom requires geometric distortion of the cluster. Incorporating another large heteroatom next to the first enhances the geometric distortion but to a lesser extent as compared to placing it at a yet undistorted site. Although, this effect is overruled by the opposite electronic effects, yet it considerably reduces the energy penalties for two adjacent larger heteroatoms. When there is a significant electronegativity difference between boron and the heteroatoms, the electronic effect dominates. However, when the electronegativity of the heteroatom is very close to that of boron, the relative position of heterogroups does not influence the electronic situation much and the geometric consequences are important.

Table 3.1. Energy penalties [kcal mol^{-1}] for HetP^{R} and HetP together with covalent radius of heteroatom (Het).

HetHet'	R_{Het} (pm)	E_{inc} (kcal mol^{-1})
NP	71	18.8
CP	77	15.1
PP	93	10.7
$\text{N}^{\text{R}}\text{P}^{\text{R}}$	71	42.5
$\text{P}^{\text{R}}\text{P}^{\text{R}}$	93	36.9
SP^{R}	104	38.8
SeP^{R}	117	35.8

Figure 3.3 shows such general trends for HetHet' and HetC energy penalties which are indirectly proportional to the covalent radii (directly proportional to electronegativity) within one group. Table 3.1 also shows very similar effects for HetP^{R} and HetP energy penalties where one heteroatom is a phosphorus atom.

Energy penalties for $\text{Het}_{5\text{k}}(1)$ and $\text{Het}_{5\text{k}}(2)$ increase down the group 14 but decrease down group 16. For both three as well as four electron donating heteroatoms in group 15, however, they show mixed trends (Figure 3.4).

The importance of geometric consequences also becomes clear by the pronounced preference for open face position for larger heteroatoms. Larger heteroatoms have much larger $\text{Het}_{5\text{k}}(1)$ and $\text{Het}_{5\text{k}}(2)$ energy penalties. The larger heteroatoms cause more geometric distortion when connected to five cage vertices (at apical position or in the middle belt), and hence larger energy penalties as compared to the smaller heteroatoms which are closer to a BH vertex in size. In the open face, larger heteroatoms are connected to four cluster vertices and hence are more suitable.

The structural feature Het(H) has very similar energy penalties for four electron donating group 16 heteroatoms (S, Se and Te have energy penalties of 6.2, 6.1 and 6.3 kcal mol⁻¹, respectively), however, Het(H) energy penalties do not follow any specific general trend for group 14 and -15 heteroatoms. Moreover, Het(H) energy penalties have a small disfavoring effect (~5 kcal mol⁻¹ in many cases) and can be considered as fine tuning increment for two structural isomers differing with respect to open face hydrogen positions, only.

3.2.3. Comparisons of the Estimated Relative Stabilities ($E_{\text{inc}}^{\text{rel}}$) Derived from Estimated Energy Penalties (E_{inc}^{\wedge}) with DFT computed Values (E_{calc}) for the 11-vertex *nido*-Hetero(carba)boranes and -borates.

Estimated (E_{inc}^{\wedge}) and statistically fitted (E_{inc}) energy penalties as well as $E_{\text{inc}}^{\text{rel}}$ were reported for 11-vertex *nido*-(carba)boranes and -borates, phospho(carba)boranes and -borates and aza(carba)boranes and -borates.¹⁶ In this section, the estimated relative stabilities ($E_{\text{inc}}^{\text{rel}}$) are compared with the DFT computed relative energies (E_{calc}) for thia(carba)boranes and -borates, phosphathiaboranes and -borates, seleno-, and telluro(carba)boranes and -borates, and selenathiaboranes and -borates. $\Delta E'$ is the difference of $E_{\text{inc}}^{\text{rel}}$ and E_{calc} .

3.2.3.1. Thia(carba)boranes and -borates

Twenty five isomers of thia(carba)boranes and -borates from *nido*-SB₁₀H₁₂ to *nido*-SC₂B₈H₁₀ are considered in this study. The estimated energy penalties for S_{5k}(1), S_{5k}(2), SS, SC, CC and S(H) were obtained as explained in section 3.1. A total of eight 11-vertex *nido*-thia(carba)borane and -borate clusters is experimentally known (labeled by “a” in Table 3.2, also see Figure 3.5). Metal complexes of *nido*-SB₁₀H₁₀²⁻ (CA) were also reported.¹⁷ Two experimentally unknown SC₂B₈H₁₀ isomers, **GC** and **GD** (see Table 3.2) are predicted as strong candidates for synthesis due to their competitive thermodynamical stabilities.

The experimentally known^{1c,9,18} most stable *nido*-SB₁₀H₁₂ isomer, i.e., *nido*-7-SB₁₀H₁₂ (**AA**) has a sulfur atom at the open face with two bridged hydrogen atoms adjacent to the sulfur atom (structural feature S(H), twice). Both $E_{\text{inc}}^{\text{rel}}$ and E_{calc} have very similar relative energy values for **AA** (*nido*-2-SB₁₀H₁₂), **AB** (*nido*-2-SB₁₀H₁₂) and **AC** (*nido*-1-SB₁₀H₁₂) (Table 3.2).

¹⁷ a) Kang, S. O.; Carroll, P. J.; Sneddon, L. G. *Inorg. Chem.* **1989**, 28, 961-964. b) Kang, S. O.; Carroll, P. J.; Sneddon, L. G. *Organometallics* **1988**, 7, 772-776. c) Zimmerman, G. J.; Sneddon, L. G. *J. Am. Chem. Soc.* **1981**, 103, 1102-1111. d) Thompson, D. A.; Rudolph, R. W. *J. Chem. Soc., Chem. Commun.* **1976**, 19, 770-771.

¹⁸ Kang, S. O.; Sneddon, L. G. *Inorg. Chem.* **1988**, 27, 3298-3300.

3. 11-VERTEX *NIDO* HETEROBORANES

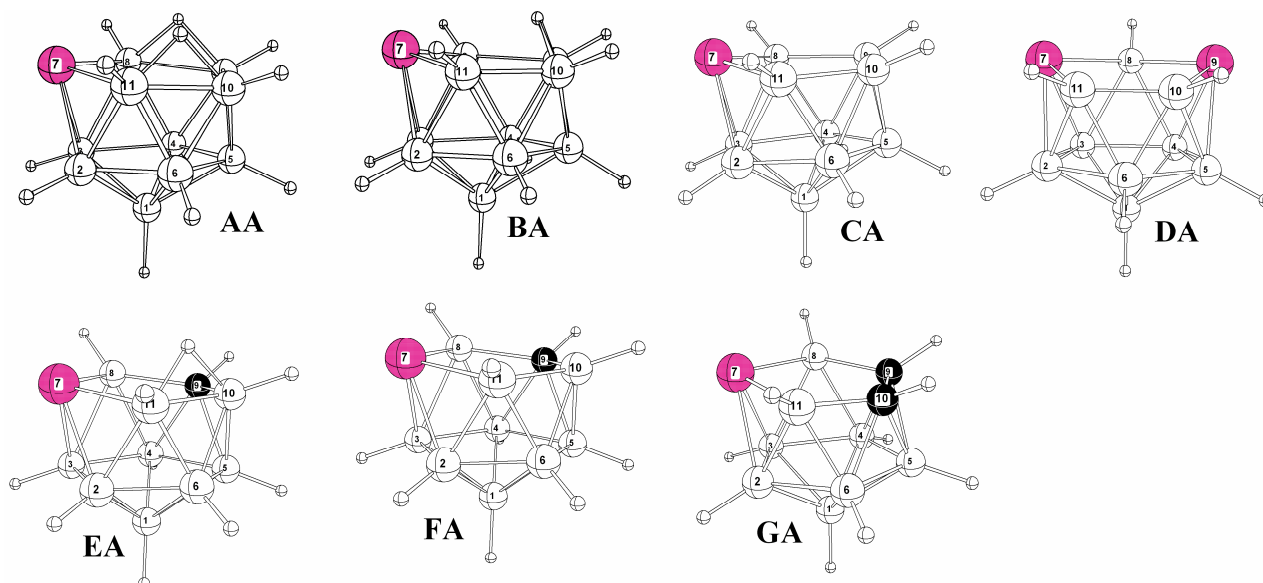


Figure 3.5: Most stable thia(carba)borane and -borate isomers. White, black and red balls represent boron, carbon and sulfur atoms, respectively. **AA**, **BA**, **DA-GA** are experimentally known. Metal complexes of **CA** are also experimentally known.

One extra hydrogen atom in *nido-7-SB₁₀H₁₁⁻* (**BA**)^{1c} bridges positions 9 and 10, resulting in no disfavoring structural feature but is adjacent to the sulfur atom in isomer **BB** resulting in $E_{\text{inc}}^{\text{S(H)}} = 6.2 \text{ kcal mol}^{-1}$. **BC**, i.e., *nido-2-SB₁₀H₁₁⁻* has a sulfur atom at position number 2 ($E_{\text{inc}}^{\text{S}_{5k}(2)} = 43.8 \text{ kcal mol}^{-1}$) and hence the structure is higher in energy than both **BA** and **BB**.

The absence of hydrogen bridges in *nido-SB₁₀H₁₀²⁻* results in only three possible isomers, i.e., *nido-7-SB₁₀H₁₀²⁻* (**CA**), *nido-2-SB₁₀H₁₀²⁻* (**CB**) and *nido-1-SB₁₀H₁₀²⁻* (**CC**), used to derive $E_{\text{inc}}^{\text{S}_{5k}(2)} = 43.8 \text{ kcal mol}^{-1}$ and $E_{\text{inc}}^{\text{S}_{5k}(1)} = 52.2 \text{ kcal mol}^{-1}$.

Experimentally known¹⁹ *nido-7,9-S₂B₉H₉* (**DA**) is the most stable isomer as it lacks any structural feature. None of the dithiaborane starting geometries with two adjacent sulfur atoms optimized successfully but converged to rearranged structures. However, a rough estimate for the SS feature was obtained by fixing the S(7)-S(8) distance in 7,8-S₂B₉H₉ to be 2.34 Å (45.5 kcal mol⁻¹). Obviously the SS feature, like N^RN^R,¹⁶ is incompatible with the *nido*-11-vertex cluster due to too large destabilization.

¹⁹ Friesen, G. D.; Barriola, A.; Daluga, P.; Ragatz, P.; Huffman, J. C.; Todd, L. J. *Inorg. Chem.* **1980**, *19*, 458-462.

3. 11-VERTEX *NIDO* HETEROBORANES

Table 3.2. Estimated energy penalties (E_{inc}^{\wedge}), estimated relative energies ($E_{\text{inc}}^{\text{rel}\wedge}$) and computed relative energies for thia(carba)boranes and -borates. All values are in kcal mol⁻¹.

Compound	$\mu\text{-H-}$	C_{5k}	$C(H)$	CC	$S_{5k(1)}^{\wedge}$	$S_{5k(2)}^{\wedge}$	$S(H)^{\wedge}$	SC^{\wedge}	$\sum E_{\text{inc}}^{\wedge}$	$E_{\text{inc}}^{\text{rel}\wedge}$	E_{calc}	ΔE^{\wedge}
		28.0	2.1	17.0	52.2	43.8	6.2	31.2				
AA ^a	7-SB ₁₀ H ₁₂						2		12.4	0.0	0.0	0.0
AB	2-SB ₁₀ H ₁₂					1	1		50.0	37.6	39.8	-2.2
AC	1-SB ₁₀ H ₁₂				1				52.2	39.8	43.8	-4.0
BA ^a	7-SB ₁₀ H ₁₁ ¹⁻								0.0	0.0	0.0	0.0
BB ^a	7-SB ₁₀ H ₁₁ ¹⁻						1		6.2	6.2	6.2	0.0
BC	2-SB ₁₀ H ₁₁ ¹⁻					1			43.8	43.8	44.3	-0.5
CA ^b	7-SB ₁₀ H ₁₀ ²⁻								0.0	0.0	0.0	0.0
CB	2-SB ₁₀ H ₁₀ ²⁻					1			43.8	43.8	43.8	0.0
CC	1-SB ₁₀ H ₁₀ ²⁻				1				52.2	52.2	52.2	0.0
DA ^a	7,9-S ₂ B ₉ H ₉								0.0	0.0	0.0	0.0
DB	1,7-S ₂ B ₉ H ₉				1				52.2	52.2	55.5	-3.3
EA ^a	7,9-SCB ₉ H ₁₁		1				1		8.3	0.0	0.0	0.0
EB	7,8-SCB ₉ H ₁₁		1					1	33.3	25.0	25.6	-0.6
EC	7,8-SCB ₉ H ₁₁						1	1	37.4	29.1	27.9	1.2
ED	2,8-SCB ₉ H ₁₁		1			1			45.9	37.6	35.0	2.6
FA ^a	7,9-SCB ₉ H ₁₀ ¹⁻								0.0	0.0	0.0	0.0
FB	7,8-SCB ₉ H ₁₀ ¹⁻							1	31.2	31.2	31.2	0.0
FC	7,1-SCB ₉ H ₁₀ ¹⁻		1						28.0	28.0	33.3	-5.3
FD	1,7-SCB ₉ H ₁₀ ¹⁻				1				52.2	52.2	54.4	-2.2
GA ^a	7,9,10-SC ₂ B ₈ H ₁₀			1					17.0	0.0	0.0	0.0
GB ^a	7,8,10-SC ₂ B ₈ H ₁₀							1	31.2	14.2	13.1	1.1
GC ^c	8,2,10-SC ₂ B ₈ H ₁₀		1						28.0	11.0	13.6	-2.6
GD ^c	7,1,9-SC ₂ B ₈ H ₁₀		1						28.0	11.0	17.5	-6.5
GE ^a	7,8,9-SC ₂ B ₈ H ₁₀			1				1	48.2	31.2	32.9	-1.7
GF	7,8,11-SC ₂ B ₈ H ₁₀							2	62.4	45.4	48.8	-3.4

^a Experimentally known isomers. ^b Only metal derivatives are experimentally known ^c Strong candidates.

Table 3.3. Estimated energy penalties (E_{inc}^{\prime}), estimated relative energies ($E_{\text{inc}}^{\text{rel}\prime}$) for phosphathiaboranes. DFT computed relative energies are also reported for **HA** to **HD**. All values are given in kcal mol⁻¹.

Compound	μ -H-	P(H)	P ^R	S(H)′	PS′	P ^R S′	$\sum E_{\text{inc}}^{\prime}$	$E_{\text{inc}}^{\text{rel}\prime}$	E_{calc}	ΔE^{\prime}
		2.2	13.3	6.1	21.4	38.8				
HA ^a 7,9-PSB ₉ H ₁₀	10,11	1		1			8.3	0.0	0.0	0.0
HB ^b 7,9-(HP)SB ₉ H ₁₀			1				13.3	5.0	3.4	1.6
HC 7,8-PSB ₉ H ₁₀	10,11	1			1		23.6	15.3	13.8	1.5
HD 7,8-(HP)SB ₉ H ₁₀			1			1	52.1	43.8	42.2	1.6
IA 7,9-PSB ₉ H ₉ ⁻							0.0	0.0	0.0	0.0
IB 7,8-PSB ₉ H ₉ ⁻					1		21.4	21.4	21.4	0.0

^a Strong candidate for synthesis ^b 7-Ph-HB, i.e., 7-Ph derivative of 7,9-PSB₉H₁₀ is experimentally known.

The *nido*-7,9-SCB₉H₁₁ with μ -H-10,11 (**EA**),²⁰ the most stable SCB₉H₁₁ isomer, has non-adjacent carbon and sulfur atoms. Isomers **EB** through **ED** are at least 25 kcal mol⁻¹ less stable than **EA**. A similar profound preference is found for the heteroatom apart *nido*-7,9-isomer (**FA**)²⁰ among SCB₉H₁₀⁻ structures.

Experimentally known *nido*-7,9,10-SC₂B₈H₁₀ (**GA**)^{1c} is the most stable of the seven computed isomers. *nido*-7,8,9-SC₂B₈H₁₀ (**GE**)^{1c} and *nido*-7,8,10-SC₂B₈H₁₀ (**GB**)^{1c} with $E_{\text{calc}} = 32.9$ and 14.2 kcal mol⁻¹, respectively, are also experimentally known. 8,2,10- (**GC**) and 7,1,9- SC₂B₈H₁₀ (**GD**) are thermodynamically more stable than 7,8,9- SC₂B₈H₁₀ (**GE**),^{1c} but are still experimentally unknown.

3.2.3.2. Phosphathiaboranes and -borates.

Relative stabilities as determined from DFT computations and from structural increments for a few phosphathiaboranes are compared in Table 3.3. PSB₉H₉⁻ structures lack extra hydrogen atoms and possess bare-phosphorus atom/s only. For *nido*-PSB₉H₁₀, however, both bare and exo-substituted phosphorus atoms are considered. The energy penalties derived for a phosphorus atom in phospho(carba)boranes and -borates¹⁶ and for a sulfur atom in thia(carba)boranes and -borates (this paper) along with energy penalties for PS (derived by comparing *nido*-7,9-PSB₉H₉⁻ with *nido*-7,8-PSB₉H₉⁻) and P^RS (derived by comparing *nido*-7,9-(PH)SB₉H₉ with *nido*-7,8-(PH)SB₉H₉) can be used to

²⁰ Holub, J.; Kennedy, J. D.; Jelínek, T.; Štíbr, B. *Inorg. Chem.* **1994**, *8*, 1317-1323.

estimate the relative stabilities of phosphathiaboranes. The estimated relative energies of four *nido*-PSB₉H₁₀ isomers (i.e., **HA**-**HD** which differ in more than one feature) were found to be in good agreement with the relative energies computed at B3LYP/6-311+G(d,p)//B3LYP/6-31G(d) (see Table 3.3, **HA** - **HD**). 7,9-PSB₉H₁₀ μ -*H*-10,11 (**HA**) with the structural features P(H) and S(H) has the least $\sum E_{\text{inc}}'$, $E_{\text{inc}}^{\text{rel}'}$ and E_{calc} values but is still experimentally unknown. *nido*-7,9-PSB₉H₁₀ with exo-substituted phosphorus atom (**HB**) is computed to be 3.4 kcal mol⁻¹ higher in energy than the former and its phenyl derivative i.e., *nido*-7-Ph-7,9-PSB₉H₉ was experimentally characterized.^{1c}

Table 3.4. Estimated energy penalties (E_{inc}'), estimated relative energies ($E_{\text{inc}}^{\text{rel}'}$) for selenaboranes and -borates. DFT computed relative energies are also reported for some structures. All values are in kcal mol⁻¹.

	Compound	μ -H-	Se _{5k} (1)'	Se _{5k} (2)'	Se(H)'	SeSe'	$\sum E_{\text{inc}}'$	$E_{\text{inc}}^{\text{rel}'}$	E_{calc}	$\Delta E'$
			48.2	40.7	6.1	35.1				
JA ^a	7-SeB ₁₀ H ₁₂	8,9:10,11			2		12.2	0.0	0.0	0.0
JB	2-SeB ₁₀ H ₁₂	7,8: 9,10		1	1		46.8	34.6	39.5	-4.9
KA ^a	7-SeB ₁₀ H ₁₁ ¹⁻	9,10					0.0	0.0	0.0	0.0
KB	7-SeB ₁₀ H ₁₁ ¹⁻	8,9			1		6.1	6.1	6.1	0.0
KC	1-SeB ₁₀ H ₁₁ ¹⁻	7,8	1				48.2	48.2	52.6	-4.4
LA ^b	7-SeB ₁₀ H ₁₀ ²⁻						0.0	0.0	0.0	0.0
LB	2-SeB ₁₀ H ₁₀ ²⁻			1			40.7	40.7	40.7	0.0
MA	7,9-Se ₂ B ₉ H ₉						0.0	0.0	0.0	0.0
MB ^a	7,8-Se ₂ B ₉ H ₉					1	35.1	35.1	35.1	0.0

^a experimentally known isomers ^b Cyclopentadienyl metal derivatives are experimentally known.

3.2.3.3. Selen(carba)boranes and -borates

Estimated energy penalties were used to give the relative stability order of 25 selen(carba)boranes and -borates (Tables 3.4 and 3.5). The relative stability order is correctly reproduced in most cases, yet $\Delta E'$ (the difference of $E_{\text{inc}}^{\text{rel}'}$ and E_{calc}) is larger for SeC₂B₈H₁₀ isomers (up to 9.8 kcal mol⁻¹ for **QB**).

The most stable SeB₁₀H₁₂ isomer i.e., *nido*-7-SeB₁₀H₁₂ (**JA**)^{10e} has the selenium atom at vertex number seven with hydrogens bridging between 8/9 and 10/11 positions (structural feature Se(H) twice). The increment system suggests the deprotonated species, i.e., *nido*-7-SeB₁₀H₁₁⁻,¹⁰ with a hydrogen bridged between positions 9/10 (**KA**) rather than positions 8/9 (**KB**) to be the most stable as in the case of exo-substituted *nido*-7-(PH)B₁₀H₁₂⁻.¹⁶

3. 11-VERTEX *NIDO* HETEROBORANES

Table 3.5. Estimated energy penalties (E_{inc}^{\prime}), estimated relative energies ($E_{\text{inc}}^{\text{rel}\prime}$) for selenacarbaboranes and -borates. DFT computed relative energies are also reported for some structures. All values are in kcal mol⁻¹.

Compound	$\mu\text{-H-}$	C _{5k}	C(H)	CC	Se _{5k} (1) [′]	Se _{5k} (2) [′]	Se(H) [′]	SeC [′]	$\sum E_{\text{inc}}^{\prime}$	$E_{\text{inc}}^{\text{rel}\prime}$	E_{calc}	ΔE^{\prime}
		28.0	2.1	17.0	48.2	40.7	6.1	30.3				
NA ^a	7,9-SeCB ₉ H ₁₁	10,11	1				1		8.2	0.0	0.0	0.0
NB ^b	7,8-SeCB ₉ H ₁₁	9,10	1					1	32.4	24.2	24.8	-0.6
NC	7,8-SeCB ₉ H ₁₁	10,11					1	1	36.4	28.2	26.5	1.7
ND	1,7-SeCB ₉ H ₁₁	9,10	1			1			42.8	34.6	32.8	1.8
NE	1,7-SeCB ₉ H ₁₁	8,9	1		1				50.3	42.1	46.7	-4.6
NF	2,4-SeCB ₉ H ₁₁	9,10	1	1		1			70.8	62.6	65.0	-2.4
OA	7,9-SeCB ₉ H ₁₀ ⁻								0.0	0.0	0.0	0.0
OB	7,8-SeCB ₉ H ₁₀ ⁻							1	30.3	30.3	30.3	0.0
OC	7,1-SeCB ₉ H ₁₀ ⁻		1						28.0	28.0	32.6	-4.6
PA	7,9,10-SeC ₂ B ₈ H ₁₀				1				17.0	0.0	0.0	0.0
PB	7,8,10-SeC ₂ B ₈ H ₁₀							1	30.3	13.3	2.5	9.8
PC	7,1,9-SeC ₂ B ₈ H ₁₀		1						28.0	11.0	7.6	3.4
PD	7,8,9-SeC ₂ B ₈ H ₁₀				1			1	47.3	30.3	22.5	8.8
PE	7,8,11-SeC ₂ B ₈ H ₁₀							2	60.6	42.6	37.4	5.2

^a Strong candidates ^b 7-cycloheptamine derivative is experimentally known.

nido-7-SeB₁₀H₁₀²⁻ (**LA**) was reported as ligand in complexes with different metal fragments.^{10a-d,11a-b,21} The geometry of *nido*-7,8-Se₂B₉H₉ (**MB**)²² unlike that of *nido*-7,8-S₂B₉H₉ could successfully be optimized and is 35.1 kcal mol⁻¹ higher in energy than the experimentally still unknown but energetically favorable 7,9-isomer (**MA**). Similarly, the heteroatom apart *nido*-7,9-SeCB₉H₁₁ (**NA**), the

²¹ a) Ferguson, G.; Faridooon; Spalding, T. R. *Acta Cryst.* **1988**, *C44*, 1368-1371. b) Ferguson, G.; Ruhl, B. L.; Ni Dhubhghaill, O.; Spalding, T. R. *Acta Cryst.* **1987**, *C43*, 1250-1253.

²² a) Base, K.; Štibr, B. *Chem. Ind.*, **1977**, 22, 919-920. b) Friesen, G. D.; Barriola, A.; Todd, L. J. *Chem. Ind.*, **1978**, 16, 631. c) Base, K. *Collect. Czech. Chem. Commun.* **1983**, 48, 2593-2603. d) Schultz, R. V.; Huffman, J. C.; Todd, L. J. *Inorg. Chem.* **1979**, 18, 2883-2886.

most stable $\text{SeCB}_9\text{H}_{11}$ isomer, is still experimentally unknown although the 7-cyclohexanamine derivative of the 7,8-isomer (**NB**) is experimentally known²³. *nido*-7,9,10- $\text{SeC}_2\text{B}_8\text{H}_{10}$ (**PA**) is experimentally known^{22a} and other computed $\text{SeC}_2\text{B}_8\text{H}_{10}$ structures (**PB-PJ**) are thermodynamically less stable (Table 3.5).

3.2.3.4. Selenathiaboranes

The energy penalty (40.2 kcal mol⁻¹) for the structural feature SSe was obtained as the energy difference of 7,8- and 7,9- SeSB_9H_9 . The latter is more stable and is experimentally known.¹⁹ Relative energies of five SeSB_9H_9 isomers are given in Table 3.6.

Table 3.6. Estimated energy penalties (E_{inc}^{\wedge}), estimated relative energies ($E_{\text{inc}}^{\text{rel}\wedge}$) for selenathiaboranes. All values are in kcal mol⁻¹.

	Compound	$E_{\text{inc}}^{\text{rel}\wedge}$	E_{calc}	ΔE	Structural Feature
QA	7,9- SeSB_9H_9	0.0	0.0	0.0	None
QB	7,8- SeSB_9H_9	40.2	40.2	0.0	SSe \wedge
QC	2,9- SeSB_9H_9	40.7	36.0	4.7	Se _{5k} (2) \wedge
QD	9,2- SeSB_9H_9	43.8	38.3	5.5	S _{5k} (2) \wedge
QE	1,7- SeSB_9H_9	48.1	51.9	-3.8	Se _{5k} (1) \wedge
QF	7,1- SeSB_9H_9	52.2	54.7	-2.5	S _{5k} (1) \wedge

3.2.3.5. Estimated Energy Penalties (E_{inc}^{\wedge}) and Corresponding Estimated Relative Stabilities ($E_{\text{inc}}^{\text{rel}\wedge}$) for Other 11-vertex *nido*-Hetero(carba)boranes and -borates.

Estimated energy penalties for sila-, germana-, stanna-, bare and exo-substituted arsa- and stiba(carba)boranes and -borates are reported in Chart 3.1 which can be used to produce the $E_{\text{inc}}^{\text{rel}\wedge}$ for the 11-vertex *nido*-hetero(carba)boranes and -borates with H-Si, H-Ge, H-Sn, As, H-As, Sb and H-Sb heterogroups, respectively.

3.2.4. Prediction of Thermodynamically Most Stable Mixed Heteroboranes and -borates with Three Open Face Heteroatoms.

Energy penalties for the HetHet \wedge structural features describe the relative energies of open face heteroboranes with two equal heteroatoms, for example, $\text{C}_2\text{B}_9\text{H}_{11}^{2-}$,¹⁴ $\text{P}_2\text{B}_9\text{H}_{11}$,¹⁶ $\text{Se}_2\text{B}_9\text{H}_9$ (section 3.4.2) or that of heteroboranes with two different heteroatoms, e.g., 7,8- and 7,9-isomers of PSB_9H_9^- and $\text{PSB}_9\text{H}_{10}$ (section 3.4.1), SeSB_9H_9 (section 3.4.3) etc. However, it is complex to predict the

²³ Arafat, A.; Friesen, G. D.; Todd, L. J. *Inorg. Chem.* **1983**, 22, 3721-3724.

thermodynamically most stable isomer in mixed heteroboranes with three open face heteroatoms, e.g. $\text{P}_2\text{CB}_8\text{H}_9^-$,²⁴ $\text{PC}_2\text{B}_8\text{H}_{10}^-$,^{25,26} $\text{SC}_2\text{B}_8\text{H}_{10}$,^{1c} $\text{SeC}_2\text{B}_8\text{H}_{10}$,^{22a} $\text{NC}_2\text{B}_8\text{H}_{11}$,²⁷ $\text{NC}_2\text{B}_8\text{H}_{10}^-$.²⁷

Here only $\text{HetC}_2\text{B}_8\text{H}_{10}^{(4-n)-}$ examples are presented, (where n = number of electrons donated by a heterogroup, and Het may be a three electron donating heteroatom/group, i.e., H-C, H-Si, H-Ge, H-Sn, N, P, As, Sb, or a four electron donating heteroatom/group, i.e., H-N, H-P, H-As, H-Sb, S, Se, Te (Chart 3.2). All four possibilities for $\text{HetC}_2\text{B}_8\text{H}_{10}^{(4-n)-}$ structures with open face heteroatoms, i.e., 7,9,10-, 7,8,10-, 7,8,9- and 7,8,11- $\text{HetC}_2\text{B}_8\text{H}_{10}^{(4-n)-}$ will be discussed. Both 7,9,10- and 7,8,10-isomers of $\text{HetC}_2\text{B}_8\text{H}_{10}^-$ have one structural feature each, i.e., CC and HetC, respectively. However, 7,8,9- and 7,8,11-isomers of $\text{HetC}_2\text{B}_8\text{H}_{10}^-$ have two structural features, each, i.e., HetC+CC and 2·HetC, respectively. For group 14 heteroatoms, i.e., H-Si, H-Ge and H-Sn, the HetC, i.e., SiC, GeC and SnC energy penalties are smaller than that of CC and therefore 7,8,10-isomers (i.e., isomers with the HetC structural feature) are more stable. The 7,8,11-isomers with twice the structural feature HetC for three electron donating group 14 heteroatoms is not a too high energy option. HetC is very small for group 14 heteroatoms and therefore the 7,8,11-isomers of $\text{SnC}_2\text{B}_8\text{H}_{10}$ is only 2.4 kcal mol⁻¹ higher in energy than the 7,8,10-isomer (see Chart 3.2). In the case of three electron donating bare nitrogen atom (N), however, the NC structural feature has a larger disfavoring effect than CC, and therefore the 7,9,10-isomer (with structural feature CC) is more stable than the 7,8,10-isomer (with structural feature NC). But for other three electron donating group 15 heteroatoms, i.e., P, As, Sb, HetC has less disfavoring effect than CC and therefore the 7,8,10-isomer is more favorable for $\text{PC}_2\text{B}_8\text{H}_{10}^-$, $\text{AsC}_2\text{B}_8\text{H}_{10}^-$, $\text{SbC}_2\text{B}_8\text{H}_{10}^-$. Estimated relative stabilities for $\text{HetC}_2\text{B}_8\text{H}_{10}$ structures for four electron donating heteroatoms are listed in Chart 3.2. H-N and H-P have HetC energy penalties ($E_{\text{inc}}^{\text{N}^{\text{R}}\text{C}} = 36.0$ kcal mol⁻¹ and $E_{\text{inc}}^{\text{P}^{\text{R}}\text{C}} = 23.6$ kcal mol⁻¹) much larger than CC ($E_{\text{inc}}^{\text{CC}} = 17.0$ kcal mol⁻¹) and hence 7,9,10-isomers with structural feature CC are more favorable than the 7,8,10-isomers. For H-As, however, 7,8,10- $\text{AsC}_2\text{B}_8\text{H}_{11}$ (with structural feature $\text{As}^{\text{R}}\text{C}$ ($E_{\text{inc}}^{\text{As}^{\text{R}}\text{C}} = 17.3$ kcal mol⁻¹)) and 7,9,10- $\text{AsC}_2\text{B}_8\text{H}_{11}$ with the structural feature CC ($E_{\text{inc}}^{\text{CC}} = 17.0$ kcal mol⁻¹) are very similar in energy.

²⁴ Bakardjiev, M; Holub, J.; Štíbr, B.; Hnyk, D.; Wrackmeyer, B. *Inorg. Chem.* **2005**, *44*, 5826-5832.

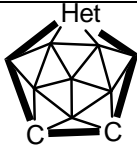
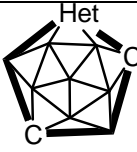
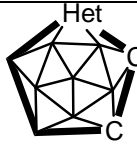
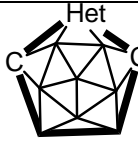
²⁵ Štíbr, B.; Holub, J.; Bakardjiev, M.; Hnyk, D.; Tok, O L.; Milius, W.; Wrackmeyer, B. *Eur. J. Inorg. Chem.* **2002**, *9*, 2320-2326.

²⁶ Holub, J.; Ormsby, D. L.; Kennedy, J. D.; Greatrex, R.; Štíbr, B.; *Inorg. Chem. Commun.* **2000**, *3*, 178-181.

²⁷ Plešek, J; Štíbr, B; Hnyk, D; Jelínek, T; Heřmánek, S; Kennedy, J. D.; Hofmann, M.; Schleyer, P. v. R. *Inorg. Chem.* **1998**, *37*, 3902-3909.

3. 11-VERTEX *NIDO* HETEROBORANES

 Chart 3.2. Estimated relative energies (kcal mol⁻¹) of 7,9,10-, 7,8,10-, 7,8,9- and 7,8,11-isomers in $\text{HetC}_2\text{B}_8\text{H}_{10}^{(4-n)-}$.^{a,b}

Heteroatom (cluster charge)	 7,9,10- ^c	 7,8,10- ^d	 7,8,9- ^e	 7,8,11- ^f
Het = H-Si (-1)	CC = 17.0 $E_{\text{rel}} = 7.5$	SiC = 8.5 $E_{\text{rel}} = 0.0$	SiC + CC = 25.5 $E_{\text{rel}} = 17.0$	2*SiC = 17.0 $E_{\text{rel}} = 8.5$
Het = H-Ge (-1)	CC = 17.0 $E_{\text{rel}} = 9.3$	GeC = 7.7 $E_{\text{rel}} = 0.0$	GeC + CC = 24.7 $E_{\text{rel}} = 17.0$	2*GeC = 15.4 $E_{\text{rel}} = 7.7$
Het = H-Sn (-1)	CC = 17.0 $E_{\text{rel}} = 14.6$	SnC = 2.4 $E_{\text{rel}} = 0.0$	SnC + CC = 19.4 $E_{\text{rel}} = 17.0$	2*SnC = 4.8 $E_{\text{rel}} = 2.4$
Het = N (-1)	CC = 17.0 $E_{\text{rel}} = 0.0$ (0.0)	NC = 28.4 $E_{\text{rel}} = 11.4$ (6.1)	NC + CC = 40.0 $E_{\text{rel}} = 23.0$	2*NC = 56.8 $E_{\text{rel}} = 39.8$
Het = P (-1)	CC = 17.0 $E_{\text{rel}} = 1.9$ (3.0)	PC = 15.1 $E_{\text{rel}} = 0.0$ (0.0)	PC + CC = 32.1 $E_{\text{rel}} = 17.0$ (17.9)	2*PC = 31.2 $E_{\text{rel}} = 15.1$ (18.1)
Het = As (-1)	CC = 17.0 $E_{\text{rel}} = 1.0$	AsC = 16.0 $E_{\text{rel}} = 0.0$	AsC + CC = 33.0 $E_{\text{rel}} = 17.0$	2*AsC = 32.0 $E_{\text{rel}} = 16.0$
Het = Sb (-1)	CC = 17.0 $E_{\text{rel}} = 1.3$	SbC = 15.7 $E_{\text{rel}} = 0.0$	SbC + CC = 32.7 $E_{\text{rel}} = 17.0$	2*SbC = 31.4 $E_{\text{rel}} = 15.7$
Het = H-N (0)	CC = 17.0 $E_{\text{rel}} = 0.0$ (0.0)	N ^R C = 37.2 $E_{\text{rel}} = 20.2$ (18.8)	N ^R C + CC = 44.2 $E_{\text{rel}} = 37.2$ (41.3)	2*N ^R C = 74.4 $E_{\text{rel}} = 57.4$ (58.8)
Het = H-P (0)	CC = 17.0 $E_{\text{rel}} = 0.0$ (0.0)	P ^R C = 24.3 $E_{\text{rel}} = 7.3$ (5.2)	P ^R C + CC = 43.6 $E_{\text{rel}} = 23.6$ (24.9)	2*P ^R C = 48.6 $E_{\text{rel}} = 31.6$ (29.5)
Het = H-As (0)	CC = 17.0 $E_{\text{rel}} = 0.0$	As ^R C = 17.3 $E_{\text{rel}} = 0.3$	As ^R C + CC = 34.3 $E_{\text{rel}} = 17.3$	2*As ^R C = 34.6 $E_{\text{rel}} = 17.6$
Het = H-Sb (0)	CC = 17.0 $E_{\text{rel}} = 4.5$	Sb ^R C = 12.5 $E_{\text{rel}} = 0.0$	Sb ^R C + CC = 29.5 $E_{\text{rel}} = 17.0$	2*Sb ^R C = 25.0 $E_{\text{rel}} = 12.5$
Het = S (0)	CC = 17.0 $E_{\text{rel}} = 0$ (0.0)	SC = 32.0 $E_{\text{rel}} = 15.0$ (13.1)	SC + CC = 49.0 $E_{\text{rel}} = 32.0$ (32.9)	2*SC = 64.0 $E_{\text{rel}} = 47.0$ (48.8)

3. 11-VERTEX *NIDO* HETEROBORANES

Chart 3.2 (continued). Estimated relative energies (kcal mol⁻¹) of 7,9,10-, 7,8,10-, 7,8,9- and 7,8,11- isomers in HetC₂B₈H₁₀⁽⁴⁻ⁿ⁾⁻.^{a,b}

Het = Se	CC = 17.0	SeC = 30.3	SeC + CC = 47.3	2*SeC = 60.6
(0)	$E_{\text{rel}} = 0$ (0.0)	$E_{\text{rel}} = 12.7$ (2.5)	$E_{\text{rel}} = 30.3$ (22.5)	$E_{\text{rel}} = 43.6$ (37.4)
Het = Te	CC = 17.0	TeC = 28.6	TeC + CC = 45.6	2*TeC = 57.2
(0)	$E_{\text{rel}} = 0$	$E_{\text{rel}} = 11.6$	$E_{\text{rel}} = 28.6$	$E_{\text{rel}} = 40.2$

^a Het may be a three or four electron donating heteroatom. n corresponds to the number of electrons donated by a given heteroatom. ^b B3LYP/6-311+G(d,p)//B3LYP/6-31G(d)+ZPE computed relative stabilities of various HetC₂B₈H₁₀⁽⁴⁻ⁿ⁾⁻ isomers are listed in parenthesis for various heteroatoms. These values are usually very close to the values predicted by estimated energy penalties. ^c 7,9,10-NC₂B₈H₁₀⁻, 7,9,10-(HN)C₂B₈H₁₀, 7,9,10-SC₂B₈H₁₀, 7,9,10-SeC₂B₈H₁₀ are experimentally known. ^d 7,8,10-SC₂B₈H₁₀ is experimentally known. ^e 7,8,9-NC₂B₈H₁₀⁻ and 7-Me and 7-Ph derivatives of 7,8,9-(HP)C₂B₈H₁₀ are experimentally known. ^f 7-Ph derivatives of 7,8,11-(HP)C₂B₈H₁₀ is experimentally known.

Since HetHet' energy penalties decrease down the group, the HetC energy penalty (Sb^RC) for four electron donating antimony atom (Sb^RC) is 4.8 kcal mol⁻¹ less than that of As^RC and therefore the 7,8,10-isomer is more stable for (HSb)C₂B₈H₁₀ as compared to the 7,9,10-isomer (7,9,10-isomer has structural feature CC and $E_{\text{inc}}\text{CC} > E_{\text{inc}}\text{Sb}^{\text{R}}\text{C}$).

HetC energy penalties for all four electron donating group 16 heteroatoms are much higher than CC and therefore 7,9,10-HetC₂B₈H₁₀ isomers are thermodynamically more stable than 7,8,10-isomers. 7,8,9- and 7,8,11-isomers have more than one structural feature, i.e., HetHet+HetC and 2·HetC, respectively, and therefore have even larger disfavoring effects for four electron donating heteroatoms.

3.3. Conclusion

Estimated energy penalties present a convenient method to predict the relative stabilities of 11-vertex *nido*-heteroboranes and -borates. Energy penalties for adjacent heteroatoms increase along the period and decrease down the group. Four electron donating heteroatoms have generally larger energy penalties than those of three electron donating heteroatoms. Larger heteroatoms have usually larger Het_{5k}(1) and Het_{5k}(2) energy penalties and smaller HetHet' energy penalties indicating that they prefer open face vertices and that the destabilizing effect of adjacent heteroatoms is smaller for larger heteroatoms. Most stable mixed heteroboranes with more than two open face heteroatoms have different but easily predictable heteroatom positions in the thermodynamically most stable 11-vertex *nido*-heteroborane isomers. Energy penalties are likely to have periodic trends in other polyborane clusters.

4. The Relative Stabilities of 11-Vertex *nido*- and 12-vertex *closo*-Heteroboranes and –borates: Facile Estimation by Structural or Connection Increments.

4.1. Introduction.

Beside their potential use in medical applications,¹ heteroboranes are of interest due to their unusual non-classical structure and their key role in stimulating new concepts and a general picture of chemical bonding.² Simple qualitative rules presented by Williams³ and Wade⁴ are helpful for both understanding the building principles and to identify possible synthetic targets. More sophisticated quantitative rules also called structural increments arising due to disfavoring structural features in heteroboranes^{2,5} have also been presented. The additive nature of these structural increments, i.e. their ability to accurately reproduce the DFT computed relative stabilities is now proven to be generally true for various *nido*-heteroboranes and -borates with diverse numbers, connectivities and types of heteroatoms. Sets of structural features and corresponding energy penalties were reported for 6-, 10- and 11-vertex *nido*-heteroboranes and –borates.^{2,5} They allow to easily derive the relative stabilities of various isomers with good accuracy, once corresponding energy increments “penalties” are assigned to relevant structural features based on

¹ a) Hawthorne, M. F.; Maderna, A. *Chem. Rev.* **1999**, *99*, 3421-3434. b) Mizusawa, E. A.; Dahlman, H. L.; Bennet, S. J.; Hawthorne, M. F. *Proc. Natl. Acad. Sci. U.S.A.* **1982**, *79*, 3011-3014.

² Kiani, F. A.; Hofmann, M. *Inorg. Chem.* **2005**, *44*, 3746-3754.

³ a) Williams, R. E. *J. Am. Chem. Soc.* **1965**, *87*, 3513-3515. b) Williams, R. E. *In Progress in Boron Chemistry* Brotherton, R. J., Steinberg, H., Eds.; Pergamon Press: England, 1970; Vol. 2, Chapter 2, p 57. c) Williams, R. E. *Chem. Rev.* **1992**, *92*, 177-207; references therein.

⁴ a) Wade, K. *Adv. Inorg. Chem. Radiochem.* **1976**, *18*, 1-66. b) Wade, K. In *Metal Interactions with Boron Clusters*; Grimes, R. N., Ed.; Plenum Press: New York, 1982; Chapter 1, pp 1– 41.

⁵ a) Hofmann, M.; Fox, M. A.; Greatrex, R.; Schleyer, P. v. R.; Williams, R. E. *Inorg. Chem.* **2001**, *40*, 1790-1801. b) Kiani, F. A.; Hofmann, M. *Eur. J. Inorg. Chem.* **2005**, *12*, 2545-2553. c) Kiani, F. A.; Hofmann, M. *Inorg. Chem.* **2004**, *43*, 8561-8571. d) Kiani, F. A.; Hofmann, M. *J. Mol. Mod.* **2006**, *12*, 597-609.

DFT results computed for a selected set of structures. The energy penalties for the structural features HetHet (two adjacent heteroatoms) and HetC (a heteroatom adjacent to a carbon atom) possess periodic trends (increase along the period and decrease down the group) for various p-block heteroatoms in 11-vertex *nido*-heteroboranes and -

borates.² Here, the study of HetHet and HetC structural features is extended to the 12-vertex *closo*-cluster for comparison with those from the 11-vertex *nido*-cluster. Both clusters have identical numbers of skeletal electrons (26) and hence have allied cluster shapes: the 11-vertex *nido*-cluster is derived from the 12-vertex *closo*-icosahedron by elimination of one vertex. Therefore, the influence of heteroatoms can be expected to be similar in both cases, particularly the positions of various heteroatoms relative to each other. For *closo*-compounds the number of possible isomers is very limited due to the high symmetry of the spherical cluster shapes. In 12 vertex *closo*-diheteroboranes, each structural feature is present only in one isomer (e.g. 1,2-C₂B₁₀H₁₂ has ortho carbon atoms, its 1,7- and 1,12-isomers have carbon atoms in meta and para positions, respectively). On the basis of these, it is therefore impossible to decide if the destabilization due to certain structural features is special for one isomer or has a general meaning. For the 11-vertex *nido*-clusters, the number of possible isomeric structures is vast due to the less symmetric cluster shape and due to the presence of additional hydrogen atoms. It has already been shown that the relative energies can, nevertheless, be estimated quite accurately by a small number of energy penalties related to certain structural features. In this chapter, quantitative rules are explored that apply both for 12-vertex *closo*- and 11-vertex *nido*-compounds.

4.2. Results and Discussion

4.2.1. Periodic Trends of Heteroatom Energy Penalties for the 12-Vertex *closo*-Cluster.

Thermodynamic stabilities of Het₂B₁₀H₁₀ isomers have been determined where Het = two-electron donating group 13 heterogroup, i.e. H-Al, H-Ga, H-In, H-Tl, three electron donating exo-substituted group 14 heteroatoms, i.e. H-C, H-Si, H-Ge, H-Sn and H-Pb, and three electron donating group 15 heteroatoms, i.e. N, P, As, Sb and Bi. The thermodynamic stabilities of the diheterododecaboranes and -borates depend on the position of the heteroatoms relative to each other and can be expressed in the following terms: HetHet_o is the energy difference of the

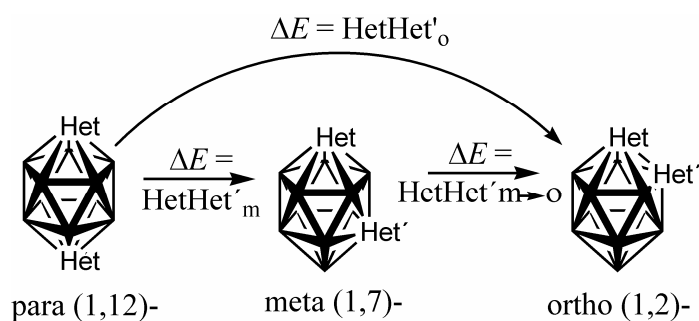


Figure 4.1: a) Structural features HetHet'_o, HetHet'_m and HetHet'_{m→o} for 12-vertex *closo*-HetHet'B₁₀H₁₀.

ortho(1,2)- with respect to the para(1,12)-isomer (Figure 4.1) while HetHet_m is the energy difference of the meta(1,7)- with respect to the para(1,12)-isomer.

$\text{HetHet}_{m \rightarrow o}$, the energy difference of the ortho(1,2)- with respect to the meta(1,7)-isomer results as the difference of HetHet_m and HetHet_o (Chart 4.1). Generally, HetHet_o and $\text{HetHet}_{m \rightarrow o}$ have larger

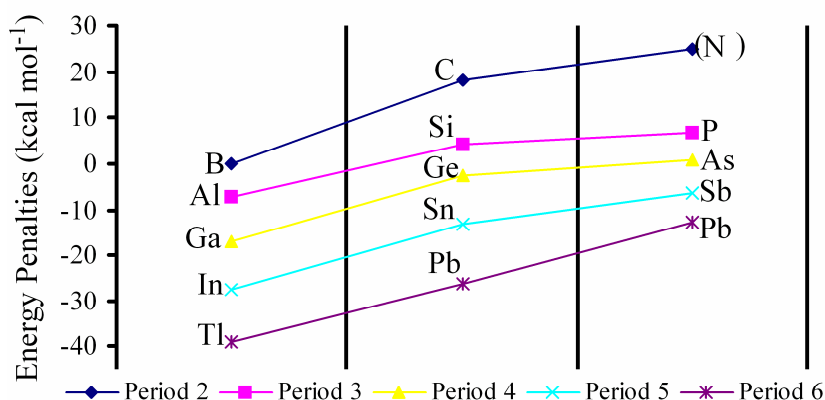


Figure 4.2: HetHet_o energy penalties for 12-vertex *closo*-clusters generally decrease down the group and increase along the period. The energy penalty for NN_o (included in parenthesis) was obtained by fixing the N-N bond distance to be 1.775 Å in the ortho- $\text{N}_2\text{B}_{10}\text{H}_{10}$ isomer because an icosahedral structure without fixed bond distances did not survive geometry optimization.

values than HetHet_m for diheteroboranes and -borates. The thermodynamic stabilities of the diheterododecaboranes and -borates also depend upon the position of heteroatoms in the Periodic Table. Energy penalties for HetHet_o (two heteroatoms adjacent to each other) decrease down the group. For example, among group 14 heteroatoms (Figure 4.2, Chart 4.1), preference of para vs. ortho of $\text{C}_2\text{B}_{10}\text{H}_{12}$ (+18 kcal mol⁻¹) is diminished in $\text{Si}_2\text{B}_{10}\text{H}_{12}$ (+4 kcal mol⁻¹) and reversed for the Ge homolog (-2.4 kcal mol⁻¹). The ortho preference is even more pronounced for Sn (-13 kcal mol⁻¹) and Pb (-26.2 kcal mol⁻¹). The same trend is observed for N (+25.0 kcal mol⁻¹) → Bi (-12.6 kcal mol⁻¹). Among exo-substituted group 13 heteroatoms, aluminium has the largest HetHet_o energy penalties while thalium has the smallest.

HetHet_o energy penalties generally increase (become more positive) along one period; e.g. along the second period, energy penalties increase from zero (for two adjacent boron atoms) to 15.9 kcal mol⁻¹ for two adjacent carbon atoms. The energy penalty for NN (two adjacent nitrogen atoms) was obtained by fixing N-N bond distance in the ortho isomer to be 1.775 Å, as otherwise the cluster distorted upon full optimization to have a four-membered open face. HetHet_o energy penalties increase along Al to P in the 3rd period, Ga to As in the 4th, In to Sb in the 5th and Tl to Bi in the 6th period (Figure 4.2, Chart 4.1). Thermodynamic stabilities of $\text{HetCB}_{10}\text{H}_{11}$ isomers (where Het = heteroatom) were also computed and corresponding values for the relative placement of a heteroatom adjacent to a carbon atom (HetC_o) are also included in Chart 4.1.

4. 12-VERTEX *CLOSO* HETEROBORANES

 Chart 4.1: Periodic trends of HetHet and HetC energy penalties in 12-vertex *closo*-hetero(carba)boranes and -borates.

Het ^a		χ^b	a. r. ^c	
HetHet ^d		HetC ^e		
o ^f		o ^f		
m→o ^g		m→o ^g		
m ^h		m ^h		
Group 13		Group 14		Group 15
B	2.04 85	C	2.55 70	N 3.04 65
0.0	0.0	18.2	18.2	25.0 ⁱ 22.6
0.0	0.0	15.9	15.9	24.6 ⁱ 16.6
0.0	0.0	2.3	2.3	0.4 6.0
Al	1.61 125	Si	1.9 110	P 2.19 100
-7.7	-1.0	4.0	14.1	6.7 15.6
-4.9	-2.6	2.7	9.6	4.4 12.7
-2.8	1.6	1.4	4.4	2.3 2.9
Ga	1.81 130	Ge	2.01 125	As 2.18 115
-16.5	-0.4	-5.4	14.5	0.8 14.7
-14.3	-8.5	-5.9	10.2	-0.7 11.8
-2.2	8.1	0.5	4.3	1.5 2.8
In	1.78 155	Sn	1.96 145	Sb 2.05 145
-25.3	-1.7	-13.0	12.4	-6.4 13.7
-22.1	-3.4	-7.1	8.2	-7.4 10.5
-3.2	1.7	-5.9	4.2	1.0 3.0
Tl	1.62 190	Pb	2.33 180	Bi 2.02 160
-39.0	-4.1	-26.2	8.1	-12.6 12.2
-33.0	-6.2	-9.2	4.6	-11.2 9.4
-6.0	-2.1	-17.0	3.5	-1.4 2.8

^a Heteroatom ^b Electronegativity values, see Pauling, L. *The Nature of the Chemical Bond* Cornell University Press: Ithaca, New York, 1960. ^c These values are an empirical set of atomic radii (pm) derived by the careful comparison of bond lengths in over 1200 bond types in ionic, metallic, and covalent crystals and molecules. For details see Slater, J. C. *J. Chem. Phys.* **1964**, *39*, 3199. ^d The energy penalties (kcal mol⁻¹) for the positions of two equal heteroatoms relative to each other ^e The energy penalties (kcal mol⁻¹) for the positions of a heteroatom relative to a carbon atom ^f The energy difference (kcal mol⁻¹) of an ortho- with respect to its para-isomer ^g The energy difference (kcal mol⁻¹) of an ortho- with respect to its meta-isomer ^h The energy difference (kcal mol⁻¹) of a meta- with respect to its para-isomer ⁱ The NN_o and NN_{m→o} energy penalties were obtained by fixing the N-N bond distance in ortho-N₂B₁₀H₁₀ to 1.775 Å. The full optimization of ortho-N₂B₁₀H₁₀ led to a distorted structure with a four-membered open face.

4. 12-VERTEX *CLOSO* HETEROBORANES

The energy range of HetC_o energy penalties is much smaller and the values generally diminish down the 13th, 14th and 15th group, although the trends are less strictly followed. For example, Ga has a higher energy penalty than Al in group 13, and Ge has a higher HetC_o energy penalty than Si in group 14. HetC_o values, however, always become more positive along the 3rd, 4th, 5th, and 6th period, without any exception. HetHet_{m→o} and HetC_{m→o} energy penalties for 12-vertex *closo*-Het₂B₁₀H₁₀ and HetCB₁₀H₁₁ clusters also decrease down the group and increase along the period (Chart 4.1).

Table 4.1. Direct comparison of HetHet energy penalties in kcal mol⁻¹, for *exo*-substituted group 14 heteroatoms in 12-vertex *closo*- and 11-vertex *nido*-clusters.

Heteroatom	12-vertex <i>closo</i> -	11-vertex <i>nido</i> - ^a	Δ
Group 13 Heteroatoms			
H-C	16	16	0
H-Si	3	9	6
H-Ge	-3	4	7
H-Sn	-7	3	10
Group 14 Heteroatoms			
N ^b	25	41	32
P	4	11	7
As	-1	7	8
Sb	-7	4	11

^a Values taken from ref. 5d. ^b The NN_{m→o} energy penalty was obtained by fixing the N-N bond distance in *ortho*-N₂B₁₀H₁₀ to 1.775 Å. The full optimization of *ortho*-N₂B₁₀H₁₀ led to a distorted structure with a four-membered open face on which the nitrogen atoms occupied opposing sites, as in a diamond-square-diamond intermediate.

Periodic trends of energy penalties can be explained on the basis of the extent of electron localization due to a heteroatom. Within the same group, all heteroatoms formally donate the same number of electrons to the cluster. However, the larger electronegativities of smaller heteroatoms, generally result in enhanced electron localization and hence larger energy penalties. There is a steady increase in HetHet and HetC energy penalties of group 14 members as compared to group

13 members but a less pronounced increase is observed for group 15 members (see HetHet_o and HetC_o curves in Figure 4.2). This is because group 13 heteroatoms formally localize two electrons at one vertex but group 14 and 15 heteroatoms localize three electrons. The increase in energy penalties for group 15 heteroatoms as compared to group 14 heteroatoms is, however, due to higher electronegativity, that further enhances the extent of electron localization.

4.2.2. Redefining $\text{Het}_{5k(2)}$ and HetHet in Terms of Connection Increments.

The $\text{HetHet}_{m \rightarrow o}$ energy penalties for group 14 heteroatoms in 11-vertex *nido*- and equivalent $\text{HetHet}_{m \rightarrow o}$ in 12-vertex *closo*-clusters are listed next to each other in Table 4.1 (also see Figure 4.3). The $\text{CC}_{m \rightarrow o}$ energy penalty for two neighboring carbon atoms is very similar for both *closo*- and *nido*-clusters. For all other heteroatoms, $\text{HetHet}_{m \rightarrow o}$ values are surprisingly smaller for the 12-vertex *closo*-cluster as compared to $\text{HetHet}_{m \rightarrow o}$ for the 11-vertex *nido*-cluster. $\text{HetHet}_{m \rightarrow o}$ values reported for the *nido*-cluster are all positive (meaning heteroatoms apart are generally more favorable) but a number of heteroatoms (especially large ones) have negative $\text{HetHet}_{m \rightarrow o}$ (and also HetHet_o) values for the 12-vertex *closo*-cluster (meaning ortho isomers are more stable). Furthermore, the difference of $\text{HetHet}_{m \rightarrow o}$ energy penalties between the 11-vertex *nido*- and 12-vertex *closo*-cluster (Δ) increases with the size of the heteroatom ($\text{Sn} > \text{Ge} > \text{Si} > \text{C}$, Figure 4.3). HetHet energy penalties are also significantly different for the 11-vertex *nido*- and the 12-vertex *closo*-cluster for group 15 heteroatoms (Table 4.1, Figure 4.3). The difference of energy penalties of a given heteroatom for the two clusters increases from P to Sb (Figure 4.3).

This apparently means different energy penalties for the same structural features in 11-vertex *nido*- and 12-vertex *closo*-cluster, in spite of very similar cluster structure and the same electronic requirement of 13 skeletal electron pairs for each cluster. Therefore increments were considered for individual “bonds” (or better bonding connections) rather than for structural features for a

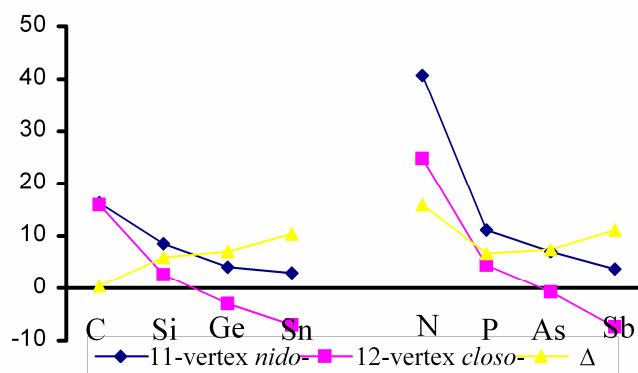


Figure 4.3: $\text{HetHet}_{m \rightarrow o}$ energy penalties for 11-vertex *nido*- and 12-vertex *closo*-clusters of Group 14 and 15 heteroatoms. The energy penalty for $\text{NN}_{m \rightarrow o}$ (included in parenthesis) was obtained by fixing the N-N bond distance to be 1.775 Å in the ortho- $\text{N}_2\text{B}_{10}\text{H}_{10}$ isomer as an icosahedral structure without fixed bond distances did not survive geometry optimization.

universal treatment of both cluster types.

Figure 4.4a shows two isomeric $[\text{CB}_{10}\text{H}_{11}]^{3-}$ structures, i.e. 7- $[\text{CB}_{10}\text{H}_{11}]^{3-}$ (**A**) and 2- $[\text{CB}_{10}\text{H}_{11}]^{3-}$ (**B**). The former has a carbon atom at the open face while the latter has the carbon atom at an unfavorable 5-coordinate vertex (vertex number 2). Hence, the difference may be described by the disfavoring structural feature $\text{C}_{5k}(2)$ with an increment of 28 kcal mol^{-1} in the latter (**B**), while the former (**A**) is a structure without any disfavoring structural feature (carbon at the lowest possible coordinated vertex).^{5c} The first structure, 7- $[\text{CB}_{10}\text{H}_{11}]^{3-}$, described in terms of heteroatom cluster connections has four C–B bonding connections while the latter has five C–B bonding connections. The presence of one additional C–B connection in **B** as compared to **A** has to reflect the stability difference of 28 kcal mol^{-1} . Hence, the C–B connection increment is attributed a (destabilizing) value of 28 kcal mol^{-1} .⁶





	a)		b)	
	A	B	C	D
Name	7- $[\text{CB}_{10}\text{H}_{11}]^{3-}$	2- $[\text{CB}_{10}\text{H}_{11}]^{3-}$	7,9- $[\text{C}_2\text{B}_9\text{H}_{11}]^{2-}$	7,8- $[\text{C}_2\text{B}_9\text{H}_{11}]^{2-}$
Skeletal Structure				
Computed Relative Energy	$E_{\text{calc}} = 0$	$E_{\text{calc}} = 28$	$E_{\text{calc}} = 0$	$E_{\text{calc}} = 16$
I Structural feature approach	No structural feature	$\text{C}_{5k}(2) = 28$	No structural feature	$\text{CC} = 16$
II Connection Increment	4 C–B	5 C–B C–B = 28	8 C–B = $8 \cdot 28 = 224$ $E_{\text{inc}}^{\text{rel}} = 0$	6 C–B = $6 \cdot 28 = 168$ 1 C–C = $1 \cdot 72 = 72$ Sum = 240 $E_{\text{inc}}^{\text{rel}} = 16$

Figure 4.4: Comparison of a) 7- $[\text{CB}_{10}\text{H}_{11}]^{3-}$ with 2- $[\text{CB}_{10}\text{H}_{11}]^{3-}$ as well as b) 7,9- $[\text{C}_2\text{B}_9\text{H}_{11}]^{2-}$ with 7,8- $[\text{C}_2\text{B}_9\text{H}_{11}]^{2-}$ using I) the structural increment approach and II) the connection increment approach (all energy values in kcal mol^{-1}). The values reported in Table 2 are slightly different due to statistical fitting procedure.

⁶ As there are no classical 2c2e bonds in the clusters considered. Bonding “connection increments” rather than bond increments are used to refer to bonding connections in clusters

The 16 kcal mol⁻¹ energy difference of 7,9-[C₂B₉H₁₁]²⁻ (C) and 7,8-[C₂B₉H₁₁]²⁻ (D) (Figure 4.4b) is due to the presence of adjacent carbon atoms (structural feature CC) in the latter with an energy penalty of 16 kcal mol⁻¹.^{5c} These two structures can also be distinguished on the basis of connection increments: 7,9-[C₂B₉H₁₁]²⁻ has eight C–B bonding connections while 7,8-[C₂B₉H₁₁]²⁻ has six C–B bonding connections in addition to one C–C bonding connection.

7,9-[C₂B₉H₁₁]²⁻ accumulates 224 kcal mol⁻¹ due to eight C–B (8·28) and is 16 kcal mol⁻¹ less stable than the 7,8-isomer. In order to reproduce the relative energy, the latter must have a total of 240 kcal mol⁻¹ of connection increment energy. Six C–B contribute 168 kcal mol⁻¹, the remaining 72 kcal mol⁻¹ are deduced as connection increment for C–C.

Two structures differing in para and meta positions of two carbon atoms may be differentiated on the basis of CC_m (Figure 4.5). It cannot be treated in terms of connection increments, due to the same number of C–B connections in the para- and meta-isomers (Figure 4.5). However, this structural feature has a very small energy penalty (2 kcal mol⁻¹) for both 11-vertex *nido*- and 12-vertex *closo*-clusters.⁷ Both 2,9-[C₂B₉H₁₁]²⁻ (E) and 2,8-[C₂B₉H₁₁]²⁻ (F) have nine C–B connections. Four C–B connections are due to a carbon atom at the open face and the remaining five C–B connections involve a carbon atom in the middle belt. Likewise *closo*-C₂B₁₀H₁₂ has ten C–B connections for both the para (G) and the meta-isomer (H).

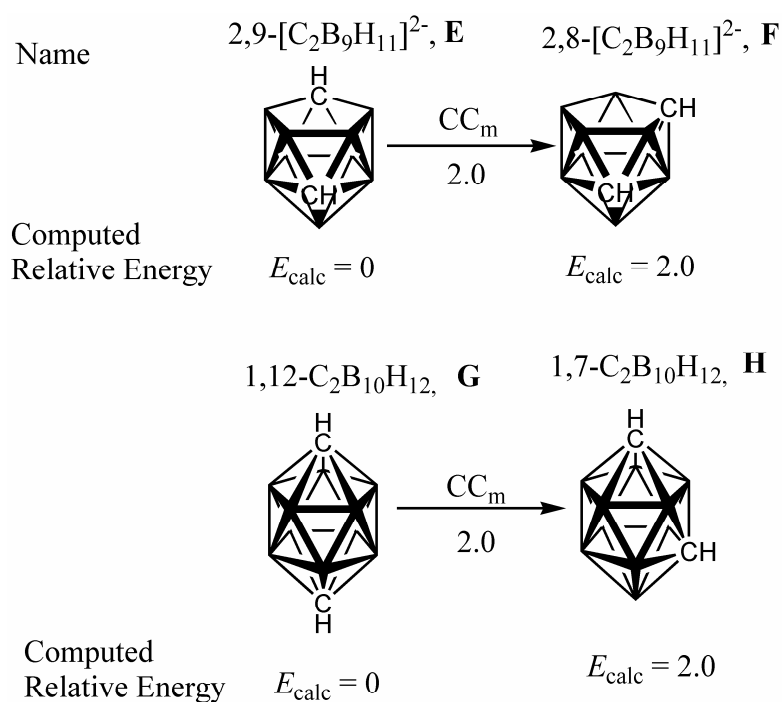


Figure 4.5: Structural feature CC_m differentiates between 2,9- (E) and 2,8-[C₂B₉H₁₁]²⁻ (F) and 1,12- (G) and 1,7-C₂B₁₀H₁₂ (H) (all values in kcal mol⁻¹).

⁷ As the preference of para over meta positions is only minor and in order to make the overall structural increment scheme simpler, a CC_m increment was not included for the 11-vertex *nido*-cluster

4. 12-VERTEX *CLOSO* HETEROBORANES

Table 4.2. The relative stabilities (kcal mol⁻¹) of 11-vertex *nido*-^a and 12-vertex *closo*-carborane isomers based on a common set of increments.

Formula	C-B	C-C	CC _m	$\sum E_{\text{inc}}$	$E_{\text{inc}}^{\text{rel}}$	$E_{\text{calc}}^{\text{b}}$	ΔE^{c}
	27	71	1				
7-CB ₁₀ H ₁₁ ³⁻	4			108	0	0	0
2-CB ₁₀ H ₁₁ ³⁻	5			135	27	26	1
7,9-C ₂ B ₉ H ₁₁ ²⁻	8		1	217	0	0	0
7,8-C ₂ B ₉ H ₁₁ ²⁻	6	1		233	16	16	0
2,9-C ₂ B ₉ H ₁₁ ²⁻	9			243	26	27	-1
2,8-C ₂ B ₉ H ₁₁ ²⁻	9		1	244	27	29	-2
2,7-C ₂ B ₉ H ₁₁ ²⁻	7	1		260	43	43	0
7,8,10-C ₃ B ₈ H ₁₁ ⁻	10	1	2	343	0	0	0
7,8,9-C ₃ B ₈ H ₁₁ ⁻	8	2	1	359	16	19	-3
1,12-C ₂ B ₁₀ H ₁₂	10			270	0	0	0
1,7-C ₂ B ₁₀ H ₁₂	10		1	271	1	2	-1
1,2-C ₂ B ₁₀ H ₁₂	8	1		287	17	18	-1
1,7,9-[C ₃ B ₉ H ₁₂] ⁺	15		3	408	0	0	0
1,2,12-[C ₃ B ₉ H ₁₂] ⁺	13	1	1	423	15	14	1
1,2,8-[C ₃ B ₉ H ₁₂] ⁺	13	1	2	424	16	17	-1
1,2,4-[C ₃ B ₉ H ₁₂] ⁺	11	2	1	440	32	33	-1
1,2,3-[C ₃ B ₉ H ₁₂] ⁺	9	3		456	48	49	-1

^a If endo-hydrogen atoms are present, additional increments as reported in ref. 5c may be needed. These can be used together with the bonding connection increments reported here. ^b Computed relative energies for 11-vertex *nido*-carboranes and -borates are taken from ref. 5c. ^c ΔE is the energy difference of $E_{\text{inc}}^{\text{rel}}$ and E_{calc} .

Upon statistical fitting to E_{calc} of the isomers reported in Table 4.2, the energy penalties for C-B, C-C and CC_m change slightly to 27, 71 and 1 kcal mol⁻¹, respectively. These energy penalties suffice to reproduce the relative energies of various 11-vertex *nido*-carborates and 12-vertex *closo*-carboranes and -borates (Table 4.2). For instance, 7,8,10-[C₃B₈H₁₁]⁻ has ten C-B connections, one C-C connection and twice the structural feature CC_m. $\sum E_{\text{inc}}$ (the sum of increments) is 343 kcal mol⁻¹. 7,8,9-[C₃B₈H₁₁]⁻ has eight C-B connections, two C-C connections and one CC_m structural feature. The sum of increments ($\sum E_{\text{inc}}$) is 359 kcal mol⁻¹ with $E_{\text{inc}}^{\text{rel}}$ (the relative energy of the

4. 12-VERTEX *CLOSO* HETEROBORANES

7,8,9-isomer as compared to the 7,8,10-isomer) is 16 kcal mol⁻¹ as predicted by the increment scheme. E_{calc} (the DFT computed relative energy) comes out to be 19 kcal mol⁻¹ for the 7,8,9-isomer as compared to the 7,8,10-isomer. The difference in relative energy between the two methods is 3 kcal mol⁻¹. The same set of increments has been applied to 11-vertex *nido*-carboranes with one, two and three carbon atoms and also to *closo*-carboranes with two and three carbon atoms (Table 4.2).

Table 4.3. The relative stabilities (kcal mol⁻¹) of 11-vertex *nido*- and 12-vertex *closo*-germaborane and germacarbaborane isomers based on a common set of increments.

Formula	C-B	Ge-B	Ge-Ge	GeGe _m	Ge-C	GeC _m	$\sum E_{\text{inc}}$	$E_{\text{inc}}^{\text{rel}}$	$E_{\text{calc}}^{\text{a}}$	ΔE
	28	44	90	2	82	1				
7-GeB ₁₀ H ₁₁ ³⁻		4					176	0	0	0
2-GeB ₁₀ H ₁₁ ³⁻		5					220	44	44	0
7,9-Ge ₂ B ₉ H ₁₁ ²⁻		8		1			354	0	0	0
7,8-Ge ₂ B ₉ H ₁₁ ²⁻		6	1				354	1	4	-4
7,9-GeCB ₉ H ₁₁ ²⁻	4	4				1	289	0	0	0
<i>nido</i> 7,8-GeCB ₉ H ₁₁ ²⁻	3	3			1		298	9	8	1
1,12-GeCB ₁₀ H ₁₂	5	5					360	0	0	0
1,7-GeCB ₁₀ H ₁₂	5	5				1	361	1	4	-3
1,2-GeCB ₁₀ H ₁₂	4	4			1		370	10	15	-5
1,12-Ge ₂ B ₁₀ H ₁₂		10					440	0	0	0
1,7-Ge ₂ B ₁₀ H ₁₂		10		1			442	2	0	1
<i>closo</i> 1,2-Ge ₂ B ₁₀ H ₁₂		8	1				442	2	-2	4

^a E_{calc} values for 11-vertex *nido*-germaboranes and -borates and germacarbaboranes and -borates are taken from ref. 5d.

Following the same approach, the relative stabilities of various other 11-vertex *nido*- and 12-vertex *closo*-heteroboranes and -borates can successfully be estimated by a single set of increments. This connection increment approach can be further expanded to 11-vertex *nido*- and 12-vertex *closo*-heterocarbaboranes and -borates with two different heteroatoms (i.e. Het and C). Table 4.3 indicates how the relative stabilities of germaboranes and -borates, germacarbaboranes and -borates can be reproduced using the additional connection increments, Ge-C, Ge-B, Ge-Ge,

and structural increments CGe_m and $GeGe_m$.

The method can be used to get the relative stabilities of other heterocarbaboranes and -borates. Some 11-vertex *nido*-heteroboranes and -borates like $2-[NB_{10}H_{11}]^{2-}$,² $2-[SnB_{10}H_{11}]^{3-}$ and $2-[AsB_{10}H_{11}]^{2-}$,^{5d} did not optimize to a regular 11-vertex *nido*-cluster due to cluster distortion.² Likewise differences of the estimated against the DFT computed relative energy larger than 5 kcal mol⁻¹ result for 2,7-, 2,8- and 2,9- $[Sn_2B_9H_{11}]^{2-}$ structures. They all have a tin atom at vertex number 2 and show significant cluster distortion. The strength of bonding interaction of one heteroatom with its cluster neighbors should depend on its overall connectivity. Bond increments therefore should also depend on the connectivity. However, at least for 4k vs. 5k, the difference seems to be small enough for the approach to work well.

4.2.3. Heavy Heteroatoms at Adjacent Positions in the Thermodynamically Most Stable 12-Vertex *closo*-Isomer; a Phenomenon Supported by Experimental Results.

Williams³ qualitative heteroatom placement rules have long remained the only theoretical tool to quickly determine the positions of heteroatoms in the thermodynamically most stable heteroboranes and -borates. These rules suggest least connected, non-adjacent vertices for heteroatoms in the thermodynamically most stable heteroborane isomers. DFT computations coupled with quantitative structural increment approach, however, helped to rationalize the presence of heteroatoms at highly connected vertices in thermodynamically most stable isomers for a number of structures in 10- and 11-vertex *nido*-heteroboranes and -borates.^{2,5b-d}

Here, computations demonstrate that if equivalently connected vertices are available (as in the 12-vertex *closo*-cluster), heavy heteroatoms tend to occupy adjacent vertices in the thermodynamically most stable isomer. Chart 4.1 shows larger (more positive) HetHet energy penalties for smaller heteroatoms. As a consequence, they rearrange to the more stable meta and para-isomers upon heating (Figure 4.6) as is known from experiments.⁸ For example, 2,1- $PCB_{10}H_{11}$ undergoes thermal rearrangement at 485 °C to form the 1,7-isomer,⁹ while at higher temperature (650 °C) significant amounts of the 1,12-isomer are formed.¹⁰

⁸ Štíbr, B. *Collect. Czech. Chem. Commun.* **2002**, 67, 843-868; references therein.

⁹ Little, J. L.; Moran, J. T.; Todd, L. J.; *J. Am. Chem. Soc.* **1967**, 89, 5495-5496.

¹⁰ Todd, L. J.; Little, J. L.; Silverstein, H. T.; *Inorg. Chem.* **1969**, 8, 1698-1703.

However, numerous experimental structures were reported with two heavy heteroatoms in the ortho position such as 1,2-As₂B₁₀H₁₀,¹¹ 1,2-Sb₂B₁₀H₁₀,^{11,12} 1,2-SbAsB₁₀H₁₀¹² or 1,2-HetBiB₁₀H₁₀¹³ (Het = P, As, Sb, Bi) but no meta or para-rearrangements were reported. As seen from smaller (more negative) HetHet energy values, the ortho-isomers are favored as compared to meta- and para-isomers for larger heteroatoms (Figure 4.6) and no isomerization takes place upon heating the ortho compounds.

The stability order of para > meta > ortho is not generally valid! Chart 4.1 shows that this is only the case for Het = C, Si, N, P.

Note that in the third column in Chart 5.1 (group 14 members) there is no parallel trend of para→ortho and meta→ortho quantitatively, i.e., both become more negative when going down, but para→ortho much more. As a consequence para→meta becomes really significant. In all other cases, it remains small.

4.3. Conclusion

A single connection increment scheme is presented that can give the relative stabilities of 11-vertex *nido*- as well as 12-vertex *closo*-clusters with different heteroatom substitution patterns. The Het_{5k} and HetHet structural increments proposed for the 11-vertex *nido*-cluster^{2,5} may be transformed to bonding connection increments that can be used for 12-vertex *closo*-clusters. Connection increments are still applicable to 11-vertex *nido*-heteroboranes and -borates along with other structural features. Hence, for the 11-vertex *nido*-cluster, the resulting estimated relative energies have exactly the previously reported values. The energy differences between para- to ortho-, and meta- to ortho-12-vertex *closo*-diheteroborane clusters follow strictly periodic trends. Smaller

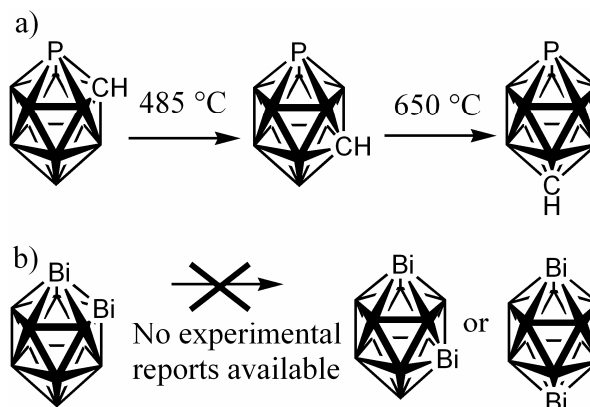


Figure 4.6: a) ortho-2,1-PCB₁₀H₁₁ undergoes thermal rearrangement to give meta and para isomers due to PC₀ energy penalty of 15.6 kcal mol⁻¹. b) ortho-Bi₂B₁₀H₁₀ does not undergo any rearrangement: it is the most stable isomer as reflected by a negative BiBi₀ energy penalty (-12.6 kcal mol⁻¹).

¹¹ Fontaine, X. L. R.; Kennedy, J. D.; McGrath, M.; Spalding, T. R. *Magn. Reson. Chem.* **1991**, *29*, 711-720.

¹² Little, J. L. *Inorg. Chem.* **1979**, *18*, 1598-1600.

¹³ Little, J. L.; Whitesell, M. A.; Kester, J. G.; Folting, K.; Todd, L. J. *Inorg. Chem.* **1990**, *29*, 804-808.

4. 12-VERTEX *CLOSO* HETEROBORANES

heteroatoms tend to occupy non-adjacent, while larger heteroatoms tend to occupy adjacent vertices in thermodynamically most stable diheteroborane isomers.

5. Ortho-, Meta- and Para-Directing Influence of Transition Metal Fragments in 12-vertex *closo*-Cyclopentadienyl Metallaheteroboranes: Additive Nature of Structural Increments

5.1. Introduction

Transition metals may occupy vertexes in deltahedral boranes and related heteroboranes as was shown for the first time by Hawthorne and co-workers.¹ Typically units of the type CpM (Cp = cyclopentadienyl; M = transition metal) replace BH or CH moieties. A large number of such structures are experimentally known² with various metals, e.g., Fe,³ Co,^{3a,4} Ni,^{4e} Ru,⁵ and Rh^{4d} in which a CpM fragment itself or its alkyl derivatives simply replace a BH vertex of a deltahedron so that the cage topology remains the same. The topology of such clusters can be derived by Wade's well-established

¹ Callahan, K. P.; Hawthorne, M. F. *Adv. Organomet. Chem.* **1976**, *14*, 145-186.

² a) Saxena, A. K.; Hosmane, N. S. *Chem. Rev.* **1993**, *93*, 1081-1124; references therein. b) Jelliss, P. A. *Organomet. Chem.* **2004**, *31*, 112-129, references therein. c) Hosmane, N. S.; Maguire, J. A. *Eur. J. Inorg. Chem.* **2003**, *22*, 3989-3999.

³ a) Shirokii, V. L.; Knizhnikov, V. A.; Vinokurov, I. I.; Bazhanov, A. A.; Mayer, N. A. *Russian Journal of General Chemistry (Translation of Zhurnal Obshchei Khimii)* **1997**, *67*, 1185-1187. b) Hawthorne, M. F., Pilling, R. L. *J. Am. Chem. Soc.* **1965**, *87*, 3987-3988. c) Štíbr, B.; Holub, J.; Teixidor, F.; Viñas, C. *Collect. Czech. Chem. Commun.* **1995**, *60*, 2023-2027. d) Zalkin, A.; Templeton, D. H.; Hopkins, T. E. *J. Am. Chem. Soc.* **1965**, *87*, 3988-3990. e) Wiersema, R. J.; Hawthorne, M. F. *J. Am. Chem. Soc.* **1974**, *96*, 761-770. f) Dustin, D. F.; Dunks, G. B.; Hawthorne, M. F. *J. Am. Chem. Soc.* **1973**, *95*, 1109-1115. g) Cerny, V.; Pavlik, I.; Kustkova-Maxova, E. *Collect. Czech. Chem. Commun.* **1976**, *41*, 3232-3244. h) Štíbr, B. *J. Organomet. Chem.* **2005**, *690*, 2857-2859. i) Garcia, M. P.; Green, M.; Stone, F. Gordon A.; Somerville, R. G.; Welch, A. J. *J. Chem. Soc., Chem. Commun.*, **1981**, *16*, 871-872.

⁴ a) Evans, W. J.; Hawthorne, M. F. *Inorg. Chem.* **1974**, *13*, 869-874. b) Evans, W. J.; Dunks, G. B.; Hawthorne, M. F. *J. Am. Chem. Soc.* **1973**, *95*, 4565-4574. c) Hawthorne, M. F.; Kaloustian, M. K.; Wiersemay, R. J. *J. Am. Chem. Soc.* **1971**, *93*, 4912-4913. d) Hanusa, T. P.; Todd, L. J. *Polyhedron* **1985**, *4*, 2063-2066. e) Rietz, R. R.; Dustin, D. F.; Hawthorne, M. F. *Inorg. Chem.* **1974**, *13*, 1580-1584.

⁵ Kudinov, A. R.; Perekalin, D. S.; Rynin, S. S.; Lyssenko, K. A.; Grintselev-Knyazev, G. V.; Petrovskii, P. V. *Angew. Chemie, Int. Ed. Engl.* **2002**, *41*, 4112-4114.

electron-counting rules.⁶ However, a systematic theoretical study of icosahedral heteroboranes incorporating various transition metals has never been carried out.

Among metal free 12-vertex *closo*-heteroboranes, usually small sized, more electronegative, formally electron withdrawing heteroatoms occupy non-adjacent vertexes in the thermodynamically most stable isomer according to Williams' heteroatom placement rule.⁷ A 12-vertex *closo*-cluster with two more electronegative heteroatoms adjacent to each other is highly unfavourable and usually rearranges to more stable meta and para isomers, if enough activation energy is provided. For example, 1,2-PCB₁₀H₁₁ successively rearranges to its 1,7- and 1,12-isomer upon heating.⁸ Larger, less electronegative, formally electron donating heteroatoms, however, tend to occupy adjacent vertexes in thermodynamically most stable 12-vertex *closo*-diheteroborane isomers.⁹ For example, due to its largest thermodynamic stability, the experimentally known ortho (1,2-) isomer of 12-vertex *closo*-Bi₂B₁₀H₁₀¹⁰ is not expected to rearrange into meta (1,7-) or para (1,12-) isomers. In the case of cyclopentadienyl metallaheteroboranes, however, one encounters both situations: Heating of 1,2-CpNiCB₁₀H₁₁ results in cluster rearrangement to a structure with the CpNi and H-C units in meta (1,7-) and para (1,12-) positions,^{4e} thus apparently obeying Williams' heteroatom placement rule.⁷ Similarly, 1-Cp-1,2,3-CoC₂B₉H₁₁ also rearranges into the isomers with carbon atoms at vertexes non-adjacent to the cyclopentadienyl cobalt fragment.^{4c} Contrarily, carbon atoms ortho to the CpFe unit in the experimentally known 1-Cp-1,2,3-FeC₂B₉H₁₁^{3b} do not rearrange to meta or para positions (at least there are no such experimental reports available). We wanted to rationalise such different behaviour of experimentally known 12-vertex *closo*-cyclopentadienyl metallaheteroboranes on the basis of theory and find rules that easily allow to identify the most stable cyclopentadienyl metallaheteroborane isomers.

Such quantitative rules in terms of structural increments or energy penalties, were already established for various *nido*- and *closo*-heteroboranes with different numbers, connectivities and types of

⁶ a) Wade, K. *Adv. Inorg. Chem. Radiochem.* **1976**, 18, 1-66. b) Wade, K. In *Metal Interactions with Boron Clusters*; Grimes, R. N., Ed.; Plenum Press: New York, 1982; Chapter 1, pp 1– 41.

⁷ a) Williams, R. E. *J. Am. Chem. Soc.* **1965**, 87, 3513. b) Williams, R. E. In *Progress in Boron Chemistry* Brotherton, R. J., Steinberg, H., Eds.; Pergamon Press: England, 1970; Vol. 2, Chapter 2, p 57. c) Williams, R. E.; *Chem. Rev.* **1992**, 92, 177-207; references therein.

⁸ Štíbr, B. *Collect. Czech. Chem. Commun.*, **2002**, 67, 843-868; references therein.

⁹ Kiani, F. A.; Hofmann, M. *Dalton Trans.*, **2006**, 5, 686-692.

¹⁰ Little, J. L.; Whitesell, M. A.; Kester, J. G.; Folting, K.; Todd, L. J. *Inorg. Chem.* **1990**, 29, 804-808.

heteroatoms.^{9,11} These allow to accurately reproduce the DFT computed relative stabilities of various 6-, 10- and 11-vertex *nido*- and 12-vertex *closo*-heteroboranes.^{9,11} Here, the structural increment studies are applied to cyclopentadienyl metallaheteroboranes, which in spite of large size and quite different nature of the CpM fragment, show structural features and in turn structural increments of very high additive nature. These structural increments allow not only to reproduce the relative stabilities of a large number of known¹⁻⁵ and unknown isomeric 12-vertex *closo*-metallaheteroboranes, but also to estimate the relative stabilities of various isomers without actually computing them. This study also helped to find out the nature of interaction of two, three and four heteroatoms in a single 12-vertex *closo*-cyclopentadienyl metallaheteroborane cluster. We find that cyclopentadienyl metal fragments are highly specific towards directing the heteroatoms to the ortho-, meta- and para positions in the thermodynamically most stable isomer.

5.2. Results and Discussion

Initially 1,2-, 1,7- and 1,12-[CpM_{CB}₁₀H₁₁]^z, where M = Fe, Ru, Os, Co, Rh, Ir, Ni, Pd and Pt, were computed. These isomers differ only with respect to the positions of the CpM fragment and the H-C moiety. The energy differences of ortho and meta isomers with respect to para isomers gave energy penalties for the structural features MC_o and MC_m, respectively (a CpM fragment at ortho and meta positions relative to a carbon atom, respectively) (see Section 2.1). The energy penalties for MC_o and MC_m reflect the highly specific preference of a CpM fragment towards the positions of a CH moiety in the thermodynamically most stable isomer (Section 2.2). The increase in the extent of electron localization results in a periodically progressive increase in energy penalties of these structural features along the period (Section 2.3). A large number of cyclopentadienyl iron containing 12-vertex *closo*-carborane structures from [CpFeCB₁₀H₁₁]²⁻ to CpFeC₃B₈H₁₁, phosphaborane structures from [CpFePB₁₀H₁₁]²⁻ to CpFeP₃B₈H₈ and phosphacarbaboranes, i.e., [CpFePCB₉H₁₀]⁻, CpFeP₂CB₈H₉ and CpFePC₂B₈H₁₀ were computed in order to check the additive nature of the structural increments for CpM containing 12-vertex *closo*-metallaheteroboranes (Section 2.4). The results help to quickly estimate the relative thermodynamically stabilities of various 12-vertex *closo*-cyclopentadienyl metallacarboranes, where M may be Fe or any other group 8, 9 or 10 metal (Section 2.5).

¹¹ a) Hofmann, M.; Fox, M. A.; Greatrex, R.; Schleyer, P. v. R.; Williams, R. E. *Inorg. Chem.* **2001**, *40*, 1790-1801 b) Kiani, F. A.; Hofmann, M. *Eur. J. Inorg. Chem.*, **2005**, *12*, 2545-2553. c) Kiani, F. A.; Hofmann, M. *Inorg. Chem.*, **2004**, *43*, 8561-8571. d) Kiani, F. A.; Hofmann, M. *Inorg. Chem.*, **2005**, *44*, 3746-3754. e) Kiani, F. A.; Hofmann, M. *J. Mol. Mod.* **2006**, *12*, 597-609.

5.2.1. Structural Features in Metallaheteroboranes.

Compared to *nido*-heteroboranes, the highly symmetrical *closo*-clusters require a small number of structural features. Only two general structural features, i.e., HetHet'_o and HetHet'_m (Figure 5.1) are required for 12-vertex *closo*-heteroboranes.⁹ As it turns out, they behave additively and may be applied to estimate quite accurately the relative stabilities of a large number of cyclopentadienyl metallaheteroborane isomers with up to four heteroatoms.

The structural feature HetHet'_o represents two equal or different heteroatoms adjacent (at ortho positions) to each other. For example, $1,2\text{-P}_2\text{B}_{10}\text{H}_{10}$ has the structural feature PP_o for two adjacent phosphorus atoms, whereas

$[1\text{-Cp-}1,2\text{-FeCB}_{10}\text{H}_{11}]^{2-}$ has the structural feature FeC_o for a CpFe unit adjacent to a carbon atom. The structural increment (energy penalty) for HetHet'_o in a 12-vertex *closo*-diheteroborane is obtained directly by comparing the relative energies of ortho- and para-isomers (Figure 5.1). HetHet'_m is the structural feature for two heteroatoms at meta positions to each other and its increment is obtained as the energy difference of a meta- and its para-isomeric 12-vertex *closo*-cluster.

The energy penalties for various MC_o and MC_m structural features, where one heteroatom is a CpM fragment (M = group 8, 9 or 10 metal) and the other heteroatom is a H-C moiety, are listed in Chart 5.1. The statistically fitted energy penalties for CC_o (two adjacent carbon atoms) = 17.2 kcal mol⁻¹, CC_m (two carbon atoms at meta positions to each other) = 2.2 kcal mol⁻¹, PC_o (a phosphorus and a carbon atoms adjacent to each other) = 12.8 kcal mol⁻¹, PC_m (a phosphorus and a carbon atom at meta positions to each other) = 0.5 kcal mol⁻¹, PP_o (two adjacent phosphorus atoms) = 6.1 kcal mol⁻¹ and PP_m (two

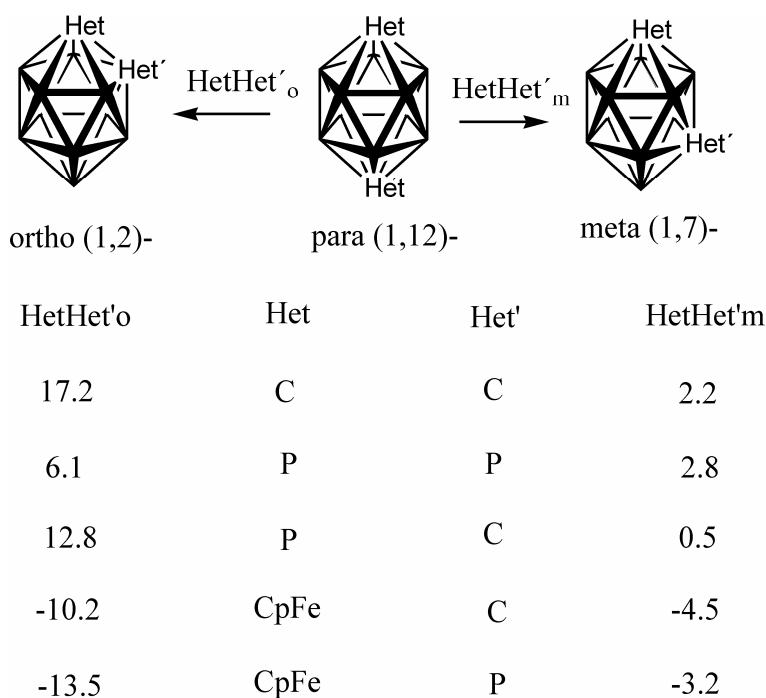


Figure 5.1: Structural features, HetHet'_o and HetHet'_m , in CpM fragment containing 12-vertex *closo*-metallaheteroboranes. Energy penalties (in kcal mol⁻¹) for HetHet'_o and HetHet'_m are the energy differences of ortho (1,2)- and meta (1,7)-isomers with respect to the para (1,12)-isomer. A negative HetHet'_o (or HetHet'_m) means that the ortho (or meta) isomer is thermodynamically more stable than the para isomer.

phosphorus atoms at meta positions to each other) = 2.8 kcal mol⁻¹ as used in 12-vertex *closo*-cyclopentadienyl ferraheteroboranes are listed in Figure 5.1. Except for cobalt, osmium and ruthenium, usually the absolute values for the HetHet'_o energy penalties (Chart 1 and Table 5.1) are larger than those of HetHet'_m. Energy penalties for these structural features can be used to obtain the relative stabilities of various 12-vertex *closo*-cyclopentadienyl metal containing metallaheteroboranes (Section 5.2.4).

5.2.2. Ortho-, Meta- and Para-Directing Influence of Metal Atoms to a Carbon Atom in Metallocarboranes.

Williams' heteroatom placement rule⁶ suggests that heteroatoms occupy as far apart vertices as possible when equivalently connected sites are available. This rule indirectly identifies para directing influences of two heteroatoms on each other in a 12-vertex *closo*-diheteroborane. In this section, the CpM fragments are also shown to be highly specific but not necessarily always para-directing towards the positions of heteroatoms in the metallocarboranes.

Chart 5.1 lists the energy penalties for the structural features MC_o (for a CpM group adjacent to a carbon atom) and MC_m (for a CpM group at meta position to a carbon atom) where M = group 8, 9 or 10 metal. The MC_o and MC_m values are negative for Fe, Ru and Os indicating ortho and meta isomers are more stable than the para-isomer for [CpMCB₁₀H₁₁]²⁻ (where M = Fe, Ru or Os). The more negative FeC_o as compared to the FeC_m energy penalty clearly indicates that the ortho isomer, [1-Cp-1,2-FeCB₁₀H₁₁]²⁻, is energetically favored over its meta isomer i.e., [1-Cp-1,7-FeCB₁₀H₁₁]²⁻, by 5.4 kcal mol⁻¹ which is the numerical difference between -9.0 and -3.6 kcal mol⁻¹, see Chart 5.1). For Ru and Os, more negative MC_m energy penalties indicate that the meta isomers are thermodynamically most stable, although this preference of meta over ortho is only slight (0.7 kcal mol⁻¹) for Os. For cobalt as well, the preference of ortho over para is negligible (-0.02 kcal mol⁻¹) and the meta isomer is thermodynamically most stable. For Rh and Ir, negative MC_m energy penalties also indicate increased thermodynamic stability of the meta isomers. When group 10 metals, i.e., Ni, Pd and Pt are incorporated as CpM fragments, both MC_o and MC_m have positive energy penalties indicating that the para isomers are thermodynamically more stable.

In short, cyclopentadienyl metal fragments of group 9 and 10 metals direct the H-C moiety to meta and para positions in the thermodynamically most stable isomer, respectively. Among group 8 heteroatoms, CpFe directs a H-C moiety to the ortho positions, while CpRu and CpOs direct it to meta positions in thermodynamically most stable isomers.

5. 12-VERTEX *CLOSO*-METALLAHETEROBORANES

 Chart 5.1: Structural increments for 12-vertex *closo*-cyclopentadienyl metallacarboranes.

M^a χ^b C.R. ^c $n(+x)^d$					
MC_o^e MC_m^a					
Group 8 heteroatoms		Group 9 heteroatoms		Group 10 heteroatoms	
Fe	1.83 125 1(+2)	Co	1.88 126 2(+3)	Ni	1.91 121 3(+4)
-9.0 ^b -3.6		-0.02 -1.2		8.5 0.9	
Ru	2.2 126 1(+2)	Rh	2.28 135 2(+3)	Pd	2.2 131 3(+4)
-2.9 -3.6		5.1 -1.2		12.2 0.9	
Os	2.2 128 1(+2)	Ir	2.2 137 2(+3)	Pt	2.28 128 3(+4)
-0.7 -3.4		8.5 -1.4		17.1 1.2	

M denotes cyclopentadienyl metal derivative of a group 8, 9 or 10 metal. ^b Electronegativity values see Pauling, L. *The Nature of the Chemical Bond* Cornell University Press: Ithaca, New York, 1960. ^c Covalent radii in pico meter, see Huheey, J. E.; Keiter, E. A.; Keiter R. L. *Inorganic Chemistry: Principles of Structure and Reactivity*, 4th edition, Harper Collins, New York, USA, 1993. ^d n is the number of electrons formally localized by a given heteroatom (+x values in parentheses indicate the formal positive charge on the metal center of a CpM unit). ^e Structural feature for a CpM fragment at ortho-position relative to a H-C moiety. ^f Structural feature for a CpM fragment at meta-position to a H-C moiety. ^g For FeC_o and FeC_m, the estimated energy penalties (-9.0 and -3.6 kcal mol⁻¹) were obtained by direct comparison of two isomers differing with respect to one structural feature, as in all other cases. Statistical fitting to a large number of isomers resulted in slightly different energy penalties of -10.2 and -4.5 kcal mol⁻¹, for FeC_o and FeC_m respectively.

5.2.3. Periodic Trends in MC_o and MC_m Energy Penalties and Their Dependence on the Extent of Electrons Localized by a CpM Fragment.

Both MC_o and MC_m energy penalties increase along the period, i.e., they are largest for group 10 heteroatoms and smallest for group 8 heteroatoms within one period (Chart 5.1).

It has already been pointed out that the energy penalties of various structural features depend directly on the extent of electron localization by a given heteroatom.^{11d-e} In cyclopentadienyl metallacarboranes, a H-C moiety formally contributes three skeletal electrons per vertex. The number of electrons contributed by a CpM fragment varies, however. The CpM fragments of group 8, 9 and 10 metals formally contribute one, two and three electrons, respectively. Thus the extent of electron localization by the CpM fragments increases along the period. It results in increased energy penalties for the structural feature MC_o (Figure 5.2) and MC_m along the period. CpM fragments of group 8 metals have the smallest while those of group 10 have the largest MC_o and MC_m energy penalties. The increase in energy penalties along the period can also be viewed in the context of positive charge accumulated on the metal center. Group 8, 9 and 10 metal ions can be considered to have formal charges of +2, +3 and +4, respectively. The increase in the energy penalties along the period can be attributed to the positive charge formally assigned to the metal center in a 12-vertex CpM fragment containing *closo*-metallaheteroborane (Figure 5.2 and 5.3).

Energy penalties for $HetHet'_o$ are usually larger as compared to $HetHet'_m$ (see also Section 2.1). As a result the trends for increase in the $HetHet'_o$ energy penalties (Figure 5.2) are much clearer and at a larger scale as compared to those of $HetHet'_m$ energy penalties.

5.2.4. Additive Nature of Structural Increments in Cyclopentadienyl Iron Containing 12-Vertex *closo*-Metallaheteroboranes.

Energy penalties for the structural features $HetHet'_o$ and $HetHet'_m$ are used to reproduce the relative stabilities of various 12-vertex *closo*-cyclopentadienyl iron containing carboranes (Section 2.4.1), phosphaboranes (Section 2.4.2) and phosphacarbaboranes (Section 2.4.3). The energy penalties for the

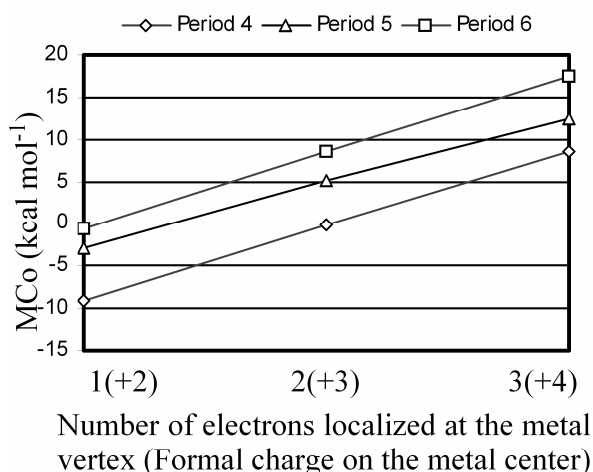


Figure 5.2: The energy penalties for MC_o i.e., a carbon atom adjacent to a cyclopentadienyl metal fragment increases with the increase in the number of electrons localized at the metal vertex (or with the increase in the formal positive charge on the metal center) in the CpM unit.

5. 12-VERTEX *CLOSO*-METALLAHETEROBORANES

two structural features, i.e., HetHet'_o and HetHet'_m were first determined empirically by comparing two isomers differing with respect to one structural feature (see Figure 5.1) and were then refined through a statistical fitting procedure in order to minimize the standard deviation. Out of a total of 101 CpFe fragment containing heteroboranes considered in this study, 14 structures are experimentally known. HetHet'_o and HetHet'_m increments can be used additively to give the relative stability of a large number of metallaheteroborane isomers. Figure 5.3 shows how the structural increment approach can be applied to reproduce the relative stabilities of selected $\text{FePC}_2\text{B}_8\text{H}_{10}$ isomers as an example. The relative stability of the computed structures was reproduced mostly within 3 kcal mol^{-1} . The difference (ΔE) of DFT computed relative energies (E_{calc}) and those derived from increments ($E_{\text{inc}}^{\text{rel}}$) is maximum for **HP** ($5.3 \text{ kcal mol}^{-1}$).

1,2,4,10- (HA)	1,2,3,5- (HB)	1,2,4,5- (HD)	1,2,3,6- (HK)	1,2,3,4- (HM)
$\text{FeC}_o = -10.2$	$2 \cdot \text{FeC}_o = -20.4$	$2 \cdot \text{FeC}_o = -20.4$	$2 \cdot \text{FeC}_o = -20.4$	$2 \cdot \text{FeC}_o = -20.4$
$\text{FeC}_m = -4.5$	$\text{CC}_m = 2.2$	$\text{CC}_o = 17.2$	$\text{CC}_m = 2.2$	$\text{CC}_o = 17.2$
$\text{CC}_m = 2.2$	$\text{FeP}_o = -13.5$	$\text{FeP}_o = -13.5$	$\text{FeP}_o = -13.5$	$\text{FeP}_o = -13.5$
$\text{FeP}_o = -13.5$	$\text{PC}_o = 0.5$	$2 \cdot \text{PC}_m = 1.0$	$2 \cdot \text{PC}_o = 25.6$	$\text{PC}_o = 12.8$
$2 \cdot \text{PC}_m = 1.0$	$\text{PC}_m = 0.5$	$\Sigma E_{\text{inc}} = -15.7$	$\Sigma E_{\text{inc}} = -6.1$	$\text{PC}_m = 0.5$
$\Sigma E_{\text{inc}} = -25.0$	$\Sigma E_{\text{inc}} = -18.4$			$\Sigma E_{\text{inc}} = -3.4$
$E_{\text{inc}}^{\text{rel}} = 0.0$	$E_{\text{inc}}^{\text{rel}} = 6.6$	$E_{\text{inc}}^{\text{rel}} = 9.3$	$E_{\text{inc}}^{\text{rel}} = 18.9$	$E_{\text{inc}}^{\text{rel}} = 21.6$
$E_{\text{calc}} = 0.0$	$E_{\text{calc}} = 5.8$	$E_{\text{calc}} = 9.1$	$E_{\text{calc}} = 18.2$	$E_{\text{calc}} = 21.3$
$\Delta E = 0.0$	$\Delta E = 0.8$	$\Delta E = 0.2$	$\Delta E = 0.7$	$\Delta E = 0.3$

Figure 5.3: DFT computed relative stabilities as well as those from the structural increments of the five selected $\text{CpFePC}_2\text{B}_8\text{H}_{10}$ isomers. Four possible $\text{CpFePC}_2\text{B}_8\text{H}_{10}$ isomers (**HB**, **HD**, **HK** and **HM**) with carbon and phosphorus atoms at ortho positions to the CpFe fragment are thermodynamically less stable as compared with **HA**, which has one carbon atom at the meta-position relative to the CpFe unit.

5. 12-VERTEX *CLOSO*-METALLAHETEROBORANES

Table 5.1. Relative stabilities of $[1\text{-CpFeC}_x\text{B}_{10}\text{H}_{11}]^{(3-x)-}$ isomers

Name	FeC _o	FeC _m	CC _o	CC _m	$\sum E_{\text{inc}}^{\text{a}}$	$E_{\text{inc}}^{\text{rel b}}$	$E_{\text{calc}}^{\text{c}}$	ΔE^{d}
AA $[1\text{-Cp-1,2-FeCB}_{10}\text{H}_{11}]^{2-}$	1				-10.2	0.0	0.0	0.0
AB $[1\text{-Cp-1,7-FeCB}_{10}\text{H}_{11}]^{2-}$		1			-4.5	5.7	3.6	2.1
AC $[1\text{-Cp-1,12-FeCB}_{10}\text{H}_{11}]^{2-}$					0.0	10.2	9.0	1.2
BA $[1\text{-Cp-1,2,4-FeC}_2\text{B}_9\text{H}_{11}]^-$	2			1	-18.2	0.0	0.0	0.0
BB $[1\text{-Cp-1,2,9-FeC}_2\text{B}_9\text{H}_{11}]^-$	1	1			-14.7	3.5	4.4	-0.9
BC $[1\text{-Cp-1,2,8-FeC}_2\text{B}_9\text{H}_{11}]^-$	1			1	-8.0	10.2	6.4	3.8
BD $[1\text{-Cp-1,2,12-FeC}_2\text{B}_9\text{H}_{11}]^-$	1			1	-8.0	10.2	10.8	-0.6
BE $[1\text{-Cp-1,2,3-FeC}_2\text{B}_9\text{H}_{11}]^-$	2		1		-3.2	15.0	16.0	-1.0
CA $1\text{-Cp-1,2,4,10-FeC}_3\text{B}_8\text{H}_{11}$	2	1		1	-20.5	0,0	0,0	0.0
CB $1\text{-Cp-1,2,3,5-FeC}_3\text{B}_8\text{H}_{11}$	3		1	2	-9.0	11.5	8.8	2.7
CC $1\text{-Cp-1,2,3,9-FeC}_3\text{B}_8\text{H}_{11}$	2	1	1	1	-5.5	15.0	14.2	0.8
CD $1\text{-Cp-1,2,4,7-FeC}_3\text{B}_8\text{H}_{11}$	2	1	1	2	-3.3	17.2	15.7	1.5
CE $1\text{-Cp-1,2,7,9-FeC}_3\text{B}_8\text{H}_{11}$	1	2	1	1	0.2	20.7	20.4	0.3
CF $1\text{-Cp-1,2,3,12-FeC}_3\text{B}_8\text{H}_{11}$	2		1	2	1.2	21.7	22.0	-0.3
CG $1\text{-Cp-1,2,3,4-FeC}_3\text{B}_8\text{H}_{11}$	3		2	1	6.0	26.5	25.5	1.0
CH $1\text{-Cp-1,2,3,8-FeC}_3\text{B}_8\text{H}_{11}$	2	1	2	1	11.7	32.2	32.4	-0.2
CI $1\text{-Cp-1,2,7,8-FeC}_3\text{B}_8\text{H}_{11}$	1	2	2	1	17.4	37.9	38.1	-0.2
CJ $1\text{-Cp-1,2,7,12-FeC}_3\text{B}_8\text{H}_{11}$	1	1	2	1	21.9	42.4	43.4	-1.0
CK $1\text{-Cp-1,2,3,7-FeC}_3\text{B}_8\text{H}_{11}$	2	1	3		26.7	47.2	46.7	0.5
CL $1\text{-Cp-1,2,7,11-FeC}_3\text{B}_8\text{H}_{11}$	1	2	3		32.4	52.9	53.3	-0.4
CM $1\text{-Cp-1,7,8,12-FeC}_3\text{B}_8\text{H}_{11}$		2	3		42.6	63.1	63.6	-0.5

^a $\sum E_{\text{inc}}$ is the sum of energy penalties for all structural features in a given structure. ^b $E_{\text{inc}}^{\text{rel}}$ is the relative stability of a given isomer with respect to the most stable one. ^c E_{calc} is the relative stability of a given isomer as obtained from calculations. ^d ΔE is the difference of $E_{\text{inc}}^{\text{rel}}$ and E_{calc} .

5.2.4.1. $[\text{CpFeC}_x\text{B}_{11-x}\text{H}_{11}]^{(3-x)-}$ ($x = 1,2,3$) isomers.

$[1\text{-Cp-1,2-FeCB}_{10}\text{H}_{11}]^{2-}$ (**AA**) is the most stable of three possible $[\text{CpFeCB}_{10}\text{H}_{11}]^{2-}$ isomers (**AA**, **AB** and **AC**, Table 5.1). Meta and para isomers **AB** and $[1\text{-Cp-1,12-FeCB}_{10}\text{H}_{11}]^{2-}$ (**AC**), are less stable than the ortho- (**AA**) by 3.6 and 9.0 kcal mol⁻¹ respectively.

Five isomeric $[\text{CpFeC}_2\text{B}_9\text{H}_{11}]^-$ structures, i.e., **BA** to **BE** were computed of which $[1\text{-Cp-1,2,4-}$

$\text{FeC}_2\text{B}_{10}\text{H}_{11}]^-$ (**BA**) with both carbon atoms adjacent to iron but at non-adjacent (meta) positions to each other is the most stable isomer. The CpFe unit prefers ortho relationships with carbon atoms (due to a negative structural increment of $\text{FeC}_o = -10.2 \text{ kcal mol}^{-1}$) while the two carbon atoms prefer para positions to each other ($E_{\text{inc}}[\text{CC}_o] = 17.2 \text{ kcal mol}^{-1}$ and $E_{\text{inc}}[\text{CC}_m] = 2.2 \text{ kcal mol}^{-1}$). The ortho Fe-C and meta C-C relationships in the most stable isomer (**BA**) comply with these preferences. The relative stabilities of other $[\text{CpFeC}_2\text{B}_9\text{H}_{11}]^-$ isomers are listed in Table 5.1.

The most stable $\text{CpFeC}_3\text{B}_8\text{H}_{11}$ isomer (1,2,4,10-CpFeC₃B₈H₁₁, **CA**) has two carbon atoms ortho to the CpFe fragment while the third carbon atom is at meta position to the CpFe fragment (Table 5.1). Structural increments predict 1-Cp-1,7,8,12-FeC₃B₈H₁₁ (**CM**) with all three carbon atoms adjacent to each other but far away from CpFe should result in the highest energy isomer as is found through computations (see Table 5.1, **CM**).

5.2.4.2. $[\text{CpFeP}_x\text{B}_{11-x}\text{H}_{11-x}]^{(3-x)-}$ ($x = 1, 2, 3$) isomers.

The FeP_o energy penalty ($E_{\text{inc}}[\text{FeP}_o] = -13.5 \text{ kcal mol}^{-1}$) is more negative than that of FeC_o ($E_{\text{inc}}[\text{FeC}_o] = -10.2 \text{ kcal mol}^{-1}$) indicating a stronger tendency of phosphorus atoms to be at the ortho position relative to a CpFe unit (see [1-Cp-1,2-FePB₁₀H₁₀]²⁻, **DA** and [1-Cp-1,2,4-FeP₂B₉H₉]⁻, **EA**). The most stable $[\text{CpFePB}_{10}\text{H}_{10}]^{2-}$ and $[\text{CpFeP}_2\text{B}_9\text{H}_9]^-$ isomers have the same substitution patterns as the carba analogues, i.e., 1,2- and 1,2,4- positions of heteroatoms, respectively. However, the most stable $\text{CpFeP}_3\text{B}_8\text{H}_8$ isomer has a different substitution pattern as compared with $\text{CpFeC}_3\text{B}_8\text{H}_{11}$: 1,2,3,5-positioning of phosphorus atoms (all ortho relative to CpFe) whereas 1,2,4,10-positioning of H-C moieties (one H-C moiety at meta position to the CpFe fragment) constitute the most stable isomer. This difference can be understood on the basis of more negative FeP_o and less positive PP_o increments as compared with those of FeC_o and CC_o .

The least stable isomers, on the other hand, have the phosphorus atoms at positions adjacent to each other but far apart from the CpFe fragment.

5.2.4.3. $[\text{CpFePCB}_9\text{H}_{10}]^-$, $\text{CpFePC}_2\text{B}_8\text{H}_{10}$ and $\text{CpFeP}_2\text{CB}_8\text{H}_{10}$ isomers.

Energy penalties for two additional structural features, i.e., PC_o and PC_m (structural feature for phosphorus and carbon atoms in ortho and meta arrangement relative to each other, respectively) are required for metallaphosphacarbaboranes. PC_o and PC_m have energy penalties of 12.8 and 0.5 kcal mol^{-1} , respectively. DFT computed relative stabilities of metallaphosphacarbaborane with three different heterogroups, i.e., CpFe, C and P can be reproduced with good accuracy. The most stable $[\text{CpFePCB}_9\text{H}_{10}]^-$ and $\text{CpFeP}_2\text{CB}_8\text{H}_9$ isomers have the heteroatoms at ortho positions to the CpFe unit. One of the carbon atoms shifts to a meta position in the thermodynamically most stable $\text{CpFePC}_2\text{B}_8\text{H}_{10}$ isomer, i.e., 1-Cp-1,2,4,10-FePC₂B₈H₁₀. Except for the most stable isomer, i.e., 1,2,4,10-, all other

FePC₂B₈H₁₀ isomers considered in Figure 5.3 have carbon and phosphorus atoms at ortho positions to the CpFe fragment. The structural features present in each of the isomers are listed. The relative energy obtained from the structural increment approach ($E_{\text{inc}}^{\text{rel}}$) for the five isomers is in excellent agreement with the computed results.

Moreover, it can be concluded that just like pure carbon and phosphorus analogues, the [CpFePCB₉H₁₀]⁻, CpFeP₂CB₈H₉ and CpFePC₂B₈H₁₀ isomers with heteroatoms far apart from the CpFe fragment and adjacent to each other have least thermodynamic stability.

5.2.5. Thermodynamically Most Stable [CpMC_yB_{11-y}H₁₁]^{Z-} (y = 0,1,2,3, M = Ru, Os, Co, Rh, Ir) Isomers.

Metallacarboranes with CpM units other than CpFe, (e.g., with M = Co,^{3a,4} Rh^{4d} and Ni^{4e}) and with a Cp*Ru fragment as in [1-Cp*-1,2,3-RuC₂B₉H₁₁]⁻ (where Cp* = pentamethylcyclopentadienyl⁵) are also known experimentally. Relative energies for isomeric metallacarboranes with a CpM unit other than CpFe can also be easily estimated by using the energy penalties for the structural features CC_o, CC_m, MC_o and MC_m. MC_o and MC_m increments for various group 8, 9 and 10 metals are listed in Chart 5.1. Values of 17.2 kcal mol⁻¹ and 2.2 kcal mol⁻¹ are used for CC_o and CC_m, throughout. They allow to estimate the relative stabilities of various isomers and in turn to rationalize some interesting facts from experiments. For example, the 1-Cp-1,2-NiCB₁₀H₁₁ isomer upon heating to 450 °C rearranges to 1,7- and 1,12-isomers,⁴ as it is the least stable in accordance with the positive NiC_o energy penalty ($E_{\text{inc}}[\text{NiC}_o] = 8.5 \text{ kcal mol}^{-1}$). Even larger PdC_o and PtC_o energy penalties allow to predict the possible thermal rearrangement of experimentally still unknown 1-Cp-1,2-PdCB₁₀H₁₁ and 1-Cp-1,2-PtCB₁₀H₁₁ to 1,7- and 1,12-isomers.

Similarly, 1-Cp-1,2,3-CoC₂B₉H₁₁ rearranges to various isomers with one or both carbon atoms non-adjacent to the CpCo fragment.^{4d} This is primarily due to the strong para-directing effect of two carbon atoms to each other ($E_{\text{inc}}[\text{CC}_o] = 17.2 \text{ kcal mol}^{-1}$) and secondly the small meta directing effect of the CpCo unit ($E_{\text{inc}}[\text{CC}_m] = -1.2 \text{ kcal mol}^{-1}$) to the carbon atom.

The complex 1,2,3-CpRhC₂B₉H₁₁ has been reported to rearrange to 1,2,4-CpRhC₂B₉H₁₁ upon heating.^{4d} This is because of the high CC_o energy penalty. Our increments suggest that further heating of the 1,2,4-isomer should result in isomeric structures with carbon atoms at meta positions to the CpRh fragment.

No experimental reports are available for iridacarboranes so far, however, thermodynamic preference for 1-Cp-1,7,9-IrC₂B₉H₁₁ can be predicted as compared with Co and Rh analogues.

CpFeC₂B₉H₁₁ structures with only Fe-C ortho relationships were reported, i.e., [1-Cp-1,2,3-FeC₂B₉H₁₁]⁻ or [1-Cp-1,2,4-FeC₂B₉H₁₁]⁻.^{3b} No meta rearrangements have been reported. This is due to

the ortho-directing nature of the CpFe unit to the carbon atoms. However, the known 1,2,3,4-CpFeC₃B₈H₁₁ structure (with three carbon atoms) rearranges to 1,2,3,5-CpFeC₃B₈H₁₁ and 1,2,4,10-CpFeC₃B₈H₁₁.¹² The latter is the thermodynamically most stable isomer and has one carbon atom in a meta position in order to counter-balance the strong mutual para-directing effect ($CC_o = 17.2 \text{ kcal mol}^{-1}$) of three carbon atoms (see Section 2.4.1).

5.2.6. Relative Stabilities of (CO)₃CoCB₁₀H₁₁ Isomers.

In order to determine the effect of the ligands on the metal fragment, (CO)₃CoCB₁₀H₁₁ isomers were also computed for comparison with CpCoCB₁₀H₁₁ isomers. The former has three carbonyl groups while the latter has a Cp fragment attached to the cobalt atom. Three possible (CO)₃CoCB₁₀H₁₁ isomers, i.e., 1,2-, 1,7- and 1,12- were computed and surprisingly, the energetics of (CO)₃CoCB₁₀H₁₁ were much different from those of CpCoCB₁₀H₁₁. Contrary to the CpCoCB₁₀H₁₁ isomers, where the meta isomer is thermodynamically most stable by 1.2 kcal mol⁻¹ (see Chart 5.1), the para isomer is the most stable for (CO)₃CoCB₁₀H₁₁. The meta isomer is only slightly more stable (0.5 kcal mol⁻¹) and the ortho isomer is 8.9 kcal mol⁻¹ less stable than the para isomer. Different energy penalties by different substituents can be rationalized: The (CO)₃Co fragment has three carbonyl groups attached to the cobalt atom. A carbonyl ligand besides being a σ -donor is also a strong π -acceptor thus it takes back electron density from the metal center through back donation. As a result, the metal withdraws more electron density from the clusters. This increased electron localization at the metal center leads to increased energy penalties and hence para isomer becomes the most stable. We note that the energy penalties of the (CO)₃Co fragment are almost equal to those of the CpNi fragment. The latter also has a higher extent of electron localization as compared with the CpCo fragment.

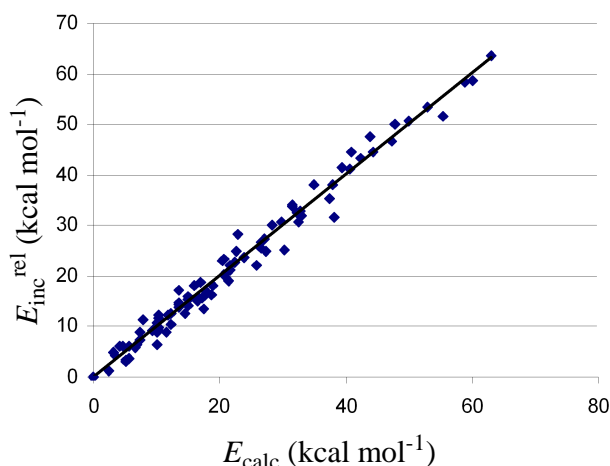


Figure 5.4: Structural increments accurately reproduce the relative stabilities of cyclopentadienyl ferraheteroboranes computed by DFT methods.

¹² Perekalin, D. S.; Holub, J.; Golovanov, D. G.; Lyssenko, K. A.; Petrovskii, P. V.; Štíbr, B.; Kudinov, A. R. *Organometallics* **2005**, *24*, 4387-4392.

5.3. Conclusion

To summarize, cyclopentadienyl metal fragments of group 8, 9 and 10 metals in 12-vertex *closo*-cyclopentadienyl metallaheteroboranes have a clear ortho-, meta- or para-directing influence on heteroatoms. Structural increments increase along one period due to increasing positive charge on the metal center along the period, i.e., as consequence of an increasing extent of electron localization. The presented structural increments can easily be used to quickly give the relative stabilities of a large number of metallaheteroboranes. These structural increments are substituent specific; a change of the substituent on the metal atom leads to different energy penalties.

6. Which *nido:nido*-Macropolyhedral Boranes are Most Stable?

6.1. Introduction

Single cluster boranes and macropolyhedral boranes have attracted a quite different attention with respect to theoretical treatment. Single cluster boranes are now well understood. The principles that govern the stabilities of macropolyhedral boranes, however, are mostly unknown and experimental research is largely exploratory.¹ Single clusters are either the most spherical deltahedra, i.e., *closo*-boranes, or are derived by the removal of one, two or three vertexes from *closo*-structures to give *nido*-, *arachno*-² and *hypho*-boranes,³ respectively. A number of theoretical efforts, e.g. Wade's skeletal electron count principle,⁴ Williams' heteroatom placement rules,^{2,5} Jemmis and Schleyer's ring cap principle,⁶ Ott-Gimarc's charge preference,⁷ and structural⁸ and connection⁹ increment systems provide insight into the structural patterns of single clusters.

¹ a) Kennedy, J. D. In *Advances in Boron Chemistry*; Siebert, W., Ed.; Royal Society of Chemistry: Cambridge, U.K., 1997; p 451. b) Grimes, R. N. *Metal Interactions with Boron Clusters*; Plenum Press: New York, 1982. c) McGrath, T. D.; Jelinek, T.; Štibr, B.; Thornton-Pett, M.; Kennedy, J. D. *J. Chem. Soc., Dalton Trans.* **1997**, 2543-2546.

² a) Williams, R. E. *Inorg. Chem.* **1971**, *10*, 210-214. b) Williams, R. E. In *Progress in Boron Chemistry Brotherton, R. J., Steinberg, H., Eds.; Pergamon Press: England, 1970; Vol. 2, Chapter 2, p 57.* c) Williams, R. E.; *Chem. Rev.* **1992**, *92*, 177-207; references therein.

³ Rudolph R. W. *Acc. Chem. Res.* **1976**, *9*, 446-452.

⁴ (a) Wade, K. *Adv. Inorg. Chem. Radiochem.* **1976**, *18*, 1-66. (b) Wade, K. In *Metal Interactions with Boron Clusters*; Grimes, R. N., Ed.; Plenum Press: New York, 1982; Chapter 1, pp 1– 41.

⁵ Williams, R. E. *J. Am. Chem. Soc.* **1965**, *87*, 3513-3515.

⁶ (a) Jemmis, E. D. *J. Am. Chem. Soc.* **1982**, *104*, 7017-7020. (b) Jemmis, E. D.; Schleyer, P. v. R. *J. Am. Chem. Soc.* **1982**, *104*, 4781-4788.

⁷ Ott, J. J.; Gimarc, B. M. *J. Am. Chem. Soc.* **1986**, *108*, 4303-4308.

⁸ a) Kiani, F. A.; Hofmann, M. *Inorg. Chem.*, **2004**, *43*, 8561-8571. b) Kiani, F. A.; Hofmann, M. *Inorg. Chem.*, **2005**, *44*, 3746-3754. c) Kiani, F. A.; Hofmann, M. *Eur. J. Inorg. Chem.*, **2005**, *12*, 2545-2553. d) Kiani, F. A.; Hofmann, M. *J. Mol. Model.* **2006**, *12*, 597-609. e) Kiani, F. A.; Hofmann, M. *Organometallics*, **2006**, *25*, 485-490

⁹ Kiani, F. A.; Hofmann, M. *Dalton Trans.*, **2006**, *5*, 686-692

Large structures are composed of smaller clusters with two different modes of combining individual single clusters: (i) a two center-two electron¹⁰ or a three center two electron bond¹¹ connects two independent units, or (ii) one,¹² two,¹³ three¹⁴ or four¹⁵ vertexes are *shared* by two individual units. The resulting clusters of *fused* polyhedral units have been termed macropolyhedra (see Scheme 1). The first case, i.e. joint clusters is not special, as one cluster is just a substituent to another one and the individual clusters remain separate entities. In the second case, the more intimate fusion of clusters results in one new and different cluster. Except for the skeletal electron count rule for macropolyhedral borane clusters,¹⁶ no further theoretical consideration has been paid to macropolyhedral boranes. Jemmis' *mno* rule - a skeletal electron count principle⁶ can be easily and correctly employed to any macropolyhedral borane. In short, the sum of the number of single cluster fragments (m), the number of vertexes in the macropolyhedron (n), the number of single vertex sharing junctions (o) and the number of missing vertexes (p) equals the number of skeletal electron pairs of a macropolyhedral borane.

¹⁰ See for example, a) Hawthorne, M. F.; Pilling, R. I.; Stokely, P. F.; Garrett, P. M. *J. Am. Chem. Soc.* **1963**, *85*, 3704. b) Hawthorne, M. F.; Pilling, R. L.; Stokely, P. F. *J. Am. Chem. Soc.* **1965**, *87*, 1893-1899. c) Ng, L. L.; Ng, B. K.; Knobler, C. B.; Hawthorne, M. F. *Inorg. Chem.* **1992**, *31*, 3669-3671. d) Grimes, R.; Wang, F. E.; Lewin, R.; Lipscomb, W. N. *Proc. Natl. Acad. Sci. U.S.A.* **1961**, *47*, 996-999.

¹¹ See for example, a) Watson-Clark, R. A.; Knobler, C. B.; Hawthorne, M. F. *Inorg. Chem.* **1996**, *35*, 2963-2966. b) Hawthorne, M. F.; Pilling, R. L. *J. Am. Chem. Soc.* **1966**, *88*, 3873-3874. c) DeBoer, B. G.; Zalkin, A.; Templeton, D. H. *Inorg. Chem.* **1968**, *7*, 1085-1090

¹² Rathke, J.; Schaeffer, R. *Inorg. Chem.* **1974**, *13*, 3008-3011.

¹³ a) Brewer, C. T.; Swisher, R. G.; Sinn, E.; Grimes, R. N. *J. Am. Chem. Soc.* **1985**, *107*, 3558-3564. b) Huffman, J. C.; Moody, D. C.; Schaffer, R. *Inorg. Chem.* **1976**, *15*, 227-232. c) Friedman, L. B.; Cook, R. E.; Glick, M. D. *Inorg. Chem.* **1970**, *9*, 1452-1458. d) Pitochelli, A. R.; Hawthorne, M. F. *J. Am. Chem. Soc.* **1962**, *84*, 3218-3220. e) Simpson, P. G.; Lipscomb, W. N. *J. Chem. Phys.* **1963**, *39*, 26-34. f) Simpson, P. G.; Lipscomb, W. N. *Proc. Natl. Acad. Sci. U.S.A.* **1962**, *48*, 1490-1491. g) Simpson, P. G.; Foltling, K.; Dobrott, R. D.; Lipscomb, W. N. *J. Chem. Phys.* **1963**, *39*, 2339-2348. h) Fontaine, X. L. R.; Greenwood, N. N.; Kennedy, J. D.; Mackinnon, P. *J. Chem. Soc., Dalton Trans.* **1988**, *7*, 1785-1793.

¹⁴ Enemark, J. H.; Friedman, L. B.; Lipscomb, W. N. *Inorg. Chem.* **1966**, *5*, 2165.

¹⁵ a) Friedman, L. B.; Dobrott, R. D.; Lipscomb, W. N. *J. Am. Chem. Soc.* **1963**, *85*, 3505-3506.

¹⁶ a) Jemmis, E. D.; Balakrishnarajan, M. M.; Pancharatna, P. D.; *J. Am. Chem. Soc.*, **2001**, *123*, 4313-4323. b) Jemmis, E. D.; Balakrishnarajan, M. M.; Pancharatna, P. D. *Chem. Rev.* **2002**, *102*, 93-144.

But unlike Wade's⁴ skeletal electron count principle for single clusters, which associates the number of skeletal electron with definite cluster shapes, the *mno* rule does not specify architectures or cluster shapes based on the given number of skeletal electrons. It rather has to be known to do the *mno* counting. Therefore, it is impossible to determine the thermodynamically most stable structure out of a large number of possibilities for a given molecular formula. Here, a detailed study is presented in order to explore the architectural patterns behind macropolyhedral boranes.

In the present paper, the relative stabilities of the various possible isomers of *nido:nido*-macropolyhedral boranes are compared with each other and also with the isomeric *nido* single clusters, each of the general formula B_nH_{n+4} ($n = 4 - 19$). We try to find computationally the turning point from *nido* single clusters to *nido:nido*-macropolyhedral preference in neutral and anionic clusters. We further explore the preferred fragment for each neutral and anionic macropolyhedral boranes in the thermodynamically most stable isomers. The single clusters used to construct macropolyhedral boranes are listed in Figure 6.1, where as the optimized geometries of various $B_{14}H_{18}$ macropolyhedra are displayed in Figure 6.2.

6.2. Result and Discussion

6.2.1. Fusion Mode of *nido:nido*-Macropolyhedral Boranes

A large number of known macropolyhedral boranes with the general formula B_nH_{n+4} consists of two *nido* units sharing two vertexes. For the sake of convenience, they are denoted as *nido*(*x*):*nido*(*y*)-macropolyhedral boranes in this paper, where *x* and *y* indicate the size of the cluster units that share two vertexes, i.e., $x+y = n+2$. B_nH_{n+4} macropolyhedra with one or three vertexes shared between two *nido*-units do not obey the *mno* rule⁶ and are experimentally unknown.

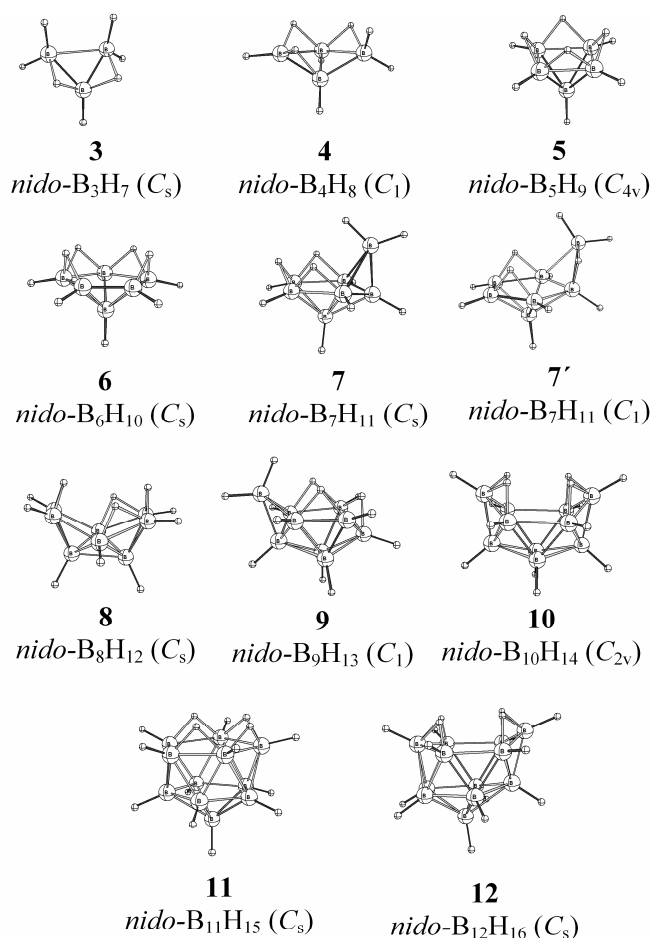


Figure 6.1: *nido* single clusters as building blocks of *nido:nido*-macropolyhedra.

In order to estimate the energetic influence of different fusion modes between two *nido*-clusters on the relative stability of isomeric structures, one and three vertex sharing $B_{18}H_{22}$ structures were computed. They are 62.7 and 52.7 kcal mol⁻¹, respectively, less stable than the experimentally known two vertex sharing C_i symmetric *nido*(10):*nido*(10)-

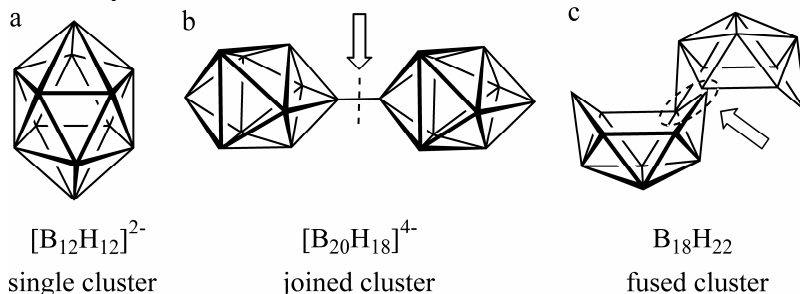
$B_{18}H_{22}$ structure.^{13d-f} We conclude that there is a large preference (>50 kcal mol⁻¹) for two vertex sharing in *nido:nido* macropolyhedral boranes.

6.2.2. Turning Point from *nido*- B_nH_{n+4} Single Cluster to *nido:nido*- B_nH_{n+4} Macropolyhedral Preference.

The largest experimentally known homonuclear *nido*-single cluster is $B_{11}H_{15}$,¹⁷ whereas the smallest experimentally known homonuclear *nido:nido*-macropolyhedral borane is $B_{12}H_{16}$ (Scheme 2).¹⁸ The latter consists of one eight vertex *nido*-unit sharing two vertexes with another six vertex *nido*-fragment. It is unclear if this also represents the turning point from *nido*-single cluster to macropolyhedral borane preference in terms of thermodynamic stability. Computation of the experimentally known *nido*(6):*nido*(8)- $B_{12}H_{16}$ and the isomeric *nido*- $B_{12}H_{16}$ indicates that the former is 3.9 kcal mol⁻¹ less stable than the *nido*- $B_{12}H_{16}$ single cluster. However, the *nido*(3):*nido*(11)- $B_{12}H_{16}$ isomer (**3:11**) was found to be 4.5 kcal mol⁻¹ more stable than the *nido*- $B_{12}H_{16}$ (**12**) cluster. The former structure, i.e., *nido*(3):*nido*(11)- $B_{12}H_{16}$ is also 8.3 kcal mol⁻¹ more stable than the experimentally known *nido*(6):*nido*(8)- $B_{12}H_{16}$.

The thermodynamic stabilities of various *nido:nido*- B_nH_{n+4} macropolyhedral borane clusters with respect to the isomeric *nido*- B_nH_{n+4} single clusters are compared in Figure 6.3 Any neutral *nido:nido*-macropolyhedral borane is less stable than the corresponding *nido* single cluster borane as long as the total number of vertexes is equal to or less than eleven. For twelve or more vertexes, i.e., for $n = 12-19$, macropolyhedra exist that are energetically preferred (Figure 6.3) over the single cluster alternatives.

Scheme 6.1: Different types of polyhedral boranes; a) $[B_{12}H_{12}]^{2-}$ represents a single cluster, b) Two single clusters may share a 2-center-2-electron bond like in $[B_{20}H_{18}]^{4-}$ and c) Two cluster units may fuse to become a macropolyhedra as two 10 vertex *nido* units share two vertexes in *nido*(10):*nido*(10)-*nido:nido*- $B_{18}H_{22}$. Arrows point to the mode of cluster connections.



¹⁷ Getman, T. D.; Krause, J. A.; Shore, S. G. *Inorg. Chem.* **1988**, *27*, 2398-2399.

¹⁸ a) Brewer, C. T.; Grimes, R. N. *J. Am. Chem. Soc.* **1984**, *106*, 2722-2723. b) Brewer, C. T.; Swisher, R. G.; Sinn, E.; Grimes, R. N. *J. Am. Chem. Soc.* **1985**, *107*, 3558-3564.

6. NIDO:NIDO-MACROPOLYHEDRAL BORANES

E.g., the most stable macropolyhedral $B_{10}H_{14}$, i.e., *nido*(6):*nido*(6)- $B_{10}H_{14}$ is 27.2 kcal mol⁻¹ less stable than single cluster *nido*- $B_{10}H_{14}$ (**10**). Similarly the most stable *nido*(5):*nido*(8)- $B_{11}H_{15}$ is 16.7 kcal mol⁻¹ less stable than the single *nido*- $B_{11}H_{15}$ (**11**) cluster. Twelve is the smallest number of vertexes for which a macropolyhedron exists that is lower in energy than its *nido*-isomer. Figure 6.3 displays an obvious trend for macropolyhedra to become more and more favored over single cluster isomers for increasing total number of vertexes.

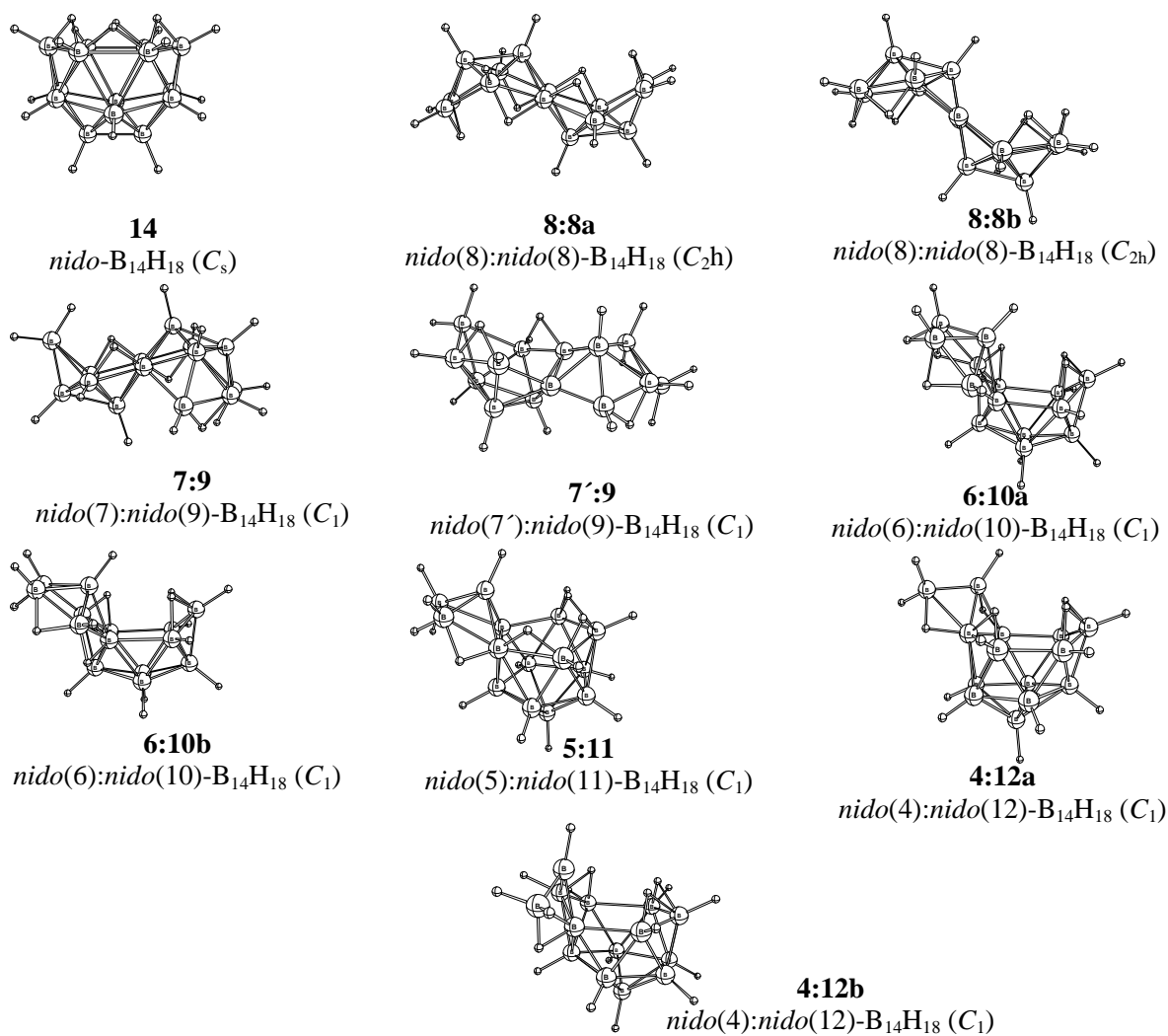


Figure 6.2: Single cluster (**14**) and macropolyhedral structures for $B_{14}H_{18}$.

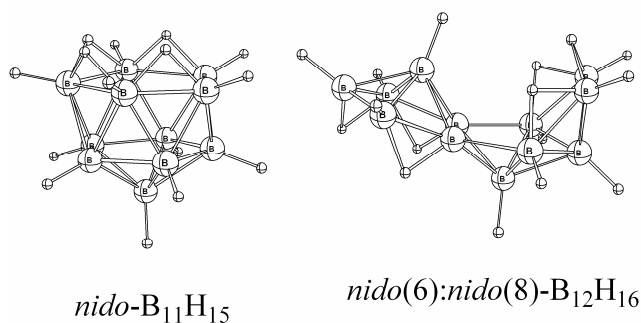
The increase in stability of *nido:nido*-macropolyhedral boranes can be explained on the basis of the connectivity of boron vertexes. Five-coordinate vertexes are especially favorable¹⁹ as is indicated by the high stability of icosahedral *closo*-[B₁₂H₁₂]²⁻.²⁰ Large sized *nido* single cluster boranes usually possess more highly connected vertexes in addition. Isomeric *nido:nido*-macropolyhedral boranes, on the other hand, are built from smaller cluster fragments and have a smaller number of highly connected vertexes (usually more 5-coordinate vertexes), and therefore get enhanced stability.

Hydrogen atoms at the open face prefer to bridge vertexes of least connectivity. Vertexes at the open face of *nido:nido*-macropolyhedral boranes are usually less connected as compared to vertexes at the open face of corresponding single *nido* clusters. The reduced thermodynamic stability of neutral *nido*-clusters may therefore be –at least in part– due to the high connectivity of open face vertexes.

6.2.3. The Effect of Open Face Hydrogen Atoms on the Relative Stabilities of *nido* Single Cluster Boranes vs. *nido:nido* Macropolyhedral Boranes.

Optimization of a *nido*(3):*nido*(10)-B₁₁H₁₅ starting geometry resulted in a structure that is 1.7 kcal mol⁻¹ more stable than the experimentally known *nido*-B₁₁H₁₅ (**11**) single cluster. It has a BH₂ unit occupying the position of a hydrogen bridge of a regular 10-vertex *nido*-fragment (**X**, Figure 6.4). This geometry can also be considered as a distorted 11-vertex *nido*-single cluster rather than a macropolyhedral borane. The presence of four open face hydrogen atoms destabilizes the *nido*-B₁₁H₁₅ (**11**) cluster: Adjacent hydrogen bridges on the open face of 11-vertex *nido*-cluster represent a high energy structural feature with an energy penalty of 25.9 kcal mol⁻¹.^{8a} This might be responsible for the

Scheme 6.2: Optimized geometries of the largest experimentally known homonuclear single *nido*-cluster (*nido*-B₁₁H₁₅¹⁷) and smallest experimentally known homonuclear *nido:nido*-macropolyhedral borane cluster (*nido*(6):*nido*(8)-B₁₂H₁₆¹⁸).



¹⁹ a) Brown, L. D.; Lipscomb, W. N. *Inorg. Chem.* **1977**, *16*, 2989. b) Jemmis, E. D.; Pavankumar, P. N. V. *Proc.-Indian Acad. Sci., Chem. Sci.* **1984**, *93*, 479. c) Boustani, I. *J. Solid State Chem.* **1997**, *133*, 182. d) King, R. B. *Inorg. Chem.* **2001**, *40*, 6369-6374

²⁰ Schleyer, Najafian and Mebel computed various *closo*-[B_nH_n]²⁻ clusters (n = 5-17) and found the least energy per vertex for n = 12. We extended the study up to 20 vertexes and find the progressive decrease in energy per vertex from [B₁₅H₁₅]²⁻ to [B₁₇H₁₇]²⁻ which was reported in ref. 21 not to continue for n = 18-20.

fact that distorted **X** with only two adjacent hydrogen atoms on the less connected vertexes can compete energetically with **11**. The latter suffers from four adjacent hydrogen bridges.

It is also known from experiments that *nido*- $B_{11}H_{15}$ (**11**) is easily deprotonated to give *nido*- $[B_{11}H_{14}]^-$.⁸ The deprotonated *nido*- $[B_{11}H_{14}]^-$, has three hydrogen atoms on the open face, only two of them adjacent to each other. Thus, *nido*-

$[B_{11}H_{14}]^-$ has two less adjacent hydrogen bridges as compared to *nido*- $B_{11}H_{15}$ and should have enhanced thermodynamic stability. In order to confirm the effect of open face hydrogen atoms, *nido*- $[B_{11}H_{14}]^-$ and corresponding *nido:nido*- $[B_{11}H_{14}]^-$ structures were computed. The *nido*- $[B_{11}H_{14}]^-$ is found to be 34.3 kcal mol⁻¹ more stable than the most stable macropolyhedral $[B_{11}H_{14}]^-$, while the neutral *nido*- $B_{11}H_{15}$ structure is 16.7 kcal mol⁻¹ more stable than the corresponding most stable macropolyhedral $B_{11}H_{15}$. Thus, removal of one open face hydrogen atom enhances the energetic preference for the regular *nido* cluster by 17.6 kcal mol⁻¹. The presence of heteroatoms in the 11-vertex *nido*-cluster also results in a reduced number of extra open face hydrogen atoms (e.g., *nido*- $CB_{10}H_{14}$ and *nido*- $HPB_{10}H_{12}$ have three and two open face hydrogen atoms, respectively). Therefore, heteroatom substituted single cluster boranes suffer less from open face hydrogen atom repulsion. As a consequence, heteroatom substituted single cluster isomers should be more competitive as compared to corresponding macropolyhedral boranes.

In order to determine the effect of open face hydrogen atoms on the relative stabilities (as in the case of $B_{11}H_{15}$ and $[B_{11}H_{14}]^-$), the anionic single clusters as well as macropolyhedra of the general formula $[B_nH_{n+3}]^-$ ($n = 4-19$) were computed. The stabilities of the most stable neutral macropolyhedra relative to the corresponding isomeric most stable neutral single clusters is usually higher (solid line in Figure 6.3) than that of the most stable anionic macropolyhedra relative to the corresponding most stable anionic *nido* single clusters (broken line in Figure 6.3). This shift can be explained on the basis of the presence of bridged hydrogen atoms on the open face. Neutral *nido*-clusters with a single open face possess four extra open face bridging hydrogen atoms while neutral macropolyhedral boranes with two open faces possess six extra open face bridging hydrogen atoms. Thus hydrogen atoms exert more stress on the open face of single *nido* clusters (four hydrogen atoms per open face) as compared to that of

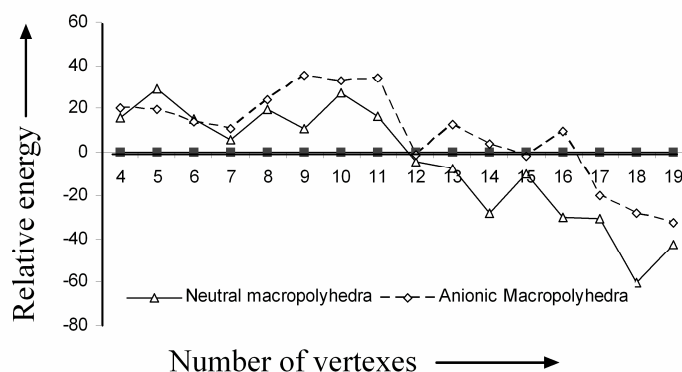


Figure 6.3: Relative energies of the most stable *nido:nido*-edge sharing macropolyhedra relative to isomeric single cluster polyhedra.

macropolyhedral boranes (three hydrogen atoms per open face).

Monoanionic clusters have one open face bridging hydrogen atom less in both cases (i.e., single *nido* clusters as well as *nido:nido*-macropolyhedral clusters) but more stress is released in single *nido* clusters as compared to macropolyhedral boranes and hence anionic *nido* clusters gain larger stability. As a consequence, the turning point from single *nido* cluster to macropolyhedral preference is shifted to a higher number of vertexes for anionic clusters: Anionic $[B_nH_{n+3}]^-$ macropolyhedral borates are clearly less stable than corresponding *nido*-clusters for $n \leq 11$ (Figure 6.3). The relative stabilities of 12-16 vertex anionic macropolyhedral clusters are close to those of the most stable single *nido* clusters. For seventeen vertexes or more, macropolyhedral borates are clearly preferred over anionic single *nido* clusters. We note that a more stable anionic macropolyhedral borate structure is obtained, when the larger cluster unit is deprotonated.

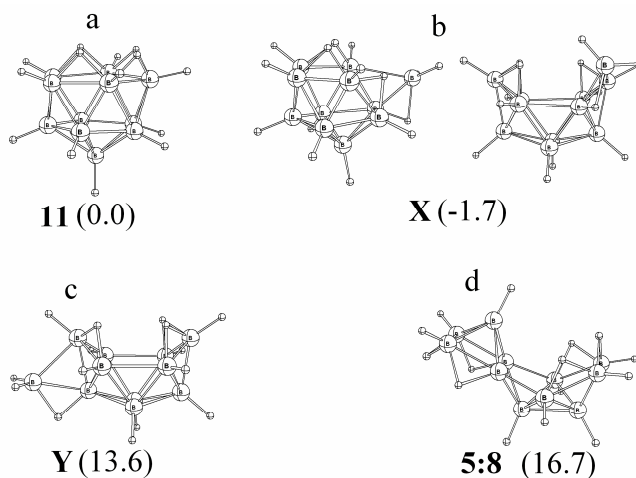


Figure 6.4: a) Optimized geometry of *nido*- $B_{11}H_{15}$ (**11**, Cs) with four adjacent hydrogen bridges b) Different views of **X** to show its relationship with the 11- and 10-vertex *nido*-clusters c) A *nido*(4):*nido*(9)- $B_{11}H_{15}$ starting geometry optimized to this distorted geometry (**Y**). d) The most stable macropolyhedral $B_{11}H_{15}$ borane has a 5-vertex *nido*-cluster sharing two vertexes with another 8-vertex *nido*-cluster (**5:8**). Relative energies in kcal mol⁻¹ are given in parentheses.

6.2.4. Preferred Units for *nido:nido*-Macropolyhedral Boranes from 12-19 Vertexes.

We further explored which *nido* clusters are best suited for the construction of macropolyhedral boranes and borates. The thermodynamic stabilities ($E_{x,y}$) of various *nido:nido*- B_nH_{n+4} macropolyhedra are indicated in the right half of Figure 6.5 relative to the most stable isomer for each number of vertexes (n). The energy range spanned by the isomers considered is always larger for even n than for the neighboring odd case of $n+1$ and $n-1$. For even n larger than 12, the energetic separation of the most stable and the second most stable isomer is also more pronounced than for the neighboring odd $n+1$ or $n-1$. Obviously, among macropolyhedra with an even number of vertexes, a clearer preference exists for the most favorable distribution of vertexes among the two building blocks. Furthermore, while isomers having a 7-vertex unit are usually energetically disfavored, the thermodynamically most stable isomer for 13 to 19 vertexes contains at least one 10-vertex *nido*-unit (Figure 6.6a).

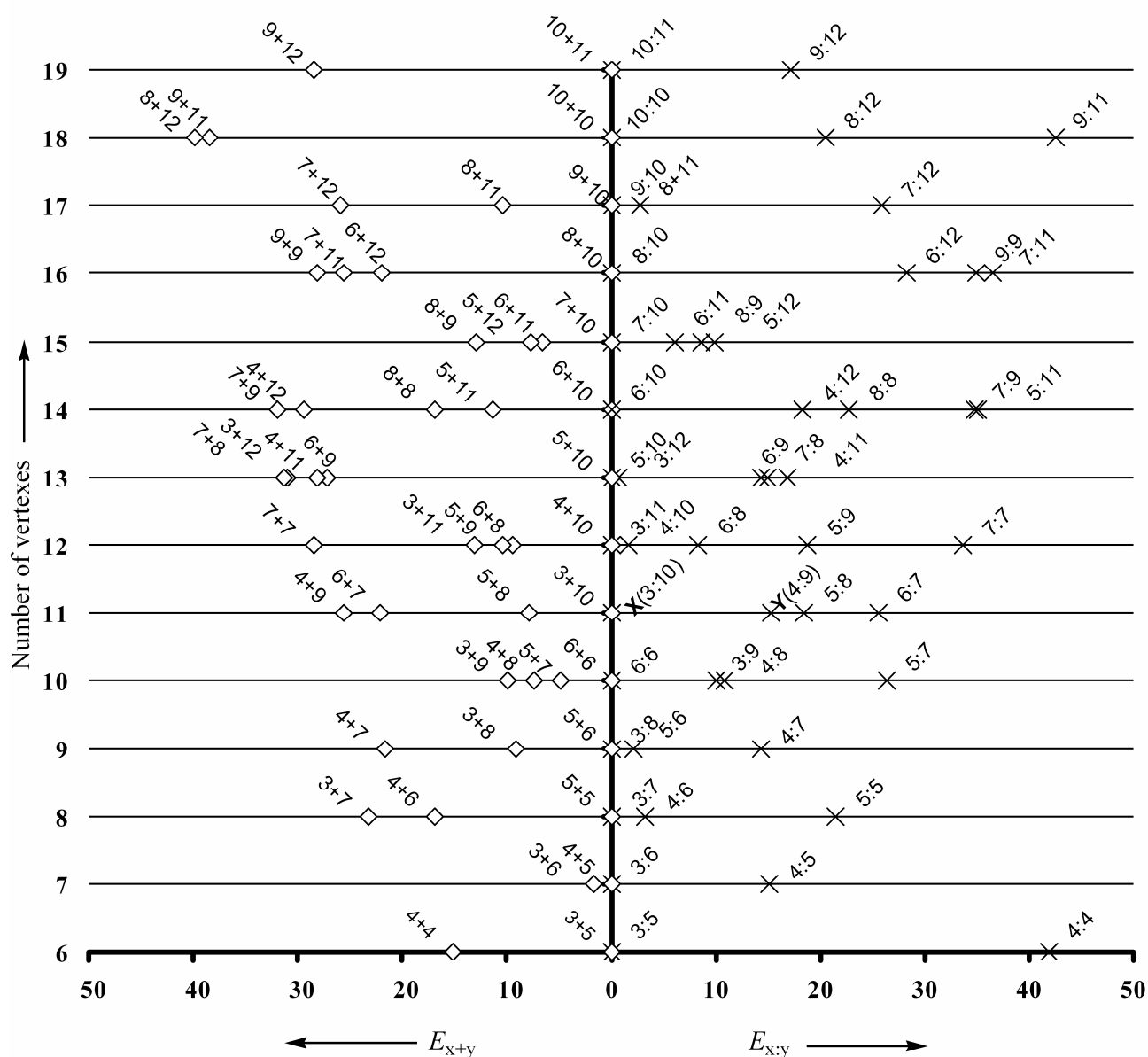


Figure 6.5: A comparison of relative energies [kcal mol^{-1}] of macropolyhedral *nido:nido*- B_nH_{n+4} boranes (labeled $x:y$, right half) with the relative energies E_{x+y} that result from the sum of energies computed for *nido* boranes corresponding to the building units $E(\text{B}_x\text{H}_{x+4}) + E(\text{B}_y\text{H}_{y+4})$ (labeled $x+y$, left half). x and y indicate the size of the two clusters making a macropolyhedron. **3:10 (X)** can also be considered as a distorted *nido*- $\text{B}_{11}\text{H}_{15}$ structure. The *nido*(4):*nido*(9)-macropolyhedra with one 4-vertex *nido*-unit and the other 9-vertex *nido*-unit rearranged to a distorted geometry **Y** (for details see Figure 4).

The thermodynamically most stable *nido:nido*-macropolyhedral borates for $n = 12 - 17$ and 19 contain one deprotonated 11-vertex *nido*-unit (Figure 6.6b). For eighteen vertexes, however, *nido*(10):*nido*(10)- $[\text{B}_{18}\text{H}_{21}]^-$ is $5.0 \text{ kcal mol}^{-1}$ more stable than *nido*(9):*nido*(11)- $[\text{B}_{18}\text{H}_{21}]^-$.

The 11-vertex *nido* unit can be expected to be the most favorable *nido* unit as it is obtained by the removal of one vertex from the highly stable icosahedral 12-vertex *closo*-cluster.²¹ However, the presence of three additional open face hydrogen atoms on the five membered open face of the 11-vertex *nido* cluster is unfavorable. Hence the structure with a *nido*-10-vertex unit, which has a larger 6-membered open face with adjacent hydrogen bridges sharing vertexes with cluster connectivity 3 rather than 4, enjoys greater thermodynamic stability in the case of neutral clusters. Loss of one extra open face hydrogen atom results in the release of stress in the 11-vertex *nido* unit and hence anionic clusters with an 11-vertex deprotonated unit become more favorable.

6.2.5. Relative Energies ($E_{x,y}$) of Macropolyhedral Boranes in Comparison to the Relative Energies (E_{x+y}) from Summation of Individual Clusters Making the Macropolyhedra.

Does the observed stability order of isomeric two vertex sharing macropolyhedra reflect that of the building units or is it different? In other words, are some *nido*-clusters better than others in forming macropolyhedra? The right half of Figure 6.5 gives a comparison of relative stabilities of various B_nH_{n+4} macropolyhedral boranes ($E_{x,y}$) for $n = 6-19$, whereas the left half of Figure 6.5 gives relative energies that result from the sum of energies of individual clusters making the macropolyhedron (E_{x+y}).

For example, the most stable 19-vertex *nido:nido*-macropolyhedra ($B_{19}H_{23}$) is a 10-vertex *nido*-unit sharing two vertexes with an 11-vertex *nido*-unit ($E_{10:11}$ is smaller than $E_{9:12}$ for $n = 19$, right half of Figure 6.5). The sum of the energies of a 10-vertex ($B_{10}H_{14}$) and an 11-vertex ($B_{11}H_{15}$) *nido* cluster (E_{10+11} , left half of Figure 6.5) is also smaller than that of the 9-vertex (B_9H_{13}) and 12-vertex ($B_{12}H_{16}$) *nido*-clusters (E_{9+12}). Although the stability order is the same in these cases, the numbers are different: $E_{9:12} = 17.2 \text{ kcal mol}^{-1}$ and $E_{9+12} = 28.4 \text{ kcal mol}^{-1}$. The 9- and 12-vertex cluster combination seems to gain some stability with respect to the 10 plus 11 alternative, when incorporated into a macropolyhedron.

One 7-vertex unit usually results in a quite unfavorable distribution of vertexes in a macropolyhedra while one 10-vertex usually means the best possible choice. The same is true for the sum of energies of two individual single *nido* clusters (E_{x+y} , listed in the left half of Figure 6.5): The sum of energies of the two units (E_{x+y}) for 11-19 vertexes is least when one component is a 10-vertex *nido*-cluster, and E_{x+y} is usually large for the sum of energies of two single clusters with at least one 7-vertex *nido*-unit.

For $n = 6, 10-11$ and $13-19$, the thermodynamically most stable macropolyhedra, i.e., 3:5, 6:6, 3:10, 5:10, 6:10, 7:10, 8:10, 9:10, 10:10, 10:11 are composed from the most stable choice of the individual clusters, i.e., 3+5, 6+6, 3+10, 5+10, 6+10, 7+10, 8+10, 9+10, 10+10 and 10+11 (Figure 6.5). As an

²¹ Schleyer, P. v. R.; Najafian, K.; Mebel, A. M. *Inorg. Chem.* **1998**, *37*, 6765.

6. NIDO:NIDO-MACROPOLYHEDRAL BORANES

example, the thermodynamically most stable 17-vertex macropolyhedron is a *nido(9):nido(10)*- $B_{17}H_{21}$ as $E_{9:10}$ gives the smallest value just as E_{9+10} is smallest.

For the clusters with smaller size, the sum of energies of the individual clusters, may not match the energies exhibited by the macropolyhedra. Moreover, the most stable isomer for smaller macropolyhedral boranes apparently contains one three vertex *nido*-unit. Such clusters resemble single cluster boranes in the sense that both may be constructed by replacement of one hydrogen bridge by a BH_2 unit. Placement of a BH_2 unit to a bridging hydrogen atom position in a convex fashion gives another single cluster while a concave orientation results in a *nido(3):nido(x)*-macropolyhedra.

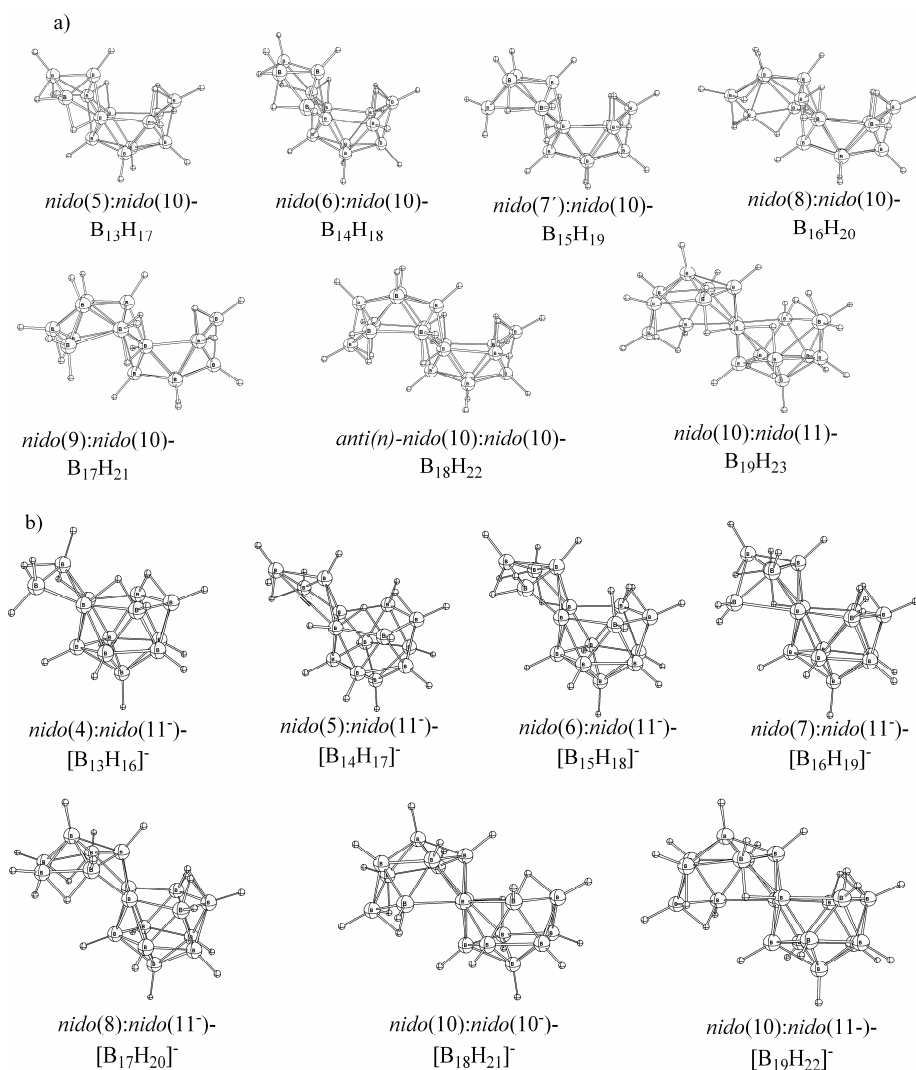


Figure 6.6: Structures of the most stable 13-19-vertex-containing (a) macropolyhedral boranes and (b) borates.

The larger relative energy splitting for an even number of boron atoms is not special to the macropolyhedra but is inherent to the subclusters fused to a macropolyhedron. This conclusion is based on the similar trends of relative stabilities of separated *nido* clusters (E_{x+y}), which are displayed in the left part of Figure 6.5 in comparison with $E_{x;y}$.

6.3. Conclusion

Neutral macropolyhedral boranes enjoy larger thermodynamic stability than single cluster isomers for twelve vertexes and more. The loss of extra open face hydrogen atoms results in enhanced stability of *nido* clusters as compared to macropolyhedra. Hence, anionic macropolyhedra are less stable with respect to anionic single clusters than in the neutral case. The same should be true for suitably substituted heteroboranes. Usually, the thermodynamically most stable neutral macropolyhedral boranes have at least one 10-vertex *nido* single cluster unit whereas the anionic macropolyhedral clusters usually possess one deprotonated 11-vertex *nido*-unit. The relative energies of the neutral macropolyhedra mostly reflect the stability patterns exhibited by the sum of the energies of two single cluster units making a given macropolyhedra (E_{x+y}).

7. Cluster Increments for Macropolyhedral Boranes

7.1. Introduction

Polyhedral (hetero)borane chemistry has experienced considerable development in the last few years with respect to both theory and experiment. Experimentalists used boron hydride clusters for the synthesis of new materials, e.g., superacids,¹ and molecular rotors or locks.² Important theoretical perspectives include the *mno* skeletal electron count rule,³ the structural relationship between the orthorhombic boron and the polyhedral borane clusters,⁴ and between various classes of macropolyhedral boranes,⁵ new definitions of electron donating or withdrawing effects of substituents,⁶ and the structural and connection increment methods to correctly reproduce the DFT calculated relative stabilities.⁷ The latter led to the prediction of competitive thermodynamic stability of some experimentally still unknown isomers,^{7a-c} the rationalization of the presence of heteroatoms at vertexes of higher connectivity,^{7a,b} or at adjacent positions,^{7e} thus quantifying and defining the limitations⁸ of Williams' qualitative heteroatom placement rules.⁹

¹ Reed, C. A.; Kim, K.-C.; Bolskar, R. D.; Mueller, L. J. *Science*, **2000**, 289, 101-104.

² Hawthorne, M. F.; Skelton, J. M.; Zink, J. I.; Bayer, M. J.; Liu, C.; Livshits, E.; Baer, R.; Neuhauser, D.; *Science*, **2004**, 303, 1849-1851.

³ a) Jemmis, E. D.; Balakrishnarajan, M. M.; Pancharatna, P. D.; *J. Am. Chem. Soc.*, **2001**, 123, 4313-4323. b) Jemmis, E. D.; Balakrishnarajan, M. M.; Pancharatna, P. D. *Chem. Rev.* **2002**, 102, 93-144.

⁴ Jemmis, E. D.; Balakrishnarajan, M. M. *J. Am. Chem. Soc.*, **2001**, 123, 4324-4330.

⁵ Kiani, F. A.; Hofmann, M. *Eur. J. Inorg. Chem.* submitted.

⁶ Teixidor F.; Barberà G.; Vaca A.; Kivekäs R.; Sillanpää R.; Oliva J.; Viñas C. *J Am. Chem. Soc.* **2005**, 127, 10158-10159.

⁷ a) Kiani, F. A.; Hofmann, M. *Inorg. Chem.* **2004**, 43, 8561-8571. b) Kiani, F. A.; Hofmann, M. *Inorg. Chem.* **2005**, 44, 3746-3754. c) Kiani, F. A.; Hofmann, M. *Eur. J. Inorg. Chem.* **2005**, 12, 2545-2553. d) Kiani, F. A.; Hofmann, M. *J. Mol. Model.* **2006**, 12, 597-609. e) Kiani, F. A.; Hofmann, M. *Dalton Trans.*, **2006**, 5, 686-692. f) Kiani, F. A.; Hofmann, M. *Organometallics*, **2006**, 25, 485-490.

⁸ Withers, N, D.; *Chemical Science*, **2006**, 1.

⁹ a) Williams, R. E. *J. Am. Chem. Soc.* **1965**, 87, 3513-3515. b) Williams, R. E. *In Progress in Boron Chemistry* Brotherton, R. J., Steinberg, H., Eds.; Pergamon Press: England, 1970; Vol. 2, Chapter 2, p 57. c) Williams, R. E. *Chem. Rev.* **1992**, 92, 177-207; references therein.

Density functional theory calculations on macropolyhedral boranes¹⁰ indicate that single cluster boranes tend to retain their individual characteristics in the macropolyhedral boranes: the energies of

macropolyhedral boranes differing in the vertex distribution between the two cluster units show very similar trends to the sum of energies for separated clusters corresponding to individual units.⁵ Therefore, macropolyhedral boranes were considered not as genuine single entities but as clusters composed of two individual cluster fragments. These have individual contributions to the total macropolyhedron which could be quantified as “cluster increments”. The studied macropolyhedral borane structures share two vertexes either between two individual *nido*-units (*nido:nido*-macropolyhedral boranes),

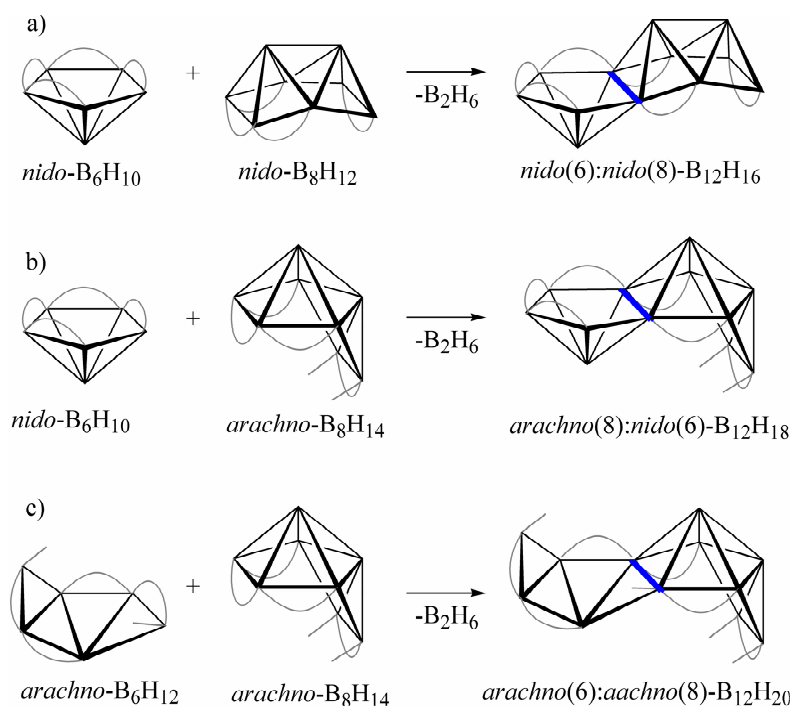
between one *arachno* and one *nido*-unit (*arachno:nido*-macropolyhedral boranes), or between two individual *arachno*-units (*arachno:arachno*-macropolyhedral boranes). These structures are formally obtained by condensation of two single clusters eliminating a B_2H_6 unit (Scheme 1). Numerous experimentally known homonuclear macropolyhedral boranes are listed in Table 7.1.

7.2. Result and Discussion

7.2.1. Relative stabilities of various types of macropolyhedral boranes

nido:nido-macropolyhedral boranes containing at least one *nido*-10-vertex cluster fragment enjoy special stability (see Figure 7.1a).⁵ The combinations 5:10, 6:10, 7:10, 8:10, 9:10, 10:10 and 10:11 are

Scheme 7.1: Macropolyhedral boranes can be formally obtained as condensation product of two single cluster boranes. Elimination of a B_2H_6 unit from corresponding six and eight vertex clusters gives rise to a) *nido*-6:*nido*-8- $B_{12}H_{16}$ b) *arachno*-8:*nido*-6- $B_{12}H_{18}$ and c) *arachno*-6:*arachno*-8- $B_{12}H_{20}$. Exo hydrogen atoms are omitted for clarity, endo hydrogen atoms are indicated as grey arcs (bridging H) or lines (endo terminal H).



¹⁰ Kiani, F. A.; Hofmann, M. *Inorg. Chem.* **2006**, 45, 6996-7003.

more stable as compared to their respective isomers. Experimentally known *nido:nido*- B_nH_{n+4} ($n = 14$,¹¹ 16,¹² 18¹³ or the anionic clusters (e.g., $n = 18$ ^{14,15} and 19^{16,17} highlighted by bold numbers in Figure 7.1a) all contain one 10-vertex *nido*-unit. Furthermore, there is a general preference for even *nido*-cluster fragments over odd ones. For example, the experimentally known $B_{12}H_{16}$ ^{18,19} isomer has two even *nido*-fragments, i.e., one 6-vertex and one 8-vertex *nido*-fragment (not two 7-vertex units or one 5- and one 9-vertex unit).²⁰

Moreover, the energy range spanned by the isomers considered is always larger for even n than for the neighboring odd case of $n+1$ and $n-1$ (Figure 7.1a).⁵ For even $n > 12$, the energetic separation of the most stable and the second most stable isomer is also more pronounced than for the neighboring odd $n+1$ or $n-1$.⁵ Obviously, there exists a clearer preference for the thermodynamically most stable *nido:nido*-macropolyhedral borane isomer when the number of vertexes are even rather than odd.

The energetic separation of various isomers of *arachno:arachno*- B_nH_{n+8} macropolyhedra (Figure 7.1c) is much less and various isomers are energetically very close to each other. Nevertheless, the thermodynamic preference of *arachno:arachno*-macropolyhedra with at least one 9-vertex *arachno*-

¹¹ Heřmánek, S.; Fetter, K.; Plešek, J.; Todd, L. J.; Garber, A. R. *Inorg. Chem.* **1975**, *14*, 2250-2253.

¹² a) Plešek, J.; Heřmánek, S.; Hanousek, F. *Collect. Czech. Chem. Commun.* **1967**, *33*, 699-705. b) Friedman, L. B.; Cook, R. E.; Glick, M. D. *J. Am. Chem. Soc.* **1968**, *90*, 6862-6863. c) Friedman, L. B.; Cook, R. E.; Glick, M. D. *Inorg. Chem.* **1970**, *9*, 1452-1458.

¹³ a) Pitochelli, A. R.; Hawthorne, M. F. *J. Am. Chem. Soc.* **1962**, *84*, 3218. b) Simpson, P. G.; Lipscomb, W. N. *J. Chem. Phys.* **1963**, *39*, 26-34. c) Simpson, P. G.; Lipscomb, W. N. *Proc. Natl. Acad. Sci. USA.* **1962**, *48*, 1490-1491. d) Simpson, P. G.; Foltz, K.; Dobrott, R. D.; Lipscomb, W. N. *J. Chem. Phys.* **1963**, *39*, 2339-2348.

¹⁴ Olsen, F. P.; Vasavada, R. C.; Hawthorne, M. F. *J. Am. Chem. Soc.* **1968**, *90*, 3946-3951.

¹⁵ Fontaine, X. L. R.; Greenwood, N. N.; Kennedy, J. D.; MacKinnon, P. *J. Chem. Soc., Dalton Trans.* **1988**, *7*, 1785-1793.

¹⁶ Dopke, J. A.; Powell, D. R.; Gaines, D. F. *Inorg. Chem.* **2000**, *39*, 463-467.

¹⁷ Jemmis et al found that the initially reported $[B_{19}H_{20}]^-$ structure did not converge at the RB3LYP/6-31G(d) level, while the reported $B_{19}H_{20}$ was a stable species only as a trianion. Hence the authors suggested $[B_{19}H_{22}]^-$ to be the correct structure. See, Jemmis, E. D.; Balakrishnarajan, M. M.; Pancharatna, P. D. *Inorg. Chem.* **2001**, *40*, 1730-1731.

¹⁸ Brewer, C. T.; Grimes, R. N. *J. Am. Chem. Soc.* **1984**, *106*, 2722-2723

¹⁹ Brewer, C. T.; Swisher, R. G.; Sinn, E.; Grimes, R. N. *J. Am. Chem. Soc.* **1985**, *107*, 3558-3564.

²⁰ In ref .18 the *nido-4:nido-10*- $B_{12}H_{16}$ was found to be slightly (1.7 kcal mol⁻¹) more stable than the experimentally known *nido-6:nido-8*- $B_{12}H_{16}$ isomer. As the current paper deals with macropolyhedral boranes with *nido*-cluster fragments between 5-12 vertexes, *nido-4:nido-10*- $B_{12}H_{16}$ is not discussed.

7. CLUSTER INCREMENTS FOR MACROPOLYHEDRAL BORANES

fragment is obvious for $n = 12-17$.²¹ For 10- and 11-vertex *arachno:arachno*-macropolyhedra, where there is no competitive 9-vertex *arachno*-cluster fragment, the 5:6 and 5:8 isomers are more stable.

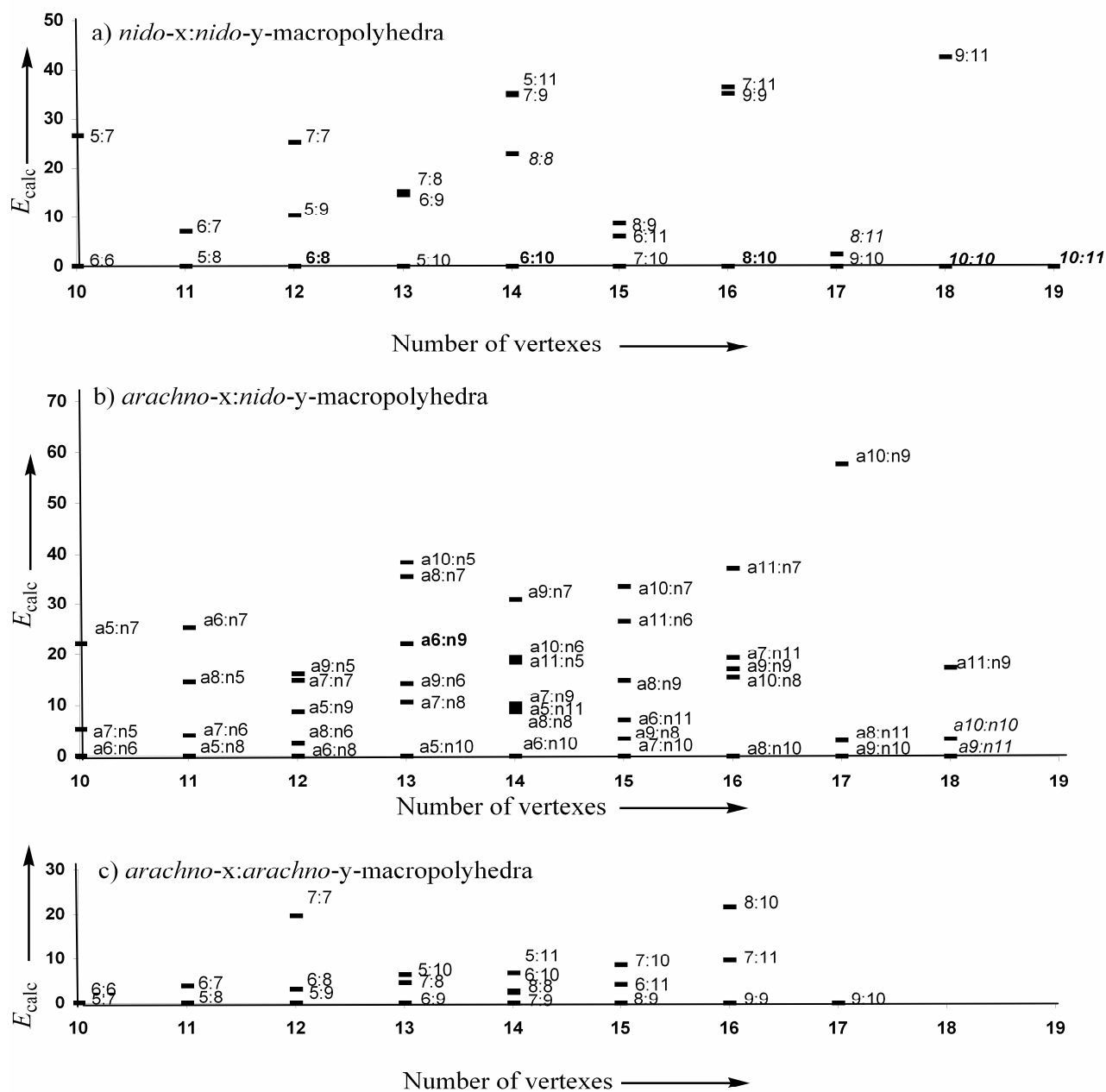


Figure 7.1: A comparison of relative energies [kcal mol⁻¹] of macropolyhedral *nido:nido*-B_nH_{n+4} (a), *arachno:nido*-B_nH_{n+6} (b) and *arachno:arachno*-B_nH_{n+8} boranes (c). Digits indicate the size of the two cluster units making a macropolyhedron. Entries in bold represent experimentally known macropolyhedral boranes while those in italic represent experimentally known macropolyhedral heteroboranes.

²¹ For B₁₇H₂₅, the isomeric *arachno*-8:*arachno*-11-B₁₇H₂₅ macropolyhedron rearranged to *arachno*-9:*arachno*-10-B₁₇H₂₅.

7. CLUSTER INCREMENTS FOR MACROPOLYHEDRAL BORANES

Table 7.1. Some experimentally known two-vertex sharing macropolyhedral (hetero)boranes and their homonuclear alternatives.^a

Example	Structure description	Homonuclear alternative	Reference(s)
B ₁₂ H ₁₆ ^b	<i>nido</i> -B ₆ : <i>nido</i> -B ₈	---	18,19
B ₁₄ H ₁₈ ^b	<i>nido</i> -B ₆ : <i>nido</i> -B ₁₀	---	11
B ₁₆ H ₂₀ ^b	<i>nido</i> -B ₈ : <i>nido</i> -B ₁₀	---	12
i-B ₁₈ H ₂₂ , n-B ₁₈ H ₂₂ ^b	<i>nido</i> -B ₁₀ : <i>nido</i> -B ₁₀	---	13
[B ₁₉ H ₂₂]	<i>nido</i> -B ₁₀ : <i>nido</i> -B ₁₁	---	16,17
B ₁₃ H ₁₉	<i>arachno</i> -B ₉ : <i>nido</i> -B ₆	---	22a
[Pt(B ₆ H ₉) ₂ (PMe ₂ Ph) ₂]	<i>nido</i> -B ₈ : <i>nido</i> -B ₈	B ₁₄ H ₂₀	22b
[(PMe ₂ Ph)PtB ₁₆ H ₁₈ (PMe ₂ Ph)] ⁻	<i>nido</i> -B ₈ : <i>nido</i> -B ₁₁	B ₁₇ H ₂₁	23
[SB ₁₇ H ₂₀]	<i>arachno</i> -SB ₉ : <i>nido</i> -B ₁₀	[B ₁₈ H ₂₃]	24a
S ₂ B ₁₆ H ₁₄ (PPh ₃)	<i>arachno</i> -SB ₈ : <i>nido</i> -SB ₁₀	B ₁₈ H ₂₄	25
S ₂ B ₁₇ H ₁₇ .SMe ₂	<i>arachno</i> -SB ₉ : <i>nido</i> -SB ₁₀	B ₁₉ H ₂₅	24b
[S ₂ B ₁₈ H ₁₉]	<i>arachno</i> -SB ₁₀ : <i>nido</i> -SB ₁₀	[B ₂₀ H ₂₅]	26

^a Macropolyhedral borates or macropolyhedral heteroboranes/borates are listed only if no homonuclear macropolyhedral borane representative is known experimentally. ^b Structure predicted as most stable isomer, both from cluster increments as well as from DFT computations.

The trends in *arachno:nido*-macropolyhedral borane relative stabilities result as superposition of *nido:nido*-, and *arachno:arachno*-trends with the former being more dominant. There is a clearer preference to have an even *nido*-fragment in the thermodynamically most stable isomer (See the most stable isomers for n = 10-17, Figure 7.1b). The most stable isomer for n = 13-17 consists of at least one

²² a) Huffman, J. C.; Moody, D. C.; Schaffer, R. *Inorg. Chem.* **1976**, *15*, 227-232. b) Greenwood, N. N.; Hails, M. J.; Kennedy, J. D.; McDonald, W. S. *J. Chem. Soc., Dalton Trans.* **1985**, *5*, 953-972.

²³ Beckett, M. A.; Crook, J. E.; Greenwood, N. N.; Kennedy, J. D.; McDonald, W. S. *J. Chem. Soc., Chem. Commun.* **1982**, *10*, 552-553.

²⁴ a) Jelínek, T.; Kilner, C. A.; Barrett, S. A.; Thornton-Pett, M.; Kennedy, J. D. *J. Chem. Soc., Chem. Commun.* **1999**, *18*, 1905-1906. b) Kaur, P.; Holub, J.; Rath, N. P.; Bould, J.; Barton, L.; Štíbr, B.; Kennedy, J. D. *Chem. Commun.* **1996**, *2*, 273-275.

²⁵ Kaur, P.; Thornton-Pett, M.; Clegg, W.; Kennedy, J. D. *J. Chem. Soc., Dalton Trans.* **1996**, 4155-4157.

²⁶ Jelínek, T.; Cisařová, I.; Štíbr, B.; Kennedy, J. D.; Thornton-Pett, M. *J. Chem. Soc., Dalton Trans.* **1998**, *18*, 2965-2968.

10-vertex *nido*-cluster fragment. For $n = 18$, however, the thermodynamically most stable macropolyhedral borane combines a *nido*-11 with an *arachno*-9-vertex fragment - the preferred fragment for *arachno:arachno*-macropolyhedral boranes.

The presence of a *nido*-7-vertex cluster usually constitutes the thermodynamically least stable isomer in *nido:nido*- as well as *arachno:nido*-macropolyhedral boranes.

7.2.2. Even *nido*-clusters are more favorable than odd *nido*-clusters in macropolyhedra

For a given molecular formula, different macropolyhedral structures are conceivable differing in the sizes of the cluster fragments that share two vertexes. Our earlier work⁵ indicated that the relative energies of the various macropolyhedral isomers are related to those of the cluster fragments. Therefore increments were established which by simple addition allow to estimate easily and quickly the relative stabilities of isomeric macropolyhedra. The statistically fitted increments for various *nido*- and *arachno*-clusters are listed in Table 7.2 and are plotted in Figure 7.2. These cluster increments correspond to individual cluster fragments in macropolyhedral boranes and are independent of the other cluster fragment present, i.e. a given cluster fragment in a macropolyhedral borane has generally the same influence on the thermodynamic stability irrespective of the size (small or large) or the type (*nido* or *arachno*) of other cluster fragment attached to it. Even *nido*-cluster fragments have smaller cluster increments as compared to odd *nido*-cluster fragments (Figure 7.2, Table 7.2). Among *nido*-cluster fragments, the 10-vertex *nido*-fragment is assigned an $E_{\text{inc}} = 0.0 \text{ kcal mol}^{-1}$. All other *nido*-cluster fragments are comparatively less favorable for incorporation in a macropolyhedral borane and have $E_{\text{inc}} > 0.0 \text{ kcal mol}^{-1}$. Smaller cluster increments for even *nido*-cluster fragments are consistent with the general energetic preference of the *nido:nido*- and *arachno:nido*-macropolyhedral boranes (Figure 7.1a and b, respectively). Thermodynamically most stable *nido:nido*-macropolyhedral boranes with $n = 10$ -19 and *arachno:nido*-macropolyhedral boranes with $n = 10$ -17 contain at least one even *nido*-cluster unit. Moreover, the 10-vertex *nido*-unit is favored by at least $10.8 \text{ kcal mol}^{-1}$ over other *nido*-units and is therefore predominant: the thermodynamically most stable 13-17 vertex containing *nido:nido*- and 13-16 vertex containing *arachno:nido*-macropolyhedral boranes have at least one 10-vertex *nido*-fragment.

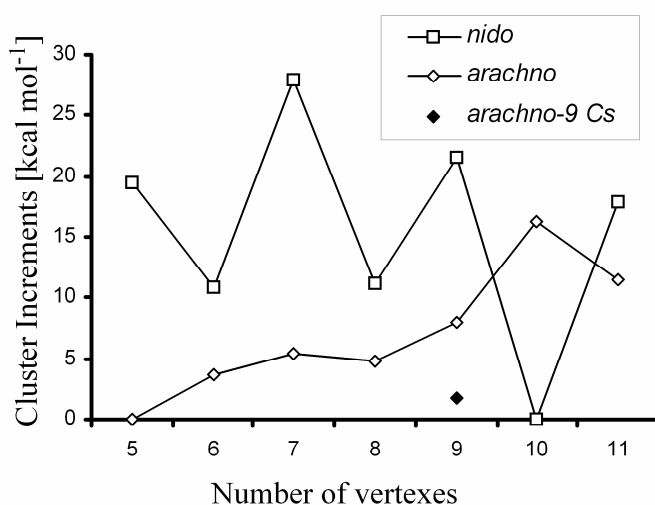


Figure 7.2: Statistically fitted cluster increments for various *nido*- and *arachno*-single cluster fragments in two-vertex sharing macropolyhedral boranes.

Table 7.2. Statistically fitted cluster increments in kcal mol⁻¹ for various *nido*- and *arachno*-fragments.

number of vertexes	Cluster increments [kcal mol ⁻¹]	
	<i>nido</i> -	<i>arachno</i> -
5	19.4	0.0
6	10.8	3.6
7	28.0	5.4
8	11.2	4.8
9	21.6	1.8 (8.0) ^a
10	0.0	16.3
11	17.8	11.5

9A has a smaller cluster increment of 1.8 kcal mol⁻¹. Its isomeric **9B** has a cluster increment of 8.0 kcal mol⁻¹.

7.2.3. Smaller *arachno*-clusters are more favorable than larger *arachno*-clusters.

The *arachno* cluster increments are usually smaller than the corresponding values for *nido* fragments and increase with the number of vertexes. Hence, smaller *arachno* cluster fragments are more suitable for macropolyhedral boranes than large ones. The cluster increments increase with the number of vertexes, ranging from $E_{\text{inc}} = 0.0$ kcal mol⁻¹ for the 5-vertex *arachno*-unit to $E_{\text{inc}} = 16.3$ kcal mol⁻¹ for the 10-vertex *arachno*-unit. The cluster increment ($E_{\text{inc}} = 11.5$ kcal mol⁻¹) for the 11-vertex *arachno*-fragment²⁷ is, however, slightly smaller than that of the 10-vertex *arachno*-fragment. Two different *arachno*-9-vertex cluster fragments, i.e. those derived from **9A** or **9B** (Figure 7.3) have significantly different cluster increments (1.8 and 8.0 kcal mol⁻¹). The former B₉H₁₅ isomer, **9A**, with a more open seven membered face is also thermodynamically preferred over **9B** by 4.6 kcal mol⁻¹. The latter has a six membered open face. We note that *arachno:arachno*- and *arachno:nido*-macropolyhedral boranes with a **9A** cluster

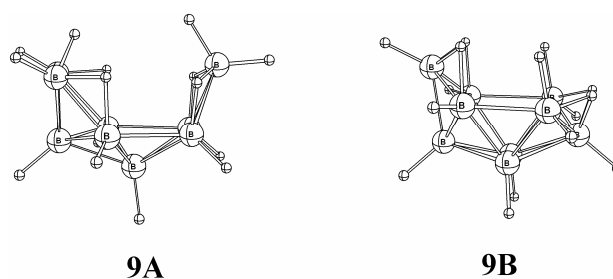


Figure 7.3: Two B₉H₁₅ isomers (**9A** and **9B**) for which two different *arachno*-9-vertex cluster fragments derive. The former is 4.6 kcal mol⁻¹ more stable than the latter.

²⁷ The *arachno*-11-vertex *nido*-fragment was derived by computing various possible B₁₁H₁₅ geometries. The most stable one looked like an outgrowth of a BH₃ vertex on the 10-vertex *arachno*-cluster.

7. CLUSTER INCREMENTS FOR MACROPOLYHEDRAL BORANES

fragment are usually particularly stable.

The smaller increments for the 5- or 9-vertex *arachno*-cluster fragments is reflected by the presence of these fragments in the thermodynamically most stable *arachno:arachno*-macropolyhedral boranes (Figure 7.1c). For $n = 12-17$, the *arachno:arachno*-macropolyhedral boranes tend to have one *arachno*-9-vertex fragment. For $n = 10-12$, the thermodynamically most stable macropolyhedral borane contains one 5-vertex *arachno*-fragment.

7.2.4. Cluster increments reproduce the DFT computed relative stabilities of macropolyhedral boranes with good accuracy.

The cluster increments may be used to derive the approximate relative stabilities of various two-vertex sharing *nido:nido*-, *arachno:nido*- and *arachno:arachno*-macropolyhedral boranes. Relative stabilities of the most stable isomer formed by two individual cluster fragments are quite accurately reproduced by the cluster increments. Table 7.3 indicates how the relative stabilities of various 16 to 18-vertex *nido:nido*-macropolyhedral boranes are reproduced.

Table 7.3. Cluster increments accurately reproduce the relative stabilities of various macropolyhedral boranes (All values are in kcal mol⁻¹).

	<i>nido</i> -5	<i>nido</i> -6	<i>nido</i> -7	<i>nido</i> -8	<i>nido</i> -9	<i>nido</i> -10	<i>nido</i> -11	$\sum E_{\text{inc}}^{\text{a}}$	$E_{\text{inc}}^{\text{rel b}}$	$E_{\text{calc}}^{\text{c}}$	ΔE^{d}
	19.4	10.8	28.0	11.2	21.6	0.0	17.8				
<i>nido:nido</i>-B₁₆H₂₀											
<i>nido</i> -8: <i>nido</i> -10 ^e				1		1		11.2	0.0	0	0.0
<i>nido</i> -9: <i>nido</i> -9					2			43.2	32.0	35.0	-3.0
<i>nido</i> -7: <i>nido</i> -11			1				1	45.8	34.6	37.9	-3.3
<i>nido:nido</i>-B₁₇H₂₁											
<i>nido</i> -9: <i>nido</i> -10					1	1		21.6	0.0	0	0.0
<i>nido</i> -8: <i>nido</i> -11				1			1	29.0	7.4	2.7	4.7
<i>nido:nido</i>-B₁₈H₂₂											
<i>nido</i> -10: <i>nido</i> -10 ^e						2		0.0	0.0	0	0.0
<i>nido</i> -9: <i>nido</i> -11					1		1	39.4	39.4	42.2	-2.8

^a The sum of increments for the two clusters making a macropolyhedral borane. ^b The relative stabilities predicted by the cluster increments. ^c DFT computed relative stabilities. ^d ΔE is the difference of the $E_{\text{inc}}^{\text{rel}}$ and $\sum E_{\text{inc}}$ values. ^e Experimentally known structures.

7. CLUSTER INCREMENTS FOR MACROPOLYHEDRAL BORANES

Among four possible *nido:nido*-B₁₆H₂₀ isomers (see Table 7.3), the *nido*-8:*nido*-10-B₁₆H₂₀ with one 10-vertex *nido*-unit is the most stable isomer due to cluster increments of 0.0 and 11.2 kcal mol⁻¹ for 10- and 8-vertex *nido*-cluster fragments, respectively. Both the cluster increments as well as the DFT computed relative stabilities are higher for *nido*-9:*nido*-9-B₁₆H₂₀ and *nido*-7:*nido*-11-B₁₆H₂₀. For 17 and 18 vertexes, again the most stable isomer incorporates a 10-vertex *nido*-fragment in each case. *nido*-8:*nido*-10-B₁₆H₂₀²⁸ and *syn*- and *anti-nido*-10:*nido*-10-B₁₈H₂₂,¹³ as well as their anions^{14,15} are experimentally known. The *syn-nido*-10:*nido*-10-B₁₈H₂₂ first reported in 1963, represented the first example of geometrical isomerism in polyhedral boranes and is 1.2 kcal mol⁻¹ higher in energy.

The relative stabilities of all *nido:nido*-B_nH_{n+4}, *arachno:nido*-B_nH_{n+6} and *arachno:arachno*-B_nH_{n+8} clusters considered are plotted in Figure 7.1. Figure 7.4 shows a good correlation between $E_{\text{inc}}^{\text{rel}}$ (the relative stabilities as produced from cluster increments) and E_{calc} (the relative stabilities from the DFT computed results). A total of 102 macropolyhedral combinations constructed by the seven *nido*- and eight *arachno*-fragments were computed. Each of these 102 combinations can have more than one possible isomer either due to different endo-hydrogen atom placement or due to different shared vertexes. Only the most stable isomers that were used in order to derive and apply cluster increments. The geometry of three isomers either distorted severely or rearranged during the course of optimization. The relative stabilities for 87 out of the remaining 99 macropolyhedral clusters investigated are reproduced with deviations of less than 6 kcal mol⁻¹. Eight clusters are border line cases with deviations ranging from 6.0 to 8.9 kcal mol⁻¹. Deviations larger than 9.0 kcal mol⁻¹ for four clusters, however, indicate that cluster increments do not reproduce satisfactorily well the DFT computed relative stabilities of these few structures.

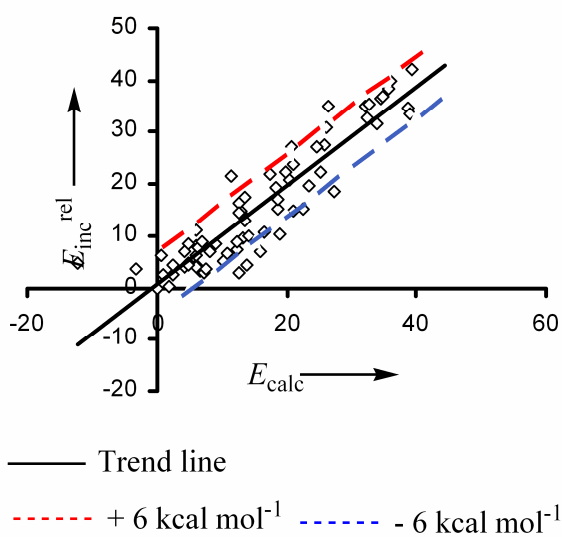


Figure 7.4: The relative stabilities [kcal mol⁻¹] of various macropolyhedral boranes are quite accurately reproduced by the cluster increments, i.e. mostly within 6.0 kcal mol⁻¹.

²⁸ Friedman, L. B.; Cook, R. E.; Glick, M. D. *Inorg. Chem.* **1970**, *9*, 1452-1458.

7.3. Conclusion

Cluster increments may be applied to reproduce the relative stabilities of various two-vertex sharing macropolyhedral boranes. Simple summation of two values (see Table 7.2) for the cluster fragments of each isomer of a given *nido:nido*-, *arachno:nido*- and *arachno:arachno*-macropolyhedral borane usually reproduces the DFT computed relative stabilities very accurately. The cluster increments are smaller for even *nido*-cluster fragments than for odd *nido*-cluster fragments. The cluster increments for *arachno*-clusters are usually smaller than for corresponding *nido*-fragments and increase with increasing cluster size. Experimentally known macropolyhedral boranes correspond to the most stable structures as computed by DFT methods and as estimated by the cluster increments produced.

8. Structural Relationships among Two Vertex Sharing Macropolyhedral Boranes

8.1. Introduction

Boron's rich polyhedral structural chemistry continues to excite chemists¹ due to its key role in invigorating new concepts and a general picture of chemical bonding,^{2,3} use in boron neutron capture therapy,⁴ and in the synthesis of new materials.⁵ Boron hydrides can be distinguished into two main classes, i.e., simple polyhedral and macropolyhedral boranes.⁶ Simple polyhedral boranes with convex curvature are either the most spherical deltahedra, i.e., *closo*-boranes, or are deltahedral fragments derived by the elimination of one, two or three vertexes from *closo*-clusters to give *nido*-, *arachno*⁷ and *hypho*-boranes,⁸ respectively. Clusters composed of merged polyhedra representing a concave fashion have been called macropolyhedra. Theoretical efforts by Wade,⁹ Williams,⁷ Jemmis and Schleyer,¹⁰ Ott

¹ Withers, N. D.; *Chemical Science*, **2006**, *1*.

² a) Teixidor F.; Barbera G.; Vaca A.; Kivekas R.; Sillanpaa R.; Oliva J.; Viñas C. *J Am. Chem. Soc.* **2005**, *127*, 10158-10159. b) Oliva J. M.; Allan N. L.; Schleyer P. V. R.; Vinas C.; Teixidor F. *J. Am. Chem. Soc.*, **2005**, *127*, 13538-13547.

³ a) Jemmis, E. D.; Balakrishnarajan, M. M.; Pancharatna, P. D.; *J. Am. Chem. Soc.*, **2001**, *123*, 4313-4323. b) Jemmis, E. D.; Balakrishnarajan, M. M.; Pancharatna, P. D. *Chem. Rev.* **2002**, *102*, 93-144.

⁴ a) Hawthorne, M. F.; Maderna, A. *Chem. Rev.*, **1999**, *99*, 3421-3434. b) Nakanishi, A.; Guan, L.; Kane, R. R.; Kasamatsu, H.; Hawthorne, M. F. *Proc. Natl. Acad. Sci. USA*, **1999**, *96*, 238-241.

⁵ a) Hawthorne, M. F.; Skelton, J. M.; Zink, J. I.; Bayer, M. J.; Liu, C.; Livshits, E.; Baer, R.; Neuhauser, D.; *Science*, **2004**, *303*, 1849-1851. b) Reed, C. A.; Kim, K.-C.; Bolskar, R. D.; Mueller, M. L. *J. Science*, **2000**, *289*, 101-104.

⁶ Kiani, F. A.; Hofmann, M. *Inorg. Chem.* **2006**, *45*, 6996-7003.

⁷ a) Williams, R. E. *J. Am. Chem. Soc.* **1965**, *87*, 3513-3515. b) Williams, R. E. *in Progress in Boron Chemistry*, Brotherton, R. J., Steinberg, H., Eds.; Pergamon Press: England, 1970; Vol. 2, Chapter 2, p 57. c) Williams, R. E.; *Chem. Rev.* **1992**, *92*, 177-207; references therein.

⁸ Rudolph R. W. *Acc. Chem. Res.* **1976**, *9*, 446-452.

⁹ (a) Wade, K. *Adv. Inorg. Chem. Radiochem.* **1976**, *18*, 1-66. (b) Wade, K. *In Metal Interactions with Boron Clusters*; Grimes, R. N., Ed.; Plenum Press: New York, 1982; Chapter 1, pp 1– 41.

¹⁰ a) Jemmis, E. D. *J. Am. Chem. Soc.* **1982**, *104*, 7017-7020. b) Jemmis, E. D.; Schleyer, P. v. R. *J. Am. Chem. Soc.* **1982**, *104*, 4781-4788.

8. TWO VERTEX SHARING MACROPOLYHEDRAL BORANES

and Gimarc,¹¹ and quite recently by us¹² offer an insight into the structural patterns of simple polyhedral boranes. Nonetheless, except for the Jemmis' skeletal electron count principle,¹⁰ macropolyhedral borane clusters did not experience a wide-ranging theoretical consideration. A large number of homonuclear as well as heteronuclear boranes with more than one fused cluster unit are experimentally known and exhibit varying architectural patterns, e.g., those with cluster units joined by a two center-two electron,¹³ or by a three center-two electron bond,^{13d,14} as well as those in which cluster units share one vertex, e.g., B₁₄H₂₂,¹⁵ two vertexes, e.g., B₁₈H₂₂,¹⁶ three vertexes, e.g., B₂₀H₁₈L₂ compounds,¹⁷ or even four vertexes, e.g., B₂₀H₁₆.¹⁸ Macropolyhedral boranes with two shared vertexes represent the group with numerous experimentally characterized examples (see Table 8.1). The simple polyhedral boranes included in this study for comparison i.e., the *nido*-B_nH_{n+4}, *arachno*-B_nH_{n+6} and *hypho*-B_nH_{n+8} series, also represent numerous experimentally known examples^{7c} including B₁₄H₂₀¹⁹ considered by Jemmis as single pseudo-spherical *arachno*-deltahedron.^{3b}

A study of the stabilities of *nido:nido*-B_nH_{n+4} macropolyhedral boranes (i.e. clusters composed of two *nido*-fragments sharing two vertexes), relative to isomeric simple polyhedral *nido*-clusters revealed that macropolyhedra are preferred for 12 and more vertexes ($n \geq 12$).⁶ In addition, *nido:nido*-macropolyhedral borane isomers with at least one ten vertex *nido*-fragment were found to be

¹¹ Ott, J. J.; Gimarc, B. M. *J. Am. Chem. Soc.* **1986**, *108*, 4303-4308.

¹² a) Kiani, F. A.; Hofmann, M. *Inorg. Chem.* **2005**, *44*, 3746-3754. b) Kiani, F. A.; Hofmann, M. *Eur. J. Inorg. Chem.* **2005**, *12*, 2545-2553. c) Kiani, F. A.; Hofmann, M. *J. Mol. Model.* **2006**, *12*, 597-609. d) Kiani, F. A.; Hofmann, M. *Dalton Trans.*, **2006**, *5*, 686-692. e) Kiani, F. A.; Hofmann, M. *Organometallics*, **2006**, *25*, 485-490. f) Kiani, F. A.; Hofmann, M. *Inorg. Chem.* **2004**, *43*, 8561-8571.

¹³ See for example, a) Srinivas, G. N.; Hamilton, T. P.; Jemmis, E. D.; McKee, M. L.; Lammertsma, K. *J. Am. Chem. Soc.* **2000**, *122*, 1725-1728. b) Hawthorne, M. F.; Pilling, R. L.; Stokely, P. F.; Garrett, P. M. *J. Am. Chem. Soc.* **1963**, *85*, 3704-3705. c) Hawthorne, M. F.; Pilling, R. L.; Stokely, P. F. *J. Am. Chem. Soc.* **1965**, *87*, 1893-1899. d) Watson-Clark, R. A.; Knobler, C. B.; Hawthorne, M. F. *Inorg. Chem.* **1996**, *35*, 2963-2966.

¹⁴ See for example, Hawthorne, M. F.; Pilling, R. L. *J. Am. Chem. Soc.* **1966**, *88*, 3873-3874.

¹⁵ Rathke, J.; Schaeffer, R. *Inorg. Chem.* **1974**, *13*, 3008-3011.

¹⁶ Simpson, P. G.; Lipscomb, W. N. *J. Chem. Phys.* **1963**, *39*, 26-34.

¹⁷ See for example, a) Enemark, J. H.; Friedman, L. B.; Lipscomb, W. N. *Inorg. Chem.* **1966**, *5*, 2165-2173. b) Cheek, Y. M.; Greenwood, N. N.; Kennedy, J. D.; McDonald, W. S. *J. Chem. Soc., Chem. Commun.* **1982**, 80-81.

¹⁸ Friedman, L. B.; Dobrott, R. D.; Lipscomb, W. N. *J. Am. Chem. Soc.* **1963**, *85*, 3505-3506.

¹⁹ Huffmann, J. C.; Moody, D. C.; Schaeffer, R. *Inorg. Chem.* **1981**, *20*, 741-745.

8. TWO VERTEX SHARING MACROPOLYHEDRAL BORANES

thermodynamically highly stable and to usually represent the most stable isomers.⁶ Further studies are carried out to determine the turning point from *arachno*- B_nH_{n+6} to *arachno:nido*- B_nH_{n+6} and from *hypho*- B_nH_{n+8} to *arachno:arachno*- B_nH_{n+8} preference in terms of thermodynamic stability. We also try to determine the “preferred fragments” for *arachno:nido*- and *arachno:arachno*-macropolyhedral borane construction. Profound structural relationships between the most stable isomers of different classes of two vertex sharing macropolyhedral boranes are determined akin to those predicted in 1965 by Williams,⁷ for simple polyhedral clusters.

The optimized geometries of various computed two-vertex sharing *arachno:nido*- $B_{14}H_{20}$ macropolyhedral boranes are displayed in Figure 8.1.

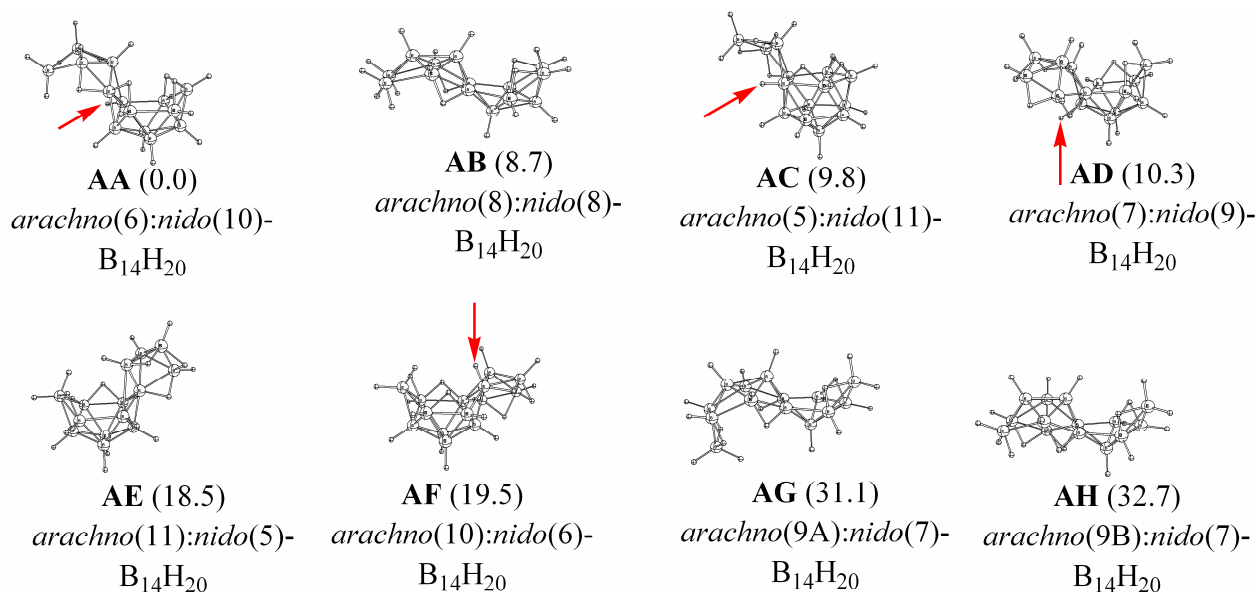


Figure 8.1: The optimized geometries and relative stabilities in parenthesis of various two-vertex sharing *arachno:nido*- $B_{14}H_{20}$ structures. Arrows indicate a hydrogen atom exo-substituted to one boron atoms of the shared B_2 unit.

8.2. Results and Discussion

8.2.1. Thermodynamic Stabilities of Neutral Macropolyhedral Boranes Relative to Corresponding Simple Polyhedral Boranes.

For the general formula B_nH_{n+4} , *nido*-boranes are more stable than isomeric two vertex sharing *nido:nido*-macropolyhedral boranes, for up to eleven vertexes ($n \leq 11$). For 12 or more vertexes macropolyhedral boranes enjoy a larger thermodynamic stability (Figure 8.2a).⁶

8. TWO VERTEX SHARING MACROPOLYHEDRAL BORANES

Table 8.1. Some experimentally known two-vertex sharing macropolyhedral (hetero)boranes and their homonuclear alternatives.^{a,b}

Example	Structure description	Homonuclear alternative
B ₁₂ H ₁₆ ^c	<i>nido</i> -B ₆ : <i>nido</i> -B ₈	---
B ₁₄ H ₁₈ ^c	<i>nido</i> -B ₆ : <i>nido</i> -B ₁₀	---
B ₁₆ H ₂₀ ^c	<i>nido</i> -B ₈ : <i>nido</i> -B ₁₀	---
<i>i</i> -B ₁₈ H ₂₂ , <i>n</i> -B ₁₈ H ₂₂ ^c	<i>nido</i> -B ₁₀ : <i>nido</i> -B ₁₀	---
[B ₁₉ H ₂₂] ⁻	<i>nido</i> -B ₁₀ : <i>nido</i> -B ₁₁	---
B ₁₃ H ₁₉	<i>arachno</i> -B ₉ : <i>nido</i> -B ₆	---
[Pt(B ₆ H ₉) ₂ (PMe ₂ Ph) ₂]	<i>nido</i> -B ₈ : <i>nido</i> -B ₈	B ₁₄ H ₂₀
[(PMe ₂ Ph)PtB ₁₆ H ₁₈ (PMe ₂ Ph)] ⁻	<i>nido</i> -B ₈ : <i>nido</i> -B ₁₁	B ₁₇ H ₂₁
[SB ₁₇ H ₂₀] ⁻	<i>arachno</i> -SB ₉ : <i>nido</i> -B ₁₀	[B ₁₈ H ₂₃] ⁻
S ₂ B ₁₆ H ₁₄ (PPh ₃)	<i>arachno</i> -SB ₈ : <i>nido</i> -SB ₁₀	B ₁₈ H ₂₄
S ₂ B ₁₇ H ₁₇ .SMe ₂	<i>arachno</i> -SB ₉ : <i>nido</i> -SB ₁₀	B ₁₉ H ₂₅
[S ₂ B ₁₈ H ₁₉] ⁻	<i>arachno</i> -SB ₁₀ : <i>nido</i> -SB ₁₀	[B ₂₀ H ₂₅] ⁻

^a Macropolyhedral borates or macropolyhedral heteroboranes/borates are listed only if no homonuclear macropolyhedral borane representative is known experimentally. ^b For experimentally known structures, see the following references: a) B₁₂H₁₆: Brewer, C. T.; Grimes, R. N. *J. Am. Chem. Soc.* **1984**, *106*, 2722-2723; Brewer, C. T.; Swisher, R. G.; Sinn, E.; Grimes, R. N. *J. Am. Chem. Soc.* **1985**, *107*, 3558-3564. b) B₁₄H₁₈: Heřmánek, S.; Fetter, K.; Plešek, J.; Todd, L. J.; Garber, A. R. *Inorg. Chem.* **1975**, *14*, 2250-2253. c) B₁₆H₂₀: Plešek, J.; Heřmánek, S.; Hanousek, F. *Collect. Czech. Chem. Commun.* **1967**, *33*, 699-705; Friedman, L. B.; Cook, R. E.; Glick, M. D. *J. Am. Chem. Soc.* **1968**, *90*, 6862-6863; Friedman, L. B.; Cook, R. E.; Glick, M. D. *Inorg. Chem.* **1970**, *9*, 1452-1458. d) B₁₈H₂₂: Pitochelli, A. R.; Hawthorne, M. F. *J. Am. Chem. Soc.* **1962**, *84*, 3218; Simpson, P. G.; Lipscomb, W. N. *Proc. Natl. Acad. Sci. USA.* **1962**, *48*, 1490-1491; Simpson, P. G.; Foltling, K.; Dobrott, R. D.; Lipscomb, W. N. *J. Chem. Phys.* **1963**, *39*, 2339-2348; Fontaine, X. L. R.; Greenwood, N. N.; Kennedy, J. D.; Mackinnon, P. *J. Chem. Soc., Dalton Trans.* **1988**, 1785-1793; Simpson, P. G.; Lipscomb, W. N. *J. Chem. Phys.* **1963**, *39*, 26-34. e) [B₁₉H₂₂]⁻: Dopke, J. A.; Powell, D. R.; Gaines, D. F. *Inorg. Chem.* **2000**, *39*, 463-467; Jemmis et al found the initially reported [B₁₉H₂₀]⁻ structure to survive RB3LYP/6-31G(d) geometry optimization only as a trianion. Hence the authors suggested [B₁₉H₂₂]⁻ to be the correct structure, on the basis of mno rule. See, Jemmis, E. D.; Balakrishnarajan, M. M.; Pancharatna, P. D. *Inorg. Chem.* **2001**, *40*, 1730-1731. f) B₁₃H₁₉: Huffman, J. C.; Moody, D. C.; Schaffer, R. *Inorg. Chem.* **1976**, *15*, 227-232. g) [Pt(B₆H₉)₂(PMe₂Ph)₂]: Greenwood, N. N.; Hails, M. J.; Kennedy, J. D.; McDonald, W. S. *J. Chem. Soc., Dalton Trans.* **1985**, *5*, 953-972. h) [(PMe₂Ph)PtB₁₆H₁₈(PMe₂Ph)]⁻: Beckett, M. A.; Crook, J. E.; Greenwood, N. N.; Kennedy, J. D.; McDonald, W. S. *J. Chem. Soc., Chem. Commun.* **1982**, *10*, 552-553. i) [SB₁₇H₂₀]⁻: Jelínek, T.; Kilner, C. A.; Barrett, S. A.; Thornton-Pett, M.; Kennedy, J. D. *J. Chem. Soc., Chem. Commun.* **1999**, *18*, 1905-1906. j) S₂B₁₇H₁₇.SMe₂: Kaur, P.; Holub, J.; Rath, N. P.; Bould, J.; Barton, L.; Štíbr, B.; Kennedy, J. D. *Chem. Commun.* **1996**, *2*, 273-275. k) [S₂B₁₈H₁₉]⁻: Jelínek, T.; Cisařová, I.; Štíbr, B.; Kennedy, J. D.; Thornton-Pett, M. *J. Chem. Soc., Dalton Trans.* **1998**, *18*, 2965-2968. ^c Structure predicted as most stable isomer, both from cluster increments as well as from DFT computations.

The energies of the most stable neutral *arachno:nido*- B_nH_{n+6} macropolyhedral boranes relative to the most stable neutral *arachno*- B_nH_{n+6} isomers are displayed in Figure 8.2b. Surprisingly, the *arachno(4):nido(3)*- B_5H_{11} is only slightly higher in energy than the thermodynamically most stable *arachno*- B_5H_{11} .²⁰ The energies of the most stable *arachno:nido*-macropolyhedral boranes relative to the corresponding most stable *arachno*-single cluster boranes increase from $n = 5$ to $n = 9$ (solid line in Figure 8.2b). For $n = 10$, the curve steeply drops down, marking the turning point from single cluster to macropolyhedral preference. For ten or more vertexes, the *arachno:nido*-macropolyhedral boranes are more stable than the single cluster *arachno*-boranes.

The comparison of thermodynamic stabilities of neutral *arachno:arachno*-macropolyhedral boranes with the isomeric single cluster *hypho*-boranes (solid line in Figure 8.2c) reveals that for six and seven vertexes, simple polyhedra are more stable than *arachno:arachno*-macropolyhedral structures.²¹ When the number of vertexes is larger than seven, *arachno:arachno*-macropolyhedral boranes are preferred.

8.2.2. Importance of Open Face Hydrogen Atoms on the Stabilities of Macropolyhedral vs. Monopolyhedral Boranes.

Figure 8.2 compares the stabilities of macropolyhedral relative to isomeric single cluster structures not only for boranes but also for borates. Solid, broken and dotted lines represent the stabilities of neutral, anionic and dianionic macropolyhedra relative to corresponding simple polyhedra, respectively.²²

Open face hydrogen atoms are known to have a significant influence on the stabilities of *nido:nido*-macropolyhedral boranes relative to corresponding *nido*-clusters.⁶ A similar effect is observed for the *arachno:nido*- versus *arachno*-curve (Figure 8.2b). The thermodynamically preferred $B_{10}H_{16}$ structure is a macropolyhedral borane (solid line in Figure 8.2b for $n = 10$). This may surprise as *arachno*-10-vertex (hetero)boranes e.g., $C_2B_8H_{14}$ or the dianionic $[B_{10}H_{14}]^{2-}$ are experimentally well known,²³ but 10-vertex

²⁰ The initial starting geometry for *arachno(3):nido(3)*- B_4H_{10} rearranged to the regular *arachno*- B_4H_{10} geometry and therefore the relative stability of both could not be compared.

²¹ An attempt to optimize *hypho*- B_4H_{12} resulted in a H_2 molecule at non-bonding distance to a regular *arachno*- B_4H_{10} structure. For $n = 5$, different starting geometries for *hypho*- B_5H_{13} and *arachno:arachno*- B_5H_{13} all converged to the same B_5H_{13} geometry.

²² Monoanionic $[B_nH_{n+3}]^-$ clusters used to generate the broken line in Figure 2a probably represent the most stable isomers as a large number of possible monoanionic clusters were computed for each number of vertexes (n). Broken or dotted lines in the case of *arachno:nido*- and *arachno:arachno*-macropolyhedral borates are based on the relative stabilities of one selected macropolyhedral borate obtained by deprotonating the respective thermodynamically most stable neutral macropolyhedron.

²³ a) Štíbr, B.; Janousek, Z.; Plešek, J.; Jelínek, T.; Hermanek, S. *Collect. Czech. Chem. Commun.* **1987**, *52*, 103-112. b) Janousek, Z.; Plešek, J.; Hermanek, S.; Štíbr, B. *Polyhedron* **1985**, *4*, 1797-1798. c) Štíbr, B.; Plešek, J.; Hermanek, S. *Collect. Czech. Chem. Commun.* **1974**, *39*, 1805-1809.

8. TWO VERTEX SHARING MACROPOLYHEDRAL BORANES

macropolyhedra are not. However, deprotonation of $B_{10}H_{16}$ to $[B_{10}H_{15}]^-$ and $[B_{10}H_{14}]^{2-}$ enormously increases the stability of simple polyhedral structures relative to corresponding macropolyhedra. This is due to the fact that two adjacent hydrogen bridges generally destabilize a structure. Neutral *archno:nido*-macropolyhedral boranes usually have seven or eight endo-hydrogen atoms on two open faces (an average of 3.5 or 4 hydrogen atoms per open face), while *archno*-boranes have six hydrogen atoms on a single open face. Loss of one hydrogen atom releases stress on both simple and macropolyhedral boranes, but more stress is released for single polyhedra and hence the curve for relative stabilities of macro- versus simple polyhedra is shifted to more positive values for anionic clusters. Therefore, macropolyhedral $[B_{10}H_{15}]^-$ and $[B_{10}H_{14}]^{2-}$ structures are far less stable than single polyhedral clusters. Moreover, the turning point from which on macropolyhedra are preferred is shifted to a larger number of vertexes for anionic clusters.

Similar relationships exist between the relative stabilities of neutral, monoanionic and dianionic *archno:archno*- versus *hypho*-macropolyhedral boranes and borates (see Figure 8.2c). Monoanionic and dianionic *archno:archno* clusters are considerably disfavored with respect to the corresponding neutral *archno:archno*-clusters except for fourteen and fifteen vertexes for which *archno:archno*-dianionic clusters are more favored than in the neutral case.

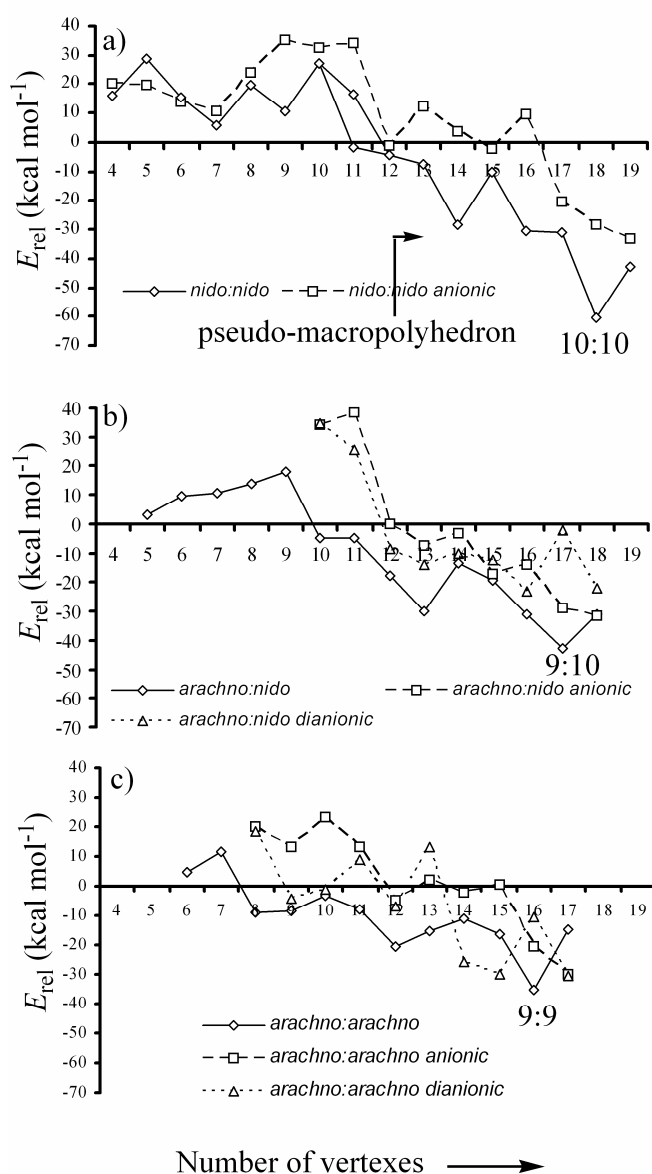


Figure 8.2: Relative stabilities of a) *nido:nido*- versus *nido*-, b) *archno:nido*- versus *archno*- and c) *archno:archno*- versus *hypho*-clusters. The curve for the relative stabilities of *nido:nido*- versus *nido*-clusters is taken from ref. 6 (also see ref. 21-23 and 25).

8.2.3. The Number of Skeletal Electron Pairs and the Stabilities of Macropolyhedral Boranes Relative to Isomeric Simple Polyhedra.

The thermodynamic stabilities of the most stable neutral *nido:nido*-,²⁴ *arachno:nido*- and *arachno:arachno*-macropolyhedral boranes relative to the corresponding neutral *nido*-, *arachno*- and *hypho*-borane clusters, respectively, are shown as solid lines in Figure 8.2.

For more than nine vertexes ($n \geq 9$), the *arachno:nido*- versus *arachno*-stability curve (solid line in Figure 8.2b) shows a pattern very similar to that of the *nido:nido*- versus *nido*-curve (solid curve in Figure 8.2a), only shifted to the left by one vertex. For example, the *nido:nido*- versus *nido*-curve (Figure 8.2a) sharply decreases between $n = 10$ and $n = 11$. A similar decrease in the *arachno:nido*- versus *arachno*-curve is found between $n = 9$ and $n = 10$ (Figure 8.2b). The similarities persist throughout both curves. The decrease of the *nido:nido*- versus *nido*- curve from eleven to fourteen vertexes is accompanied by a similar decrease of the *arachno:nido*- versus *arachno*-curve from ten to thirteen vertexes. A sharp increase between $n = 14$ and $n = 15$ for the *nido:nido*- versus *nido*-curve, and between $n = 13$ and $n = 14$ for the *arachno:nido*- versus *arachno*- curve continues to decrease beyond the points to reach minima at $n = 18$ in the *nido:nido*- versus *nido*- and $n = 17$ in the *arachno:nido* versus *arachno*-curve, respectively.

For larger cluster size ($n \geq 9$), the relative stabilities of neutral *arachno:arachno*- versus *hypho*-curve also follows the trends exhibited by the neutral *nido:nido*-versus *nido*- and neutral *arachno:nido*- versus *arachno* curves but is shifted to the left by one more unit with respect to the latter: The trends between n

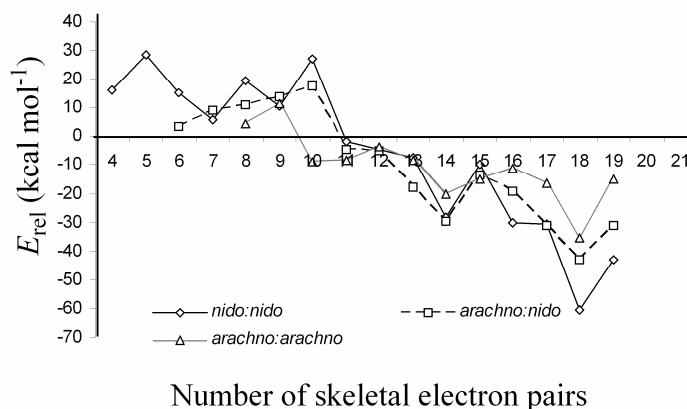


Figure 8.3: Stabilities of *nido:nido*-, *arachno:nido*- and *arachno:arachno*- macropolyhedral boranes relative to isomeric monopolyhedra are plotted against the number of skeletal electron pairs.

²⁴ A structure with one exo-substituted hydrogen atom on one boron atom of the shared B_2 unit in *nido:nido*-macropolyhedral boranes was regarded as pseudo macropolyhedron including the *nido(3):nido(10)*- $B_{11}H_{15}$. However, many optimized *arachno:nido*- and *arachno:arachno*-macropolyhedral geometries contain this feature. In order to compare *nido:nido*-macropolyhedral boranes with *arachno:nido*- and *arachno:arachno*-macropolyhedral boranes, *nido(3):nido(10)*- $B_{11}H_{15}$ is included in Figure 2a, which slightly changes the curve shape.

= 10 to $n = 17$ in the *arachno:arachno*-curve are very similar to those observed between $n = 11$ and $n = 18$ in the *arachno:nido*- and between $n = 12$ and $n = 19$ in the *nido:nido*-curve.

The similar trends of the neutral curves in Figure 8.2a-c for larger number of vertexes can be rationalized on the basis of the number of skeletal electrons. According to Wade's skeletal electron counting rule,⁹ the loss of one vertex from *closo* to *nido*, from *nido* to *arachno* and from *arachno* to *hypho* clusters does not alter the skeletal electron requirement. For example, $n+1$, $n+2$, $n+3$ and $n+4$ skeletal electron pairs are required for the 12-vertex *closo*-, 11-vertex *nido*-, 10-vertex *arachno*- and 9-vertex *hypho*-clusters, respectively, i.e., 26 skeletal electrons in each case. In a similar fashion, the loss of one vertex from a *nido:nido*-cluster to give an *arachno:nido*-cluster and the loss of another vertex from an *arachno:nido*-cluster to give an *arachno:arachno*-cluster does not alter the total skeletal electronic requirement. An *arachno:arachno*-cluster with a total number of vertexes n has the same number of skeletal electrons as an *arachno:nido*-cluster with $n+1$ vertexes and as a *nido:nido*-cluster with $n+2$ vertexes. Hence, the stability curve in Figures 8.2a through 2c match each other roughly when they are plotted against the number of skeletal electrons rather than the number of vertexes (Figure 8.3).

The smaller the cluster size, the larger is the ratio of the open face hydrogen atoms to the boron atoms. The importance of endo-hydrogen atoms on the stability of borane clusters has already been demonstrated vastly.^{6,7,12} The *arachno*- and *hypho*-clusters have more open face hydrogen atoms as compared to the *nido*-clusters. Therefore, the trends of the three curves in Figure 8.3 are dominated by the extra open face hydrogen atoms for smaller number of vertexes. As a consequence, in this region they show significantly different patterns.

The anionic (broken line) and dianionic (dotted line) curves in Figure 8.2 do not show similarities to the same extend. This might be due to the fact that the anionic curves for *arachno:nido*- and *arachno:arachno*-macropolyhedral borates were not obtained by a thorough scanning of all possible anionic clusters. They rather represent the relative stabilities of optimized deprotonated most stable neutral structures, which may not necessarily be the most stable anionic isomers.

8.2.4. Preferred Fragments for Two Vertex Sharing *arachno:nido*- and *arachno:arachno*-Macropolyhedral Boranes.

Generally, the thermodynamically most stable two vertex sharing macropolyhedral boranes with two fused *nido*-units consist of at least one 10-vertex *nido*-unit.⁶ Table 8.2 indicates that the most stable isomers of the two vertex sharing *arachno:arachno*-macropolyhedral boranes with $n = 12-17$ contain at least one *arachno*-9-vertex unit. Thus the 10-vertex *nido*-unit and the 9-vertex *arachno*-unit seem to be the preferred building blocks for two vertex sharing *nido:nido*- and *arachno:arachno*-macropolyhedral boranes, respectively.

When one *arachno*-fragment is combined with a *nido*-fragment, the choice for the *nido* fragment rules out the *arachno* counterpart: The thermodynamically most stable *arachno:nido*-macropolyhedral boranes from $n = 12-17$ have one 10-vertex *nido*-unit. Only for $n = 10, 11$ and 18 , one *arachno*-9-vertex unit is present instead.

Moreover, the deepest point of the neutral *nido:nido*-curve (Figure 8.2a) corresponds to 18 vertexes, i.e. *nido*(10):*nido*(10), which involves two *nido*-10-vertex fragments. The latter is the preferred building block for *nido:nido*-macropolyhedral boranes. Likewise the lowest point, i.e., the highest preference of a macropolyhedron over the corresponding single polyhedron (Figure 8.2c), is found for $n = 16$, i.e., *arachno*(9):*arachno*(9). The preference of *arachno*-9-vertex and *nido*-10-vertex clusters for *arachno:nido*-macropolyhedral boranes is also reflected by the high thermodynamic preference of *arachno*(9):*nido*(10)- $B_{17}H_{25}$ for $n = 17$.

8.2.5. Structural Relationships between Different Macropolyhedral Borane Classes.

Williams⁷ first pointed out that the elimination of one most highly coordinated vertex from *closo*-clusters results in a *nido*-deltahedral fragment. The loss of another most highly coordinated vertex from the open face of *nido*-deltahedra generates *arachno*-deltahedra. The removal of one more vertex from the open face of *arachno*-deltahedra produces *hypho*-deltahedra.⁸ Similar structural relationships exist for the most stable isomers within different classes of two vertex sharing macropolyhedral boranes.

Generally a variety of choices exists how to distribute the vertexes to the two cluster units making a macropolyhedral borane. The thermodynamically most stable isomers for *nido:nido*-, *arachno:nido*- and *arachno:arachno*-macropolyhedral boranes are listed in Table 8.2. For eighteen vertexes, three possible structures are *nido*(9):*nido*(11)- $B_{18}H_{20}$, *nido*(8):*nido*(12)- $B_{18}H_{20}$ and *nido*(10):*nido*(10)- $B_{18}H_{20}$. The latter consists of two equally sized *nido*-10-vertex units and is the thermodynamically most stable structure in accordance with the experimentally established $B_{18}H_{22}$ structures.²⁵ The thermodynamically most stable 17-vertex *arachno:nido*-macropolyhedral borane consists of one 9-vertex *arachno* unit sharing two vertexes with another 10-vertex *nido* unit. Alternatives like *arachno*(8):*nido*(11)-, *arachno*(11):*nido*(8) or *arachno*(10):*nido*(9) are energetically disfavored. The removal of one BH vertex from the *nido*(10):*nido*(10)- $B_{18}H_{22}$ structure (and addition of two open face hydrogen atoms) results in an *arachno*(9):*nido*(10) structure which is the most stable $B_{17}H_{23}$ isomer. The most stable $B_{16}H_{24}$ structure, i.e. *arachno*(9):*arachno*(9)- $B_{16}H_{24}$ can also be obtained by a similar one vertex elimination from the *nido*-part of the most stable *arachno*(9):*nido*(10)-macropolyhedron (Figure 8.4).

²⁵ Two $B_{18}H_{22}$ isomers were reported, which combine two 10-vertex *nido*-fragments in a two vertex sharing macropolyhedron with C_2 and C_i symmetry, respectively.

8. TWO VERTEX SHARING MACROPOLYHEDRAL BORANES

Table 8.2. Structural relationships^a between thermodynamically most stable isomers of various *nido:nido*-, *arachno:nido*- and *arachno:arachno*-macropolyhedral boranes.^{b,c}

Number of vertexes (n)	<i>nido:nido</i> -B _n H _{n+4} ^d	<i>arachno:nido</i> -B _n H _{n+6}	<i>arachno:arachno</i> - B _n H _{n+8}
19	10:11		
18	10:10	9:11	
17	9:10	9:10	9:10
16	8:10	8:10	9:9
15	7:10	7:10	8:9
14	6:10	6:10	7:9
13	5:10	5:10	6:9
12	3:11 (4:10) ^e	4:10	5:9
11	3:10	9:4	5:8 (4:9) ^e
10	6:6	9:3	5:7 (4:8) ^e
9	3:8	6:5	4:7
8	3:7	5:5	5:5
7	3:6	4:5	4:5
6	3:5	4:4	3:5
5	3:4	3:4	3:4 ^f
4	3:3	3:3 ^g	3:3 ^h

^a The diagonal arrows indicate the loss of one vertex. The question mark on the arrow indicates that the corresponding macropolyhedral borane structures are not related simply by the loss of one vertex. ^b The 14 to 19 vertex containing *nido:nido*-macropolyhedral boranes are structurally related to the 13 to 18-vertex *arachno:nido*-clusters by the loss of one vertex. Further loss of one vertex from *arachno:nido*-macropolyhedral boranes results in corresponding *arachno:arachno*-macropolyhedral boranes with $n = 12$ to 17 . ^c The boxes with light gray shade indicate that isomeric single cluster boranes are thermodynamically more stable than macropolyhedral boranes. ^d See ref. 6 ^e The structures in parenthesis are only slightly (i.e. less than $1.7 \text{ kcal mol}^{-1}$) higher in energy than the most stable isomer. ^f Different starting geometries for *hypho*-B₅H₁₃ and *arachno:arachno*-B₅H₁₃ converged to the optimized *arachno:arachno*-B₅H₁₃ geometry. ^g The initial starting geometry for *arachno*(3):*nido*(3)-B₄H₁₀ rearranged to regular *arachno*-B₄H₁₀ upon geometry optimization. ^h An attempt to optimize *hypho*-B₄H₁₂ resulted in a geometry with one H₂ unit at non-bonding distance to the regular *arachno*-B₄H₁₀ structure.

8. TWO VERTEX SHARING MACROPOLYHEDRAL BORANES

These correlations hold generally true (Table 8.2) starting with the most stable 14-19 vertex containing *nido:nido*-macropolyhedra, which give the preferred 13-18 vertex containing *arachno:nido*-deltahedra which in turn give the most favorable *arachno:arachno*-deltahedra by successive removal of one open face vertex from the smallest *nido*-unit. The following rules emerge how to derive the most stable structure for a macropolyhedral borane:

-For B_nH_{n+4} , the most stable isomer adopts a two vertex sharing *nido*(n-8):*nido*(10)-macropolyhedron.

-The most stable $B_{n-1}H_{n+5}$ isomer is derived from the most stable macropolyhedral B_nH_{n+4} by the removal of one vertex from the smaller unit, i.e. it constitutes either an *arachno*(n-9):*nido*(10) for $n \leq 18$ or an *arachno*(9):*nido*(n-8)-macropolyhedron for $n \geq 18$.

-The most stable $B_{n-2}H_{n+6}$ structures correspond to an *arachno*(n-9):*arachno*(9)-macropolyhedron.

-The loss of one vertex from *nido:nido*- to *arachno:nido*-deltahedra is always from the open face but, unlike monopolyhedra, not the most highly coordinated vertex is removed, which usually is either one of the shared vertexes or directly attached to one of them.

8.2.6. Comparison of $E_{n+1}-E_n$ for Simple Polyhedral and Macropolyhedral Boranes.

The difference of the computed absolute energies of consecutive members of the *nido*(10):*nido*(n)- $B_{8+n}H_{12+n}$ as well as for members of the *nido*- B_nH_{n+4} series is plotted against n for $n = 3-10$ in Figure 8.4a. I.e. the lowering of the absolute energy is plotted as a *nido*-cluster is increased as a part of a macropolyhedron or by itself. The average values are indicated as horizontal lines for both cases. A data point above this line means that incorporation of another BH group is accompanied with a less than average energy gain while a point below indicates a more than average favorable cluster increase from n to n+1.

The *nido* line is slightly below the *nido:nido* line, which means that in the chosen range of n on average it is more favorable to expand a *nido* cluster by one vertex as compared to a *nido:nido* macropolyhedron. There is a preference for *nido*- as well as *nido:nido*-clusters with an even number of

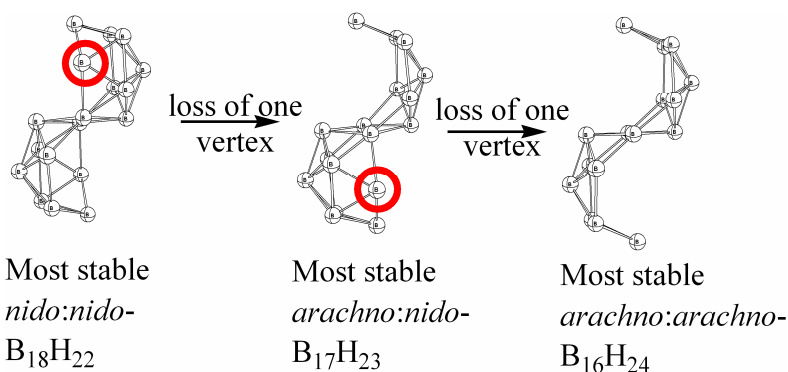


Figure 8.4: The most stable *nido:nido*- $B_{18}H_{22}$, *arachno:nido*- $B_{17}H_{23}$ and *arachno:arachno*- $B_{16}H_{24}$ are structurally related by the removal of one open face vertex (highlighted by a circle).

8. TWO VERTEX SHARING MACROPOLYHEDRAL BORANES

vertexes over neighboring odd numbered cases. The absolute of $E_{n+1}-E_n$ is always smaller than the average for even n , while it is larger for an odd n . As an example, E_9-E_8 is higher than the average of $E_{n+1}-E_n$ but $E_{10}-E_9$ is much smaller than the averaged $E_{n+1}-E_n$. Moreover, this trend of favoring the even cluster is progressively increasing with the increase in number of vertexes.

A similar plot (Figure 8.4b) of $E_{n+1}-E_n$ of the *nido*- and *arachno:nido*-macropolyhedral boranes shows that a similar trend exists. The even clusters are more favorable than the odd clusters. However, the plot of $E_{n+1}-E_n$ of the *arachno*- and *arachno:nido*-clusters and the *arachno* and *arachno:arachno*-clusters do not clearly indicate any specific trends.

8.3. Conclusion

Two vertex sharing *nido:nido*-, *arachno:nido*- and *arachno:arachno*-macropolyhedral boranes are structurally related to each other: Loss of one vertex from the thermodynamically most stable *nido:nido*-macropolyhedral borane isomers results in the thermodynamically most stable *arachno:nido*-macropolyhedral boranes. Loss of another vertex from the *nido*-part of the most stable *arachno:nido*-macropolyhedral boranes results in the thermodynamically most stable *arachno:arachno*-macropolyhedral boranes. The *arachno*-9-vertex and *nido*-10-vertex cluster fragments are the preferred fragments that usually constitute the thermodynamically most stable macropolyhedral borane isomers. Open face hydrogen atoms enormously influence the thermodynamic stability of macropolyhedra relative to corresponding monopolyhedral boranes. For larger number of vertexes, thermodynamic stabilities of macropolyhedra relative to their corresponding simple polyhedra exhibit similar trends (but shifted to the left by one vertex) due to the same number of skeletal electrons.

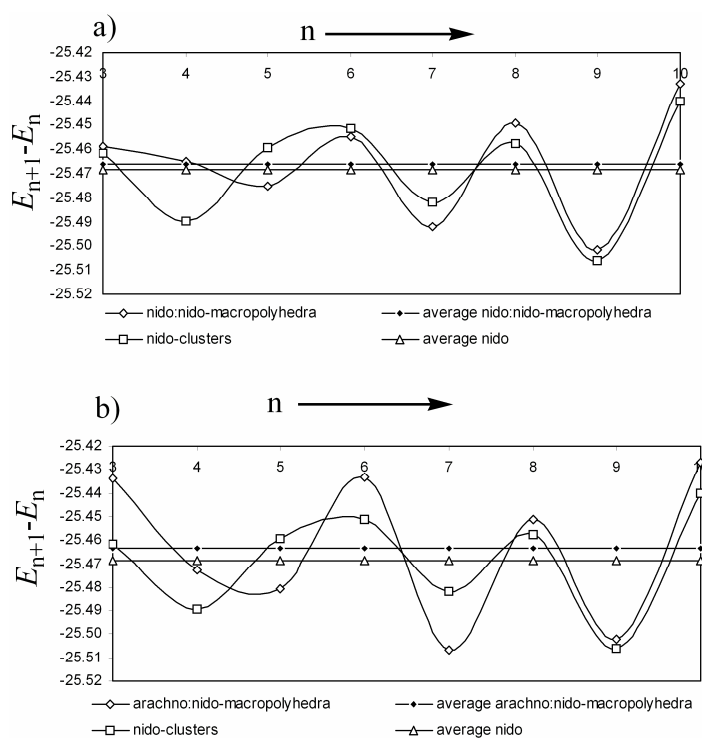


Figure 8.5: $E_{n+1}-E_n$ for a) *nido:nido*-macropolyhedral boranes and corresponding *nido*-single cluster boranes b) *arachno:nido*-macropolyhedral boranes and corresponding *nido*-single cluster boranes.

9. Summary and Conclusion

Quantitative rules governing the relative stabilities of single cluster boranes have been determined. Five structural increments obtained as the energy difference of two clusters differing with respect to one structural feature can be conveniently used to derive the relative stabilities of various 11-vertex *nido*-hetero(carba)boranes. The magnitude of structural increments depends largely upon the extent of electron localization which is determined primarily by the number of electrons donated by a heteroatom and secondarily by the electronegativity of the heteroatom. The energy penalties for two disfavoring structural features, i.e. HetHet (two heteroatoms adjacent to each other) and HetC (a heteroatom adjacent to a carbon atom) show highly periodic trends i.e. increase along the period while decrease down the group (Figure 9.1). Smaller heteroatoms have larger while larger heteroatoms have smaller HetHet and HetC energy penalties. Energy penalties for Het_{5k}(1) (a heteroatom at a five-coordinate vertex) and Het_{5k}(2) (a heteroatom in the middle belt of an 11-vertex *nido*-cluster) increase down the group 14 but decrease down group 16. For both three as well as four electron donating heteroatoms in group 15, however, they show mixed trends. The importance of geometric consequences also becomes clear by the pronounced preference for open face position for larger heteroatoms due to their larger Het_{5k}(1) and Het_{5k}(2) energy penalties. Structural increments very accurately predict the DFT computed relative stabilities of various 11-vertex *nido*-hetero(carba)boranes and –borates. Most stable mixed heteroboranes with more than two open face heteroatoms have different heteroatom positions in the thermodynamically most stable 11-vertex *nido*-heteroborane isomers, easily predictable on the basis of structural increments.

Structural and connection increments can be used to give the relative stabilities of numerous 11-

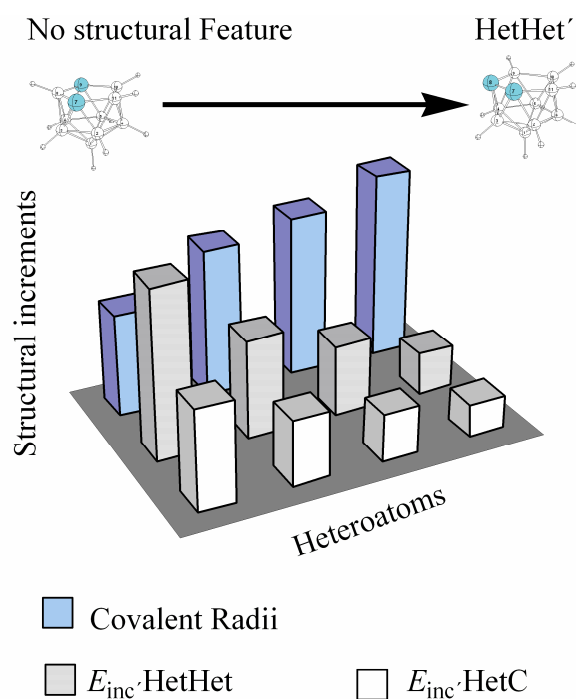


Figure 9.1: Structural Increments for various heteroatoms are inversally related to covalent radii.

vertex *nido*- and 12-vertex *closo*-hetero(carba)boranes with a unique set of increments. Usually more electronegative (smaller) heteroatoms tend to occupy non-adjacent, whereas less electronegative (larger) heteroatoms tend to occupy adjacent vertices in the thermodynamically most stable *closo*-diheterododecaborane isomers (Figure 9.2). The energy differences of para- and meta- relative to ortho-isomers of 12-vertex *closo*-heteroboranes generally depend on the extent of electron localization by a given heteroatom and show highly periodic trends, i.e., increase along the period and decrease down the group, as in the case of 11-vertex *nido*-heteroboranes.

The energy penalties for the HetHet structural feature (two heteroatoms adjacent to each other) for the 12-vertex *closo*-cluster are

apparently significantly different from those for the 11-vertex *nido*-cluster. Reformulating two 11-vertex *nido*-structural features, i.e. Het_{5k}(2) and HetHet, in terms of connection increments along with the additional structural feature HetHet_m give the relative stabilities of various isomeric 11-vertex *nido*- as well as 12-vertex *closo*-heteroboranes and -borates with different heteroatom substitution patterns. The Het_{5k} and HetHet structural increments proposed for the 11-vertex *nido*-cluster may be transformed to bonding connection increments that can be used for 12-vertex *closo*-clusters. Connection increments are still applicable to 11-vertex *nido*-heteroboranes and -borates along with other structural features.

Cyclopentadienyl metal fragments in the 12-vertex *closo*-cyclopentadienyl metallaheteroboranes have a clear preference with respect to the positions relative to carbon and other heteroatoms in the thermodynamically most stable isomer. Cyclopentadienyl derivatives of group 9 and 10 metals direct a carbon atom to meta- and para-positions, respectively. CpM fragments of two group 8 metals, i.e., Ru and Os have the tendency to direct carbon atoms to meta positions while that of Fe directs carbon atoms to ortho positions. Structural increments for two general structural features, i.e., HetHet'_o (two heteroatoms at ortho positions) and HetHet'_m (two heteroatoms at meta positions) reproduce the DFT-

12-Vertex *closo*-cluster

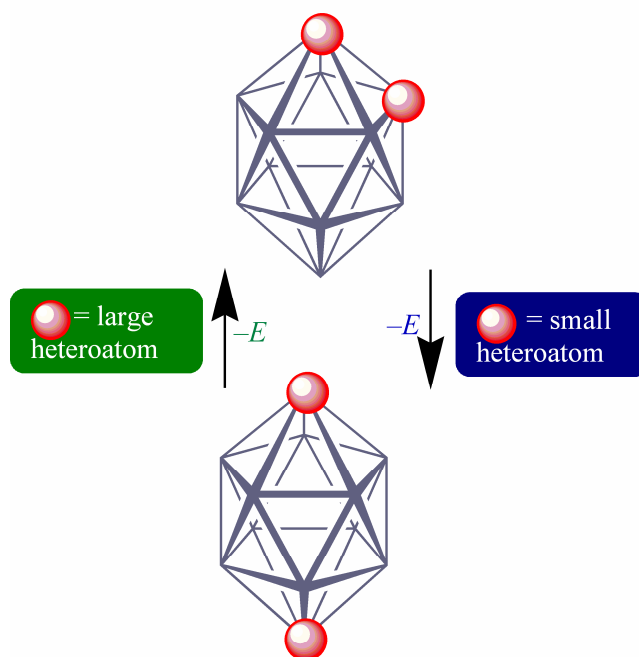


Figure 9.2: Smaller, more electronegative heteroatoms tend to occupy non-adjacent, whereas larger, less electronegative heteroatoms occupy adjacent vertices in the thermodynamically most stable isomers of Het₂B₁₀H₁₀ isomers.

9. CONCLUSION

computed relative stabilities of more than one hundred 12-vertex *closo*-cyclopentadienyl metallaheteroboranes isomers quite accurately (Figure 9.3).

Structural increments increase along one period due to increasing positive charge on the metal center along the period, i.e., as consequence of an increasing extent of electron localization. These structural increments are substituent specific; a change of the substituent on the metal atom leads to different energy penalties.

Thermodynamic stabilities of various neutral B_nH_{n+4} and anionic $[B_nH_{n+3}]^-$ for *nido*-single cluster boranes and borates with corresponding *nido:nido*-macropolyhedral boranes and borates are compared at the RB3LYP/6-311+G(d,p)//RB3LYP/6-31G(d) + ZPE level of theory. Neutral macropolyhedral boranes enjoy larger thermodynamic stability than single cluster isomers for larger cluster size ($n \geq 12$, Figure 9.4). For anionic species, a clear cut turning point for macropolyhedral preference is shifted to not less than seventeen vertexes. Extra hydrogen atoms at the open face have a significant influence on the relative stabilities of the single cluster *nido* boranes vs. *nido:nido*-macropolyhedral boranes. The loss of extra open face hydrogen atoms results in enhanced stability of *nido* clusters as compared to macropolyhedra. Hence, anionic macropolyhedra are less stable with respect to anionic single clusters than in the neutral case. The same should be true for suitably substituted

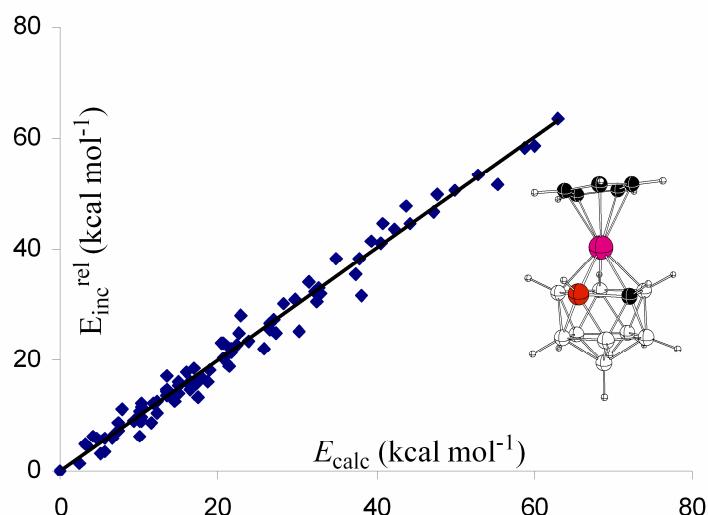


Figure 9.3: Structural increments may be applied to quickly derive the relative stabilities of various possible isomers of cyclopentadienyl metallaheteroboranes.

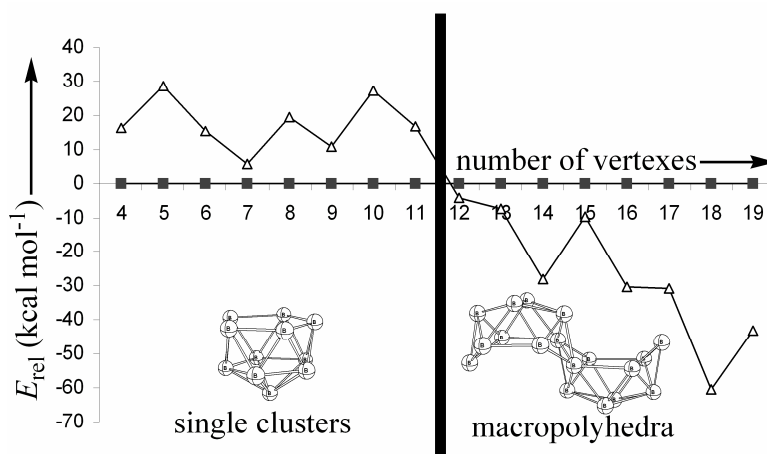


Figure 9.4: Twelve vertexes is the turning point from *nido*- B_nH_{n+4} single cluster to *nido:nido*-macropolyhedral borane preference. The thermodynamically most stable neutral *nido:nido*-macropolyhedral boranes consist of at least one 10-vertex *nido*-unit.

9. CONCLUSION

heteroboranes. Usually, the thermodynamically most stable neutral macropolyhedral boranes have at least one 10-vertex *nido* single

cluster unit whereas the anionic macropolyhedral clusters usually possess one deprotonated 11-vertex *nido*-unit. The relative energies of the neutral macropolyhedra mostly reflect the stability patterns exhibited by the sum of the energies of two single cluster units making a given macropolyhedra (E_{x+y}).

Cluster increments may be applied to estimate the relative stabilities of various two-vertex sharing macropolyhedral boranes (Figure 9.5). Such increments reproduce the DFT computed relative stabilities of macropolyhedral boranes usually within ± 6 kcal mol⁻¹. A simple summation procedure helps to select the best partner for a given cluster fragment in order to construct the thermodynamically most stable *nido:nido*-, *arachno:nido*- and *arachno:arachno*- macropolyhedral boranes. Cluster increments are considerably smaller for even *nido*-cluster fragments than for odd *nido*-cluster fragments pointing towards high thermodynamic stability of macropolyhedral boranes with even numbered *nido*-units. The cluster increments for *arachno*-clusters are usually smaller than for corresponding *nido*-fragments and increase with increasing cluster size. Experimentally known macropolyhedral boranes correspond to the most stable structures as computed by DFT methods and as estimated by the cluster increments produced.

Various two vertex sharing macropolyhedral boranes were

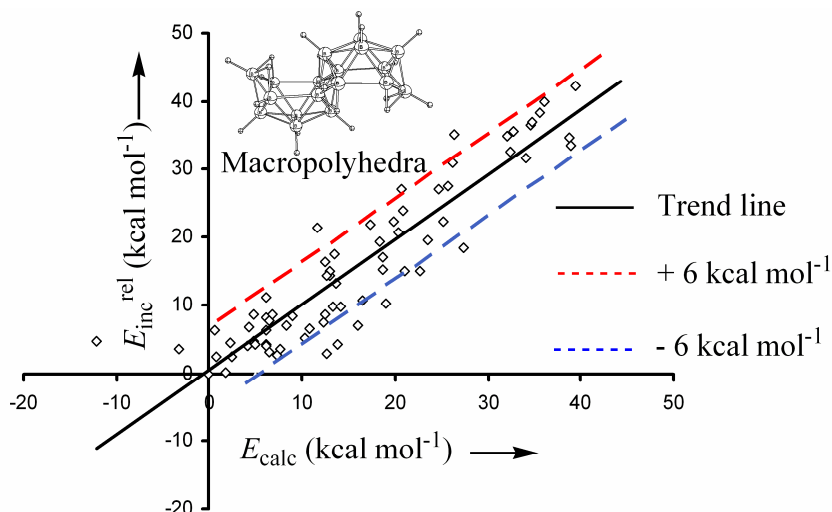


Figure 9.5: Cluster increments derived for individual cluster fragments reproduce the DFT computed relative stabilities of macropolyhedral boranes usually within ± 6 kcal mol⁻¹.

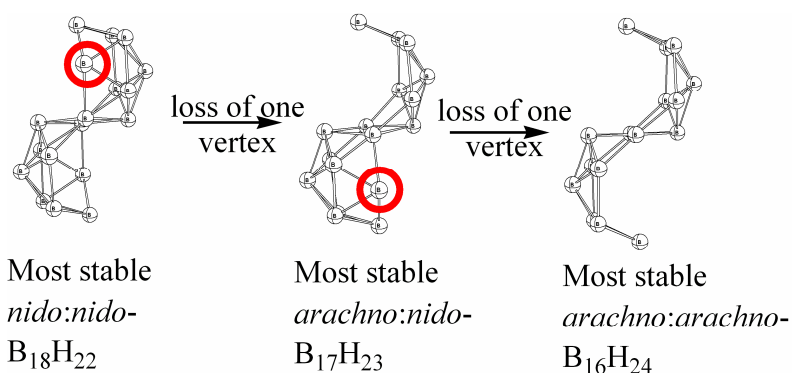


Figure 9.6: Most stable isomers of *nido:nido*-, *arachno:nido*-, and *arachno:arachno*-macropolyhedral boranes are structurally related to each other by the loss of one open face vertex.

9. CONCLUSION

computed at the B3LYP/6-311+G**//B3LYP/6-31G* level of theory to determine the preferred fragments for the thermodynamically most stable isomers. The *arachno*-9-vertex and *nido*-10-vertex cluster fragments usually constitute the thermodynamically most stable macropolyhedral borane isomers. Two vertex sharing *nido:nido*-, *arachno:nido*- and *arachno:arachno*-macropolyhedral boranes are structurally related to each other: Loss of one vertex from the thermodynamically most stable *nido:nido*-macropolyhedral borane isomers results in the thermodynamically most stable *arachno:nido*-macropolyhedral boranes. Loss of another vertex from the *nido*-part of the most stable *arachno:nido*-macropolyhedral boranes results in the thermodynamically most stable *arachno:arachno*-macropolyhedral boranes (Figure 9.6). Open face hydrogen atoms enormously influence the thermodynamic stability of macropolyhedra relative to corresponding monopolyhedral boranes. For larger number of vertexes, thermodynamic stabilities of macropolyhedra relative to their corresponding simple polyhedra exhibit similar trends (but shifted to smaller number of vertexes by one unit) due to the same number of skeletal electrons. For small numbers of vertexes ($n \leq 10$), however, this effect is overruled by the extra open face hydrogen atoms.

Related articles in peer-reviewed journals

The following articles in peer-reviewed journals have been derived from the material presented in or related to this thesis;

1. A Structural Increment System for 11-Vertex *nido*-Boranes and Carboranes. Kiani, F. A.; Hofmann, M. *Inorg. Chem.* **2004**, *43*, 8561-8571.
2. Structural Increments for 11-Vertex *nido*-Phospha and Aza(carba)boranes and -borates; Dependence of Energy Penalties on the Extent of Electron Localization. Kiani, F. A.; Hofmann, M. *Inorg. Chem.* **2005**, *44*, 3746-3754.
3. The Additive Nature of Energy Penalties in 10-Vertex *nido*-(Car)boranes. Kiani, F. A.; Hofmann, M. *Eur. J. Inorg. Chem.* **2005**, *12*, 2545-2553.
4. The Relative Stabilities of 11-Vertex *nido*- and 12-vertex *closo*-Heteroboranes and -borates: Facile Estimation by Structural or Connection Increments. Kiani, F. A.; Hofmann, M. *Dalton Trans.*, **2006**, *5*, 686-692.
5. Ortho-, Meta- and Para-Directing Influence of Transition Metal Fragments in 12-vertex *closo*-Cyclopentadienyl Metallaheteroboranes: Additive Nature of Structural Increments. Kiani, F. A.; Hofmann, M. *Organometallics*, **2006**, *25*, 485-490.
6. Periodic Trends and Easy Estimation of Relative Stabilities in 11-Vertex *nido*-p-Block Heteroboranes and -borates. Kiani, F. A.; Hofmann, M. *J. Mol. Mod.* **2006**, *12*, 597-609.
7. On the Stability of *nido:nido*-Macropolyhedral Boranes. Kiani, F. A.; Hofmann, M. *Inorg. Chem.* **2006**, *45*, 6996-7003.
8. Structural Relationships between Two Vertex Sharing Macropolyhedral Boranes. Kiani, F. A.; Hofmann, M. *Eur. J. Inorg. Chem.* submitted.
9. Cluster Increments for Macropolyhedral Boranes. Kiani, F. A.; Hofmann, M. *Dalton Trans.* accepted.
10. Structural Paradigms in Macropolyhedral Boranes. Kiani, F. A.; Hofmann, M. *Manuscript in Preparation*.

Acknowledgement

I express my sincere gratitude to the following;

Prof. Dr. Roland Krämer for giving me place in his group and for his kind formal supervision.

Prof. Dr. Peter Comba as speaker of the “Graduate College-850” for providing an excellent additional education through the program of the college.

I must acknowledge the nice company of Tobias Graf over the years. Moreover, he was always ready to help me in any problem related to computers.

I express my gratitude to all the present and past members of AK Krämer during my PhD time, especially Nora Graf, Mareike Göritz, Malgorzata Jagoda, Zuhail Kaya, Ann-Kathrin Marguerre, Andriy Mokhir, Larisa Mokhir and Volker Seifried.

I am also thankful to all members of “Graduate College-850, Modeling of Molecular Properties” including Bodo Martin, Ulrike Blumbach, Karin Memminger, Sven Reinhardt, Tobias Rosendahl, Heidi Rohwer and Mate Tarnai for their nice company at local as well as outstation seminars and conferences.

I am thankful to my lab-fellows over the years including Sascha K. Goll, Carola Darge and Birgit Esser.

The most needed administrative staff including Jeanette Grosse, Claudia Aßfalg, Karin Stelzer and Marlies Schilli.

I am thankful to professors and researchers with whom I discussed various boron hydride issues. Those include Prof. A. J. Welsh, Prof. J. Plešek, Prof. L. Wesemann, Prof. B. Wrackmeyer, Dr. D. Hnyk, and Dr. I. Maulana.

The best wishes of my parents, family members and friends are a precious asset for me. I remember my favorite teachers especially Ghulam Hassan Kiani, my maternal grandfather, Maqsood Sahib, my chemistry teacher at Govt. Post Graduate College Chakwal and Prof. Dr. Christy Munir at Quaid-I-Azam University Islamabad, Pakistan. I am indebted to Prof. Dr. Amin Badshah for his help and guidelines in getting M.Phil scholarship.

My nice and beloved wife, Faiza Farooq! I am thankful to you and Shees for bearing ‘hours of mindlessness’, during which I was thinking research problems while physically being at home.

The inspirations that I got from the book “Alchemist” by Paulo Coelho, the poetry of Dr. Muhammad Iqbal-the national poet of Pakistan, the sayings of Muhammad Ali Jinnah-the founder of Pakistan, and those of Prof. Dr. Abdus Salam-Pakistani Nobel laureate in theoretical physics, were always with me during the course of my research work.

Erklärung

Erklärung gemäß § 7 (3) b) und c) der Promotionsordnung:

a) Ich erkläre hiermit an Eides statt, dass ich die vorgelegte Dissertation selbst verfasst und mich keiner anderen als der von mir ausdrücklich bezeichneten Quellen und Hilfen bedient habe.

b) Ich erkläre hiermit an Eides statt, dass ich an keiner anderen Stelle ein Prüfungsverfahren beantragt bzw. die Dissertation in dieser oder anderer Form bereits anderweitig als Prüfungsarbeit verwendet oder einer anderen Fakultät als Dissertation vorgelegt habe.

Heidelberg, den 21.08.2006

Farooq Ahmad Kiani

